Qualitative und quantitative Analyse von lokalen Progenitorzellen in humanen Myokardbiopsien von Patienten mit Myokarditis und Kardiomyopathie

Dissertation
zur Erlangung des akademischen Grades
Dr. med.
an der Medizinischen Fakultät
der Universität Leipzig

eingereicht von: Marie Gerisch, geb. Wegener

Geburtsdatum / Geburtsort: 21.09.1991 in Peine

angefertigt am Biotechnologisch-Biomedizinischen Zentrum, Professur für Zelltechniken und angewandte Stammzellbiologie, Universität Leipzig

Betreuer: Univ.-Prof. Dr. med. Augustinus Bader

Ko-Betreuer: Dr. rer. nat. Shibashish Giri
Ko-Betreuer: Dr. med. Jan Smettan

Beschluss über die Verleihung des Doktorgrades vom: 12. Februar 2019

INHALTSVERZEICHNIS

I ABKÜRZUNGSVERZEICHNIS

Abk.	Erläuterung
ADSC	Adipose tissue-derived stem cell
BMC	Bone marrow-derived cell
CD	Cluster of Differentiation
CDC	Cardiosphere-derived cell
c-Myc	Myc-Protoonkogen
DCM	Dilatative Kardiomyopathie
ED	Erstdiagnose
EF	Ejektionsfraktion
ICM	Ischämische Kardiomyopathie
IPSC	Induzierte pluripotente Stammzelle
KHK	Koronare Herzerkrankung
Klf4	Gut-enriched Krüppel-like factor
MSC	Mesenchymale Stammzelle
Oct3/4	Oktamer-bindender Transkriptionsfaktor 4
pAVK	Periphere arterielle Verschlusskrankheit
Sca-1	Stem cell antigen-1
SCFR	Stem cell factor receptor
SCIPIO	Cardiac stem cells in patients with ischaemic cardiomyopathy
Sox2	Sex determining region Y (SRY)-box 2
Thy-1	Thymocyte differentiation antigen-1
WSI	Whole Slide Imaging

II VORBEMERKUNGEN

Für die Darstellung der Ergebnisse wurde die kumulative Form der Promotion gewählt. Eine ausführliche Literaturrecherche erschien in Form eines Reviews im Juni 2015 in der wissenschaftlichen Fachzeitschrift „Drug Discovery Today“. Die experimentellen Daten sowie eine ausführliche Diskussion der Ergebnisse wurden in Form eines Original Research Artikels im März 2018 bei „Frontiers in Genetics“ veröffentlicht. Beide Publikationen wurden in diese Arbeit eingefügt.

Bibliografischer Nachweis der Publikationen:

Wegener M, Bader A, Giri S (2015) How to mend a broken heart: adult and induced pluripotent stem cell therapy for heart repair and regeneration. Drug Discov Today. 20:667-85. doi: 10.1016/j.drudis.2015.02.010

Gerisch M, Smettan J, Ebert S *et al.* (2018) Qualitative and Quantitative Analysis of Cardiac Progenitor Cells in Cases of Myocarditis and Cardiomyopathy. Front Genet. 6;9:72. doi: 10.3389/fgene.2018.00072

1. EINFÜHRUNG IN DIE THEMATIK

1.1 Hintergrund

Herz-Kreislauf-Erkrankungen sind eines der zentralen Themen in der Gesundheitsforschung. Im Jahr 2015 starben rund 17,7 Millionen Menschen weltweit aufgrund kardiovaskulärer Erkrankungen, das entsprach 31 % aller Todesfälle weltweit [1]. Speziell die ischämische Herzkrankheit führte laut WHO die Liste der zehn häufigsten Todesursachen im Jahr 2015 mit 8,756 Millionen Fällen an [2].

Eine ischämische Herzkrankheit kann durch ein akutes kardiales Ereignis ausgelöst werden, wie zum Beispiel einem Myokardinfarkt. Dieser löst im betroffenen Myokardareal eine Entzündungsreaktion aus, welche zu einer Aktivierung lokaler Fibroblasten führt. Diese wiederum formen eine kollagenreiche Narbe als schnellen und sicheren Reparaturmechanismus [3]. Der Verlust der Kardiomyozyten führt anschließend zu Funktionsverlusten und folglich zur Herzinsuffizienz oder gar zum Tod [4]. Wegen augenscheinlich fehlender Regenerationsmechanismen galt deshalb lange die Meinung, dass das menschliche Herz ein postmitotisches Organ mit enddifferenziertem Gewebe sei [5].

Die bisherigen Therapiemöglichkeiten von Herz-Kreislauf-Erkrankungen zielten daher darauf ab, das Fortschreiten des kardialen Funktionsverlustes zu begrenzen [6]. Dabei spielt bis heute die medikamentöse Behandlung eine große Rolle. Aber auch invasive Eingriffe, wie zum Beispiel perkutane Koronarinterventionen, koronare Bypassoperationen oder Klappenrekonstruktionen zählen zu den gegenwärtigen Behandlungsstrategien. Als Ultima Ratio gilt die Herztransplantation. Im Jahr 2015 wurden weltweit insgesamt 5.074 Herztransplantationen in 285 Zentren bei der „International Society for Heart and Lung Transplantation“ registriert [7]. Die mediane Überlebensdauer nach einer Herztransplantation beträgt 10,7 Jahre bei Erwachsenen und 16,1 Jahre bei Kindern [7].

Neue Therapiestrategien mit dem Ziel, die kardiale Funktion durch Regeneration des geschädigten Myokards wiederherzustellen und dadurch die hohe Mortalität kardiovaskulärer Erkrankungen zu reduzieren, haben sich in den letzten Jahren zu einem großen Schwerpunkt in der Herz-Kreislauf-Forschung entwickelt. Verschiedene Stamm- und Progenitorzellen unterschiedlichen Ursprunges werden dabei bis heute analysiert. Ziel dieser Arbeit ist es, lokale Progenitorzellen direkt in Myokardbiopsien nachzuweisen und mögliche Unterschiede bezüglich Anzahl und Verteilung in verschiedenen Krankheitsbildern zu analysieren.

1.2 Pluripotente Stammzellen

Auf der Suche nach geeigneten Stammzellen zur Regeneration des Herzens fiel der Blick zunächst auf die sogenannten pluripotenten Stammzellen. Diese Zellen besitzen die Fähigkeit zur Selbsterneuerung durch Teilung. Sie können sich in jede Zelle des menschlichen Körpers entwickeln [8]. Zu den pluripotenten Stammzellen gehören die embryonalen Stammzellen, welche aus der inneren Zellmasse von Blastozysten stammen [9]. Sie haben die Fähigkeit, sich in alle drei Keimblätter zu differenzieren: Ektoderm, Endoderm und Mesoderm. Darüber hinaus haben sie eine unbegrenzte Kapazität zur Selbsterneuerung [9]. Es wurde bereits bewiesen, dass sich humane embryonale Stammzellen auch in Kardiomyozyten differenzieren können [10]. Der Gebrauch von menschlichen Embryonen zur Gewinnung von Stammzellen steht jedoch im Mittelpunkt weltweiter ethischer Diskussionen. Auf der Suche nach Alternativen gelang es Wissenschaftlern im Jahr 2006, somatische, also bereits differenzierte, nicht-pluripotente Zellen in ein pluripotentes Stadium - ähnlich dem von embryonalen Stammzellen - zurück zu „reprogrammieren“. Unter Verwendung von vier Transkriptionsfaktoren, *Oct3/4* („Oktamer-bindender Transkriptionsfaktor 4“), *Sox2* („sex determining region Y (SRY)-box 2“), *c-Myc* („Myc-Protoonkogen“) und *Klf4* („gut-enriched Krüppel-like factor“), induzierten sie die Reprogrammierung von Fibroblasten zu pluripotenten Stammzellen. Sie nannten die entstandenen Zellen „induzierte pluripotente Stammzellen“ (iPSCs) [11]. Erste Experimente versprachen ein großes Potential der iPSCs. So zeigte sich bei Myokardischämie nach Injektion von iPSCs eine verbesserte Kontraktilität in einem Mausmodell [12]. Im Schweinemodell zeigte sich eine verbesserte regionale Perfusion und linksventrikuläre Funktion [13]. In einer weiteren Studie wurde das kardiale Differenzierungspotential von iPSCs mit embryonalen Stammzellen verglichen. Es wurden Ähnlichkeiten in der Aktivierung kardialer Gene gefunden, ebenso wie in der elektrischen Aktivität der Zellen. IPSCs galten somit als vielversprechende Alternativtherapie zu embryonalen Stammzellen [14]. Neben den Vorteilen, die diese Zelltherapie erreichen kann, wurden jedoch bereits negative Auswirkungen bei der Implantation von iPSCs berichtet. So ist die Implantation von iPSCs höchstwahrscheinlich mit einer erhöhten Inzidenz der Tumorgenese assoziiert [15].

1.3 Multipotente Stammzellen

Neben den pluripotenten Stammzellen existieren die multipotenten Stammzellen, welche sich lediglich in verschiedene Zelltypen einer Zelllinie differenzieren können [16]. Als potentielle Kandidaten für die kardiale Regeneration gelten Stamm- und Progenitorzellen aus dem Knochenmark, die „Bone marrow-derived cells“ (BMCs). Diese Zellen werden aus dem menschlichen Knochenmark aspiriert und sie enthalten unterschiedliche Zellgruppen, unter anderem hämatopoetische Stammzellen, mesenchymale Stammzellen und endotheliale Stammzellen [17]. Die BMCs werden direkt, ohne vorherige *in vitro* Transdifferenzierung transplantiert [16]. Es erwies sich, dass BMCs vor allen Dingen parakrine Effekte verursachen [16]. BMCs gelten momentan als die am meist genutzte Stammzellquelle in Bezug auf kardiale Regeneration [16]. Es wurden mehrere klinische Studien durchgeführt, welche die Injektion von BMCs beinhalteten, zum Beispiel die BOOST-Studie, die REGENERATE-AMI-Studie, die TIME-Studie und einige weitere [18–23]. Meist führten die Studien jedoch nicht zu signifikanten Verbesserungen der linksventrikulären Pumpfunktion des Herzens [21–23]. Auch wurde nachgewiesen, dass BMCs sich nach einem Myokardinfarkt *nicht* in Kardiomyozyten differenzieren [24]. Außerdem gibt es Hinweise darauf, dass BMCs Tumorwachstum und Tumorprogress fördern [25].

Mesenchymale Stammzellen (MSCs) sind sowohl im Knochenmark, als auch in verschiedenen anderen Geweben zu finden, unter anderem der Nabelschnur, der Plazenta, in Muskel- und Fettgewebe [26]. In einer Studie konnte eine signifikanten Verbesserung der linksventrikulären Pumpfunktion durch eine Therapie mit MSCs nachgewiesen werden [27]. Eine Meta-Analyse bestätigte, dass MSCs einen positiven Effekt auf die kardiale Funktion bei der Behandlung von Myokardinfarkten ausüben [28]. Auch bei den MSCs geht man davon aus, dass der positive Effekt der Zellen jedoch nicht auf einer Transdifferenzierung in kardiale Zellen beruht, sondern durch die Sekretion von parakrinen Faktoren bedingt ist [29]. Es sind jedoch größere, randomisierte kontrollierte Studien notwendig, um diesen Effekt zu verifizieren [28].

Als weitere Kandidaten für die kardiale Regeneration gelten auch die sogenannten Skelettmyoblasten. Bei diesen handelt es sich um „ruhende“ Zellen, die unter der Basalmembran von Muskelfasern liegen [30]. Nach einer Verletzung werden sie aktiviert, sie proliferieren und differenzieren sich in neue Muskelfasern [30]. In Untersuchungen konnte die

Injektion dieser Skelettmyoblasten jedoch keine signifikante Verbesserung der regionalen oder globalen linksventrikulären Funktion zeigen [31].

Stammzellen aus dem Fettgewebe ("Adipose tissue-derived stem cells", ADSCs) weisen ähnliche Eigenschaften wie BMCs auf. Sie können in einem einfachen chirurgischen Eingriff aus subkutanem Fettgewebe gewonnen werden [32]. In einem Tierversuch konnte gezeigt werden, dass die Therapie mit ADSCs zu einer verbesserten Ejektionsfraktion (EF) und einem verbesserten kardialen Output im Vergleich zur Kontrollgruppe führte [33]. Jedoch haben Studien bereits erwiesen, dass ADSCs die Proliferation von Tumorzellen unterstützen können und somit ADSCs möglicherweise das Wachstum bereits vorhandener Tumoren fördern [34].

1.4 Lokale kardiale Stammzellen

Wissenschaftler gehen inzwischen davon aus, dass im Herzen selbst ein lokaler Pool an Stamm- bzw. Progenitorzellen vorhanden ist. Es ist belegt, dass Kardiomyozyten sowohl unter physiologischen als auch unter pathologischen Konditionen Mitose und Zytokinese durchlaufen können [35]. In Untersuchungen wurde gezeigt, dass in Myokardbiopsien von Patienten, die nach einem akuten Herzinfarkt starben, typische Charakteristika der Zellteilung, wie zum Beispiel die Formation von Spindelapparaten, Karyo- und Zytokinese zu finden waren. Daraus wurde geschlussfolgert, dass nach einem Myokardinfarkt eine Myozytenproliferation stattfindet [36]. Es wurden primitive Zellen entdeckt, welche Stammzelleigenschaften aufweisen und in der Lage waren, neue Muskelzellen zu bilden [37, 38]. Andere Arbeiten unterstützen die Aussage, dass das Herz kardiale Progenitorzellen besitzt, welche unter bestimmten pathologischen Konditionen eine aktive Rolle in der Regeneration des Herzens spielen [39].

In experimentellen Studien am Schweinemodell wurden so genannte „Cardiosphere-derived cell"s (CDCs) als residente kardiale Stammzellen beschrieben, welche aus endomyokardialen Biopsien isoliert und anschließend kultiviert wurden. In dieser Studie konnte nachgewiesen werden, dass CDCs neues Myokard generieren können und die kardiale Funktion verbessern können [40]. Für eine prospektive, randomisierte Phase-1-Studie, der „CADUCEUS"-Studie („Cardiosphere-derived autologous stem cells to reverse ventricular dysfunction"), wurden 25 Patienten ausgewählt, die wenige Wochen zuvor einen Myokardinfarkt erlitten hatten. Sie wurden in eine CDC- Behandlungsgruppe und eine

Kontrollgruppe, welche lediglich die Standardtherapie erhielt, eingeteilt. Der Behandlungsgruppe wurden 1,5 - 3 Monate nach einem Myokardinfarkt autologe CDCs in eine vom Infarkt betroffene Arterie infundiert. 6 Monate nach Injektion der Zellen konnte zwar eine Reduktion des Narbengewebes und eine Vergrößerung der Herzmuskelmasse festgestellt werden, jedoch zeigte sich kein signifikanter Unterschied zwischen beiden Gruppen in Bezug auf das enddiastolische und endsystolische Volumen oder der linksventrikulären EF [41].

1.5 Das Oberflächenantigen CD117

Der c-Kit Rezeptor, auch CD117 („Cluster of Differentiation" 117) bzw. SCFR („Stem Cell Factor Receptor") genannt, ist ein Oberflächenprotein, welches zur Gruppe der Zytokinrezeptoren gehört [42]. Zellen, die dieses Antigen tragen, gelten als potenzielle lokale Progenitorzellen, sie wurden schon in einigen Studien im humanen Myokard nachgewiesen [43–45]. Typische Stammzellcharakteristika wie Klonogenität, Multipotenz und Selbsterneuerung wurden an $CD117^+$ Zellen bestätigt [38, 46]. Eine vermehrte Expression von $CD117^+$ Zellen fand man in unterschiedlichen Erkrankungen, wie zum Beispiel Herzinsuffizienz, kardialer Hypertrophie, ischämischer Kardiomyopathie (ICM), Herzschädigung und Drucküberlastung [37, 43, 47–51]. In einer Studie wurde jedoch geschlussfolgert, dass $CD117^+$ Zellen unter pathologischen Konditionen keine terminale Differenzierung und funktionale Kompetenz erreichen konnten [52].

Es wurden bereits erste klinische Studien zur Analyse der therapeutischen Wirkung von $CD117^+$ Zellen durchgeführt. In der Phase-1-Studie „SCIPIO" („Cardiac stem cells in patients with ischaemic cardiomyopathy") wurden Myokardinfarkt-Patienten mit eingeschränkter linksventrikulärer Funktion (EF < 40 %) vor einer koronaren Bypassoperation in eine Behandlungs- und eine Kontrollgruppe aufgeteilt [53]. Die Behandlungsgruppe erhielt einige Zeit nach der Operation eine einmalige intrakoronare Injektion von 1 Mio. autologen $CD117^+$ Stammzellen, die Kontrollgruppe erhielt keine Zelltherapie. In der Behandlungsgruppe konnte eine verbesserte linksventrikuläre Pumpfunktion gezeigt werden und ebenso eine Reduzierung des Infarktareales [53]. Bei den guten Ergebnissen sollte jedoch bedacht werden, dass es sich um eine sehr kleine Probandenzahl handelte (n = 16) und der Placebo-Effekt nicht berücksichtigt wurde. Erheblich größere Studien werden nötig sein, um die Sicherheit und die Erfolge dieser Therapiestrategie zu verifizieren.

1.6 Das Oberflächenantigen CD90

Zur Charakterisierung kardialer Progenitorzellen wurde bereits eine ganze Reihe an Oberflächenantigenen in Kombination mit CD117 untersucht, dazu zählen unter anderem CD29, CD44, CD31, CD34, Sca-1 („stem cell antigen-1“), sowie CD105 und CD90 [54–61].

Von besonderem Interesse für diese Arbeit ist das Oberflächenantigen CD90 bzw. Thy-1 („Thymocyte differentiation antigen-1“), welches vor allen Dingen als Zelltypmarker für mesenchymale Stammzellen gilt [62]. In dieser Arbeit wurde die These verfolgt, dass CD90 sowohl Fibroblasten charakterisiert, welche in die Narbenbildung involviert sind, als auch Progenitorzellen, welche die funktionale Geweberegeneration induzieren können. Das Interesse an kardialen Fibroblasten ist in den letzten Jahren explosionsartig angestiegen [63]. Viele Studien beschäftigen sich mit dem Ursprung kardialer Fibroblasten, der Reprogrammierung von Fibroblasten und der Entwicklung neuartiger Medikamente zur Reduzierung kardialer Fibrose [63].

In dieser Arbeit wird die These aufgestellt, dass im menschlichen Körper $CD90^+$ Progenitorzellen vorhanden sind, welche lokal im Gewebe ruhen und nach Entzündung, Verletzung oder nach natürlichem Altern der Zellen aktiviert werden. Frühere Studien unterstützen diese Annahme, so wurden bereits $CD90^+$ Progenitorzellen in der Haut nachgewiesen und deren Abhängigkeit von lokaler Zytokinstimulation zur Proliferation untersucht [64, 65]. Durch die Aktivierung lokaler Progenitorzellen wurden bei Patienten mit akuten oder chronischen Wunden und Hautulzerationen erste klinische Erfolge erzielt [64, 66].

1.7 Direkter Nachweis von CD117 und CD90 in Myokardbiopsien

Die Antigene CD117 und CD90 konnten bereits am menschlichen Herzen nachgewiesen werden [54, 56, 58–60]. Oftmals geschah dieser Nachweis jedoch nicht direkt in der Gewebsbiopsie, sondern an isolierten Zellen oder an bereits kultivierten Zellen [45, 52, 53, 59]. In wenigen Studien wurde CD117 direkt im humanen Myokard untersucht [51, 56, 67]. In einer Arbeit wurden 12 explantierte Herzen von Kindern untersucht, davon handelte es sich in acht Fällen um univentrikuläre Herzen („Single Ventricle mit funktionstüchtigem rechtem Ventrikel") und in vier Fällen um eine dilatative Kardiomyopathie (DCM). Es wurde nachgewiesen, dass hohe Druckbelastung zu einem Anstieg der $CD117^+$ Zellen führt, denn bei

den Patienten mit einem Single Ventricle konnte eine dreifach höhere Konzentration an $CD117^+$ Zellen im Vergleich zu den Patienten mit DCM gemessen werden [51].

Im Gegensatz zu CD117 wurde CD90 in der Vergangenheit häufig als zusätzlicher mesenchymaler Stammzellmarker analysiert und meist an kultivierten $CD117^+$ Zellen getestet [54, 56, 68]. In der hier vorliegenden Arbeit jedoch erfolgte der Nachweis von CD117 und CD90 direkt an Serienschnitten humaner Myokardbiopsien verschiedener Patientengruppen mittels immunhistochemischer Analyse. Die Ergebnisse spiegeln somit den Nativzustand der Biopsie wider und enthalten Informationen über die unverfälschte Anzahl und Verteilung der Progenitorzellen.

1.8 Myokarditis und Kardiomyopathie

Neben dem allgemeinen Nachweis von Progenitorzellen im menschlichen Myokard soll in dieser Arbeit auch die unterschiedliche Ausprägung dieser Zellen bei verschiedenen kardialen Krankheitsbildern untersucht werden. Dazu wurden zum einen Patienten ausgewählt, bei denen die Diagnose „Myokarditis“ gestellt wurde. Die Myokarditis im Allgemeinen ist definiert als eine entzündliche Erkrankung der Herzmuskelzellen. Histologisch zeigt sich eine Infiltration von mononuklearen Zellen im Myokard [69]. Die klinische Manifestation der Myokarditis ist stark variabel und reicht von asymptomatischen Stadien bis hin zu schweren Myokardschäden mit Arrhythmien und kardiogenem Schock [69]. Die Ursachen der Erkrankung sind ebenfalls vielfältig. Häufig ist eine Myokarditis viral bedingt, aber auch Bakterien und andere nicht infektiöse Trigger können diese auslösen [69].

Neben dieser oft akut verlaufenden, von Entzündungsreaktionen geprägten Erkrankung wurden zum anderen Patienten mit der Diagnose „Kardiomyopathie“ ausgewählt. Dabei handelt es sich um eine chronische, progredient verlaufende Erkrankung. Die Kardiomyopathie umfasst eine Gruppe von unterschiedlichen Krankheitsbildern, welche alle den Herzmuskel betreffen. Dieser kann dabei hypertrophiert, dilatiert oder auch durch Narbengewebe ersetzt sein. Anfänglich verläuft die Erkrankung meist symptomarm, es können Kurzatmigkeit und Schwindel auftreten, aber auch Benommenheit und Müdigkeit. Ein Progress der Erkrankung kann zu Herzinsuffizienz und Arrhythmien führen [70]. Oftmals ist die genaue Ursache unbekannt, prinzipiell kann eine Kardiomyopathie jedoch erworben oder gar bereits angeboren sein [70].

1.9 Virtuelle Mikroskopie

Die standardmäßige Auswertung immunhistochemischer Färbungen ist die visuelle Analyse unter einem gewöhnlichen Lichtmikroskop. Das Anliegen dieser Arbeit war es, zur Auswertung der durchgeführten immunhistochemischen Analysen neuartige Mikroskopiertechniken zu verwenden. Die virtuelle Mikroskopie, oder auch „Whole Slide Imaging“ (WSI) genannt, revolutioniert die traditionelle Lichtmikroskopie. Das WSI besteht grundsätzlich aus zwei verschiedenen Prozessen. Der erste Prozess beinhaltet die Digitalisierung der Objektträger mittels einer speziellen Software. Ein sogenannter “Whole Slide Scanner” wird benötigt, um die Objektträger digitalisieren zu können. Der „Whole Slide Scanner“ besteht im Wesentlichen aus einem Mikroskop mit Objektiven, einer Lichtquelle, einer digitalen Kamera zur Bildaufzeichnung, einer Robotertechnik, welche die Objektträger verschiebt, einem Computer und einer Software zur Bearbeitung der entstandenen digitalen Bilder, den so genannten „Digital Slides“ [71]. Im zweiten Prozess können die entstandenen „Digital Slides“ angesehen und analysiert werden [71]. Eine Studie belegte die Umsetzbarkeit und die Genauigkeit der WSI in der Diagnostik und bestätigte die Eignung für die Interpretation von immunhistochemischen Analysen und auch von In-situ-Hybridisierung [72].

1.10 Hypothesen, Frage- und Zielstellungen

Durch den oben aufgezeigten Einstieg in die Problematik wird deutlich, dass der Erforschung kardialer Stammzellantigene eine wichtige Bedeutung bei der Suche nach neuartigen Therapiestrategien kardiovaskulärer Erkrankungen zukommt. Bisherige Veröffentlichungen zu diesem Schwerpunkt beinhalten oftmals tierexperimentelle Studien oder sind fokussiert auf die Kultur von extrahierten Stamm- und Progenitorzellen, und nicht auf deren Nachweis direkt im Biopsiematerial. Daher wurden in der vorliegenden Arbeit folgende Fragestellungen und Ziele formuliert:

1. Die Neuentwicklung und Etablierung spezieller Protokolle zur immunhistochemischen Analyse von Progenitorzellmarkern der in Paraffin eingebetteten Gewebeproben

2. Die Durchführung von immunhistochemischen Färbungen zum Nachweis der Progenitorzellmarker CD90 und CD117 direkt in humanen Myokardbiopsien
3. Die Erstellung hochauflösender, digitaler Bilder der immunhistochemischen Färbungen, welche sowohl einen Überblick über den gesamten Gewebeschnitt geben, als auch die Möglichkeit bieten, jeden Abschnitt bis auf Zellebene vergrößern zu können
4. Das Entwickeln einer Methode zur automatisierten quantitativen Analyse des gesamten Gewebeschnittes, welche über die traditionelle qualitative Analyse der histologischen Bilder hinaus geht
5. Können im menschlichen Herzen lokale $CD90^{+}/CD117^{+}$ Progenitorzellen nachgewiesen werden?
6. Gibt es Unterschiede in Anzahl und Verteilung von CD90 und CD117 in Hinblick auf verschiedene Krankheitsbilder? Und unterscheiden sich die Anzahl und Verteilung von CD90 und CD117 untereinander?

2. PUBLIKATIONEN

How to mend a broken heart: adult and induced pluripotent stem cell therapy for heart repair and regeneration

Marie Wegener, Augustinus Bader, Shibashish Giri

erschienen als Publikation bei: *Drug Discovery Today* (Impact Factor 2017: **6.848**)
Juni 2015; 20(6):667-85. doi: 10.1016/j.drudis.2015.02.010

Qualitative and Quantitative Analysis of Cardiac Progenitor Cells in Cases of Myocarditis and Cardiomyopathy

Marie Gerisch, Jan Smettan, Sabine Ebert, Maria Athelogou, Beate Brand-Saberi, Nick Spindler, Wolf C. Mueller, Shibashish Giri, Augustinus Bader

erschienen als Publikation bei: *Frontiers in Genetics* (Impact Factor 2017: **4.151**)
6. März 2018; 9:72. doi: 10.3389/fgene.2018.00072

We describe recent advances in the development of molecular and cellular targets in the heart for the reactivation and regeneration of cardiomyocytes. The conversion of primary adult stem cells and induced pluripotent stem cells into cardiomyocytes provides unprecedented opportunities for safer and more effective drug development and cell therapy for patients with cardiovascular disease.

How to mend a broken heart: adult and induced pluripotent stem cell therapy for heart repair and regeneration

Marie Wegener, Augustinus Bader and Shibashish Giri

Centre for Biotechnology and Biomedicine, Department of Cell Techniques and Applied Stem Cell Biology, Medical Faculty of University of Leipzig, Deutscher Platz 5, Leipzig D-04103, Germany

The recently developed ability to differentiate primary adult stem cells and induced pluripotent stem cells (iPSCs) into cardiomyocytes is providing unprecedented opportunities to produce an unlimited supply of cardiomyocytes for use in patients with heart disease. Here, we examine the evidence for the preclinical use of such cells for successful heart regeneration. We also describe advances in the identification of new cardiac molecular and cellular targets to induce proliferation of cardiomyocytes for heart regeneration. Such new advances are paving the way for a new innovative drug development process for the treatment of heart disease.

Introduction

Heart disease is a major global health problem and the main cause of illness and death worldwide. In 2008, cardiovascular disease (CVD) resulted in more than 17 million deaths, representing 30% of all deaths worldwide (http://www.who.int/en). A frequently observed form of heart disease is cardiomyopathy, which, the American Heart Association (AHA) defined as a

> *heterogeneous group of diseases of the myocardium associated with mechanical and/or electrical dysfunction that usually (but not invariably) exhibit inappropriate ventricular hypertrophy or dilatation and are due to a variety of causes that frequently are genetic. Cardiomyopathies either are confined to the heart or are part of generalized systemic disorders, often leading to cardiovascular death or progressive heart failure-related disability.* ***[1]***

Currently, a heart transplant is the only possible option for such patients. However, in Germany, while waiting for a suitable donated organ, 18.9% of patients registered from 2001 to 2009 died within a year of being listed for heart transplantation [2] and the probability of undergoing heart transplantation in this 1-year period was 40.2% [2]. Over the past 10 years, 3600–3850 heart transplants have been registered annually [3], accounting for approximately 66% of all heart transplants globally [3]. However, survival rates show that 83% of heart transplant patients survive for 1 year, 72% have a survival rate of 5 years and 50% survive for

Corresponding author: Giri, S. (shibashish.giri@bbz.uni-leipzig.de)

Marie Wegener

began her medical degree in October 2010 at the University of Leipzig. In 2013, she started her dissertation at the Centre for Biotechnology and Biomedicine (BBZ), University of Leipzig, under the direction of Augustinus Bader. Her dissertation focuses on stem cell research for use in the human heart.

Augustinus Bader

is a German physician and biomedical scientist, and one of the leading experts in the field of stem cell research. He oversees a group at the Centre for Biotechnology and Biomedicine (BBZ), University of Leipzig, where he has been the head of cell techniques and applied stem cell biology since 2003. He was the founder of the International World Congress on Regenerative and is president of the World Federation & World Virtual Institute of Preventive & Regenerative Medicine. Augustinus has given more than 450 lectures at national and international conferences, more than 300 being invited, plenary, or keynote lectures. He has contributed to more than 160 peer-reviewed papers and book chapters. His clinically most relevant inventions include a biological process that imitates bionic principles for stem cell activation and tissue regeneration. Most of his patents have a global coverage. The currently active patent families are 27 with 200+ international filings. In 2010, Augustinus received the most prestigious European scientific price (the Cicatrix Price) organised by a patient organisation for the development of a therapeutic method to prevent scar formation following severe thermal injuries (burns). He is also a member of the Scientific Advisory Committee of the umbilical-cord stem-cell blood bank.

Shibashish Giri

earned his BSc in 1998 from Rairangpur College (Autonomous), Utkal University. He received his MPhil in zoology from the University of Delhi, India in 2003 and a Master's degree in zoology with specialisation in cytogenetics from North Orissa University in 2001. After completing his PhD thesis on´Bioreactor development for hepatocyte culture model, stem cell expansion and efficient hepatic differentiation using self assembling peptides, he joined the applied stem cell biology and cell technology group at BBZ as its deputy head. He has 11 years of research experience with hepatocyte culture models. Currently, he is working on epigenetic targets for liver diseases, hepatic differentiation from human-induced pluripotent stem cells, boosting factors for biotrachea construction, scarless healing mechanisms, and biomaterials for stem cell research under the directorship of Augustinus Bader at BBZ. He has 20 peer-reviewed publications on bioreactor-based hepatocyte culture models and is a scientific member of the World Federation & World Virtual Institute of Preventive & Regenerative Medicine.

http://dx.doi.org/10.1016/j.drudis.2015.02.010

9.4 years or more, with the survival outcome being influenced by features of the recipient and donor [4]. Graft dysfunction is the leading cause of death during the first month following a transplant [4], and the recipient must take immunosuppressive drugs for the rest of their life to avoid rejection [5], despite the adverse effects of such drugs, including weariness, lack of energy, and nervousness [6].

Therefore, given the prevalence of CVD (CVD is the main reason for death in Europe for people younger than 75 years [7]) and related conditions and the predicted increase in the number of deaths resulting from CVD (estimated to be more than 23 million by 2030; http://www.who.int/en), combined with the lack of sufficient treatment options, researchers have begun to investigate whether it is possible to repair damaged hearts. At the forefront of this research is the use of adult stem cells, which have shown some preclinical and clinical success. The use of bone-marrow stem cells (BMSCs), mesenchymal stem cells (MSCs), skeletal myoblasts and embryonic stem cells (ESCs) for heart repair has been reviewed elsewhere [8–11]. Here, we focus on the use of iPSCs for heart repair.

iPSCs

In 2006, Takahashi and Yamanaka reported that it was possible to reprogram differentiated cells, so-called 'iPSCs', into an undifferentiated state, such as embryonic stem cells (ESCs) [12]. Initial experiments in mice demonstrated the beneficial effects of iPSCs on the heart. For instance, when iPSCs were injected into mice following myocardial ischaemia, the results showed beneficial effects in terms of cardiac contractility [13], and a similar result, in the form of enhanced regional perfusion and upgraded cardiac function, was reported using a porcine acute anterior myocardial infarction (AMI) model [14]. Additionally, in another experiment, iPSCs were differentiated into endothelial cells and transplanted into mice after AMI, resulting in enhancement of the ejection fraction [15]. By contrast, a negative effect of iPSC injection was shown in a rat model, where the treated rats had a higher incidence of tumourigenesis [16]. Halbach *et al.* [17] evaluated the effect of iPSC-derived cardiomyocytes (iPSCCMs) on electrical integration and action potential (AP) properties when transplanted into healthy areas of injured hearts in an adult male wild type mouse model. Their results showed an electrophysiological maturation over a period of 6–8 months of transplanted iPSCCMs, which also exhibited AP. Miki *et al.* [18] bioengineered myocardium from mouse iPSCs and tested its cardiac properties in a rat chronic MI model. The authors reported that the implanted bioengineered myocardium survived at the epicardial implantation site following implantation and resulted in attenuated left ventricular (LV) remodelling, suggesting this as a new promising step in the treatment of heart failure [18]. Zwi-Dantsis *et al.* [19] highlighted the clinical importance of gap junctions between host cells tissue and transplanted cells for long-term heart repair. These authors evaluated the potential of heart failure human-iPSC-derived cardiomyocyte cells (HF-hiPSCCMs) *in vivo* in the hearts of female Sprague-Dawley rats. They found that transplanted HF-hiPSCCMs survived and integrated structurally with host cardiomyocytes to form electromechanical junctions within the healthy rat heart. The authors reported a functional cardiac syncytium and adequate chronotropic responses to adrenergic and cholinergic stimulation based on multielectrode array recordings [19]. Carpenter *et al.* [20] induced ischaemia reperfusion injury in the coronary artery of female RNU-RNU rats and injected either iPSCs in culture medium or medium alone into the peri-infarct region of the rats. Although the cardiac morphology and function of iPSC-treated hearts was not significantly different from nontreated infarcted hearts at any time point, iPS-derived cardiac differentiated cells showed improved cardiac performance ($62 \pm 4\%$) compared with infarct controls ($45 \pm 9\%$) after 10 weeks. The authors highlighted the importance of engraftation following transplantation of iPS-derived cardiac differentiated cells because transplanted cells are often lost over time, even in immunocompromised models. On the basis of their results, Carpenter *et al.* also showed that the retention of iPS-derived cardiac differentiated cells at 10 weeks was helpful for recovery from infarct and resulted in improved cardiac performance.

It has been assumed that iPSCs and hESCs are similar in many aspects. Chong *et al.* [21] produced hESCCMs on a clinical scale (more than 1 billion cells per batch) and cryopreserved them with good viability. They showed that cryopreservation and intramyocardial delivery of 1 billion hESCCMs generated extensive remuscularisation of the infarcted heart. Such results are likely to be beneficial to patients with CVD, given the difficulty in regenerating myocardium. Kawamura, *et al.* [22] highlighted the need for high numbers of cells for myocardium therapy. To overcome the difficulty of producing such a high number of cells, the authors developed a simple cell-sheet technique for the creation of hiPSCCM sheets using thermoresponsive dishes. The technique eliminated undifferentiated iPSCs from hiPSCCMs, which is an important step for the large-scale generation of homologous hiPSCCMs and to avoid teratoma formation. The team successfully yielded approximately 2.5×10^7 pure hiPSCCMs and created hiPSCCM sheets from homologous hiPSCCMs. The cardiac performance of hiPSCCM sheets was evaluated in a porcine model of ischaemic cardiomyopathy, induced by ameroid constriction of the left anterior descending coronary artery. After transplantation of hiPSCCMs into myocardial infarcts, hiPSCCMs survived in damaged myocardium and significantly improved cardiac function, increasing neovascularisation and attenuating LV remodelling. This newly developed culture system could be useful for the purification of hiPSCCM to avoid teratoma formation and improve cardiac performance. However, despite its promise, cell sheet technology results in poor long-term survival of the cells that it produces. Kawamura *et al.* [23] overcame this limitation by using omentum, which has a rich vasculature resulting in an enhanced blood supply. They hypothesised that the combined use of hiPSCCM sheets with an omentum flap would enhance cardiac performance on a long-term basis. They transplanted hiPSCCM sheets to porcine hearts with or without an omentum flap and, after 2 months, showed increased angiogenesis in the transplanted area in mini-pigs with the omentum compared with those without omentum. Pecha *et al.* [24] created hiPSC-derived engineered heart tissue (hEHT) grafts from hiPSCCM (7 million cardiomyocytes per EHT) and transplanted them into a LV myocardial cryoinjury of adult female guinea pigs. They found that hEHT implantation improved LV function [23].

Resident cardiac stem cells

The origins of cardiac stem cells (CSCs) are still unknown, but research has shown them to be a promising treatment option for

heart repair (reviewed in [25–31]). The Stem Cell Infusion in Patients with Ischemic Cardiomyopathy (SCIPIO) trial was the first trial of CSC therapy in human patients and the results demonstrated an improvement in LV function and a decrease in infarct size [30], which was also consistent with cardiac regeneration. However, larger trials with more patients are needed to investigate the efficiency and safety of such cell therapies.

Cardiac differentiation

Zhang *et al.* [32] conducted a comparative study of cardiac differentiation of ESCs with hiPSCs and found similarities in the upregulation of cardiac genes and in the electrical activity. They concluded that hiPSCs are an alternative treatment option to ESCs. Matsuura *et al.* [33] used a bioreactor for cardiac differentiation of hiPSCs and showed that 80% of these cells differentiated into cardiac cells and exhibited synchronous and spontaneous beating. Another suspension culture model for cardiac differentiation was developed using iPSCs without a bioreactor [34] and was used to show a significant upregulation of cardiac markers in the differentiated cells. Using a CARM/SB cardiac differentiation procedure, Wei *et al.* [35] showed that hiPSCs were able to differentiate into both cardiomyocytes and mesenchymal stem cells. The resulting cardiomyocytes recorded a whole AP and there was a cardiac differentiation efficiency for the hiPSCs of 20–30%. Another group of researchers differentiated iPSCs into cardiomyocytes and investigated the pharmacological and electrophysiological features of hiPSC cardiomyocytes (hiPSCCMs) by using the patch-clamp technique [36]; they identified the expression genes involved in key ion channels and recorded AP waveforms in hiPSCCMs. Lee *et al.* [37] designed hiPSCCMs and compared them with cardiomyocytes derived from human ESCs. They showed that hiPSCCMs were less effective at calcium handling compared with cell (hESC)-derived cardiomyocytes and that hiPSCCMs also had functional sarcoplasmic reticulum (SR), but that it was immature compared with hESC-derived cardiomyocytes. hiPSCs were also used by Gai *et al.* [38] to demonstrate that such cells have as much cardiomyocyte differentiation efficiency as the hESC line, H9. Specific cardiac genes were identified and the iPSCCMs were also found to respond to cardioactive drugs. The authors also demonstrated that 5-azacytidine (5-Aza) was able to improve cardiac differentiation, whereas low serum and bone morphogenetic protein 2 (BMP2) showed fractional increases, but dimethylsulfoxide (DMSO) had no impact. So *et al.* [39] used a two-medium combination culture protocol [Dulbecco's modified eagle medium (DMEM) plus endothelial basal medium 2 (EBM2)] to differentiate iPSCs into cardiomyocytes. Results showed that these cardiomyocytes express cardiac specific genes and proteins. They reported that the efficiency of cardiac differentiation of the iPSCs [44.8% contracting embryoid bodies (EBs) from iPS-S-6 cells] was superior to that of ESCs (33.3%). Germanguz *et al.* [40] identified cardiac-specific proteins and Ca^{2+}-handling proteins in their iPSCCMs, whereas Kim *et al.* [41] induced differentiation of BMSCs from mice into cardiomyocytes, which resulted in upregulation of the expression of cardiac-specific genes and of sodium/iodide symporter (NIS) gene activity.

Another group of scientists [42] differentiated human dermal MSCs (hDMSCs) into cardiomyocytes by treating them with 5-Aza, demonstrating a simple way of producing cardiomyocytes by using these readily available cells. Xing *et al.* [43] were able to induce the differentiation of rat BMSCs into cardiomyocytes by treating them with angiotensin II (Ang II) and 5-Aza, which both resulted in cardiac differentiation. Li *et al.* [44] investigated the differentiation of BMSCs into cardiac-like cells using a semipermeable membrane. They co-cultured neonatal rat ventricular myocytes with BMSCs using semipermeable membranes to create a myocardial environment. They showed that BMSCs were able to differentiate into cardiac-like cells without the need for cell–cell contact with cardiomyocytes. Another study by Tokcaer-Keskin *et al.* [45] used 5-Aza to reduce the culture time for MSCs by 5 days. 5-Aza was also used by Carvalho *et al.* [46], who compared three different protocols to induce differentiation: (i) Planat-Benard; (ii) 5-Aza, and (iii) Planat-Benard + 5-Aza. With all protocols, the authors identified sarcomeric α-actinin protein, connexin-43, and formation of gap junctions, but they could not find spontaneous cell contraction. Ge *et al.* [47] investigated the differentiation of human amniotic MSCs (hAMSC)-derived iPSCs (MiPSCs) into cardiomyocytes and demonstrated a high expression of cardiac genes. The authors also showed the reprogramming of hAMSCs into MiPSCs. Choi *et al.* [48] tested different culture methods for human adipose-derived stem cells (ASCs), including 5-Aza, a modified cardiomyogenic medium (MCM), a histone deacetylase inhibitor [trichostatin A (TSA)], and co-culture with neonatal rat cardiomyocytes. They reported no success with 5-Aza treatment, whereas MCM and TSA resulted in partial differentiation, but there was no spontaneous contraction. By contrast, direct cell–cell interaction with rat cardiomyocytes induced differentiation of ASCs into beating cardiomyocytes. In addition, Jumabay *et al.* [49] used adipocyte-derived dedifferentiated fat (DFAT) cells and demonstrated that, when the cells were co-cultured with cardiomyocytes or grown in 'MethoCult' medium without cardiomyocytes, they were able to differentiate into cardiomyocyte-like cells (CLCs) *in vitro* and *in vivo* and expressed cardiac phenotype markers. Van Dijk *et al.* [50] also cultured human ASCs on fibronectin-coated, laminin-coated, and uncoated culture dishes and treated the cells with 5-Aza-2-deoxycytidine, resulting in differentiation towards cardiomyocytes. The authors also showed that laminin promoted late ASC differentiation, but fibronectin did not. Li *et al.* [51] cultured CD117+ BMSCs from mice in a RPMI 1640 medium and treated them with transforming growth factor (TGF)-β. TGF-β activated genes in the TGF-β signal transduction pathway and increased the expression of cardiac-specific markers. However, there was no spontaneous beating, indicating that the differentiated cells were CLCs rather than mature cardiomyocytes.

Labovsky *et al.* [52] conducted experiments with human MSCs. They treated the cells with rat cardiomyocyte extract (EX) + streptolysin O (SLO) or with 5-Aza and compared the results. Real-time polymerase chain reaction (RT-PCR) analysis demonstrated the upregulation of cardiomyocyte-related genes in both groups. Labovsky *et al.* described their EX+ SLO− treatment as a possible risk-free alternative to 5-Aza. Another way to produce cardiac cells was developed by Zhao *et al.* [53], who cultured human umbilical cord MSCs (hUMSCs) in a cardiomyocyte-conditioned medium (CMCM) alone, with sphingosine-1-phosphate (S1P) or in DMEM with 10% foetal bovine serum (FBS) + S1P. In CMCM or CMCM + S1P cultured cells, α-actinin and myosin heavy chain (MHC) proteins were identified, but only the CMCM + S1P

cultured cells showed cardiomyocyte-like AP. Zhu *et al.* [54] tried to induce differentiation by direct or indirect co-culturing. They utilised human adipose tissue-derived stem cells (ADSCs) and cultured them directly or indirectly using cell culture inserts. The authors reported that cardiac-specific markers were more expressed in direct co-cultured cells compared with indirectly co-cultured cells. Yan *et al.* [55] conducted a study with rat BMMSCs and divided the cells into four treatment groups: (i) control; (ii) p53 inhibitor alpha (PFT-α); (iii) 5-Aza, and (iv) PFT-α + 5-AZA. The authors showed that, by delaying the p53− cyclin-dependent kinase inhibitor 1 (p21) pathway with PFT-α, BMMSCs were encouraged to differentiate into CLCs. Immunofluorescence staining demonstrated strong expression of cardiac Troponin I (cTnI) and Connexin-43 (Cx43) in all experimental groups and Western blot analysis showed no significant difference in cTnI expression among groups (ii)–(iv). Jin *et al.* [56] also investigated an alternative to 5-Aza and examined the effects of icariin (ICA) on mouse ADSCs. The authors divided ADSCs into ADSCs co-cultured with cardiomyocytes and either with or without ICA or both with ICA and a specific ERK inhibitor (PD98059). Their results indicated that mouse ADSCs can differentiate into cardiomyocytes when treated with ICA. Kaichi *et al.* [57] investigated the differentiation of different iPSC lines into cardiomyocytes and their responses to TSA. They used two Nanog-iPSC lines (38C2 and 20D17) and one Myc(−) iPSC line (256H18) and cultured them on feeder-free gelatinised dishes. They concluded that both Nanog-iPS and Myc(−) iPSCs have the potential to differentiate into cardiomyocytes and that TSA evokes cardiac differentiation. However, 20D17 iPSCs did not differentiate into cardiomyocytes after day 5, perhaps because of the high expression of Octamer-binding transcription factor 3/4 (Oct3/4). Uosaki *et al.* [58] co-cultured mouse ESCs with the endodermal cell line End2, one group by co-aggregation and one group by using an End2-conditioned medium. The authors concluded that their co-aggregation method was a simple and efficient alternative to induce cardiac progenitor cells. Another study was conducted by Kuzmenkin *et al.* [59] using murine iPSCs. These authors used Iscove's-modified Dulbecco medium (IMDM) for cardiac differentiation and showed that cardiac development of N10 and O9 iPSC lines was decelerated compared with ESCs. In addition, Zwi *et al.* [60] induced the differentiation of hiPSCs using an EB differentiation system. The differentiated cells had molecular, structural, and functional features that were specific to cardiac cells. The cardiomyocyte differentiation of different types of iPSCs and adult stem cells is given in Table 1.

A novel approach was used by Lian *et al.* [61], who demonstrated that the generation of cardiomyocytes from various hiPSC lines was possible by using regulatory elements of Wnt/β-catenin signalling, if applied at the right time. They were able to generate populations comprising up to 98% cardiomyocytes. Lin *et al.* [62] conducted a study with hiPSCs and ESCs. For differentiation, they used a basal differentiation medium, endothelial basal medium 2 (EGM2) and smooth muscle growth medium 2 (SmGM2) medium and small molecules, such as vascular endothelial growth factor (VEGF) and basic fibroblast growth factor (bFGF). The resulting cells exhibited cardiovascular cell types with a high degree of purity. Shinozawa *et al.* [63] differentiated murine ESCs and hiPSCs into cardiomyocytes and used a thin glass pipette to preserve cardiomyocyte-rich beating cell clusters (CCs). They demonstrated that their method increased the proliferative activity of murine ESCCMs and hiPSCCMs. Carpenter *et al.* [20] also conducted a study with hiPSCs and described a protocol that resulted in efficient cardiac differentiation after just 14 days. Authors have recommended the use of a human cardiac extracellular matrix for the cardiac differentiation of PSCs towards a cardiomyocyte phenotype [64]. Mauritz *et al.* [65] differentiated murine iPSCs into cardiomyocytes with the use of a standard EB-based differentiation protocol for ESCs. Functionally, the cells created were similar to ESCCMs. In most of the tests, iPSCCMs were almost equivalent to ESCCMs in terms of the expression of typical markers, for instance of endoderm and mesoderm, cardiac mesoderm, or cardiomyocytes.

Molecular and cellular targets for cardiac regeneration

miRNA, MMPIs, macrophages, and exosomes

In most cases of heart disease, cardiomyocytes are unable to regenerate naturally because the human heart lacks regenerative capacity. Chen *et al.* [66] investigated the role of the miR-17–92 cluster in cardiomyocyte proliferation under pathological conditions in normal healthy and damaged mouse hearts. They observed the decreased proliferation of cardiomyocytes in embryonic and postnatal hearts of miR-17–92-knockout (KO) mice. This suggests that deleting the miR-17–92 cluster reduces cardiomyocyte proliferation. Furthermore, the authors found that the heart could be protected from injuries resulting from a heart attack or MI by the addition of miR-17–92. As discussed above, miR-19 is member of the miR-17–92 cluster, which is required to induce cardiomyocyte proliferation [66]. These results highlight miRNAs in the heart as targets for reducing the risk of developing MI or chronic heart failure.

Inhibition of matrix metalloproteinases (MMPs) using MMP inhibitors (MMPIs) is one of the best-validated clinical targets for heart repair. Over more than three decades, several drugs have been designed as MMPIs, although none have reached clinical application because of dose-limiting adverse effects in clinical trials. Brendan *et al.* [67] investigated the electrostatic interactions of sugars with MMPIs using a microdialysis technique to design an injectable and bioresponsive hydrogel that could be used to overcome these adverse effects. The inhibitors are physically held within the polysaccharide-based hydrogel by interactions of sugars and the injectable hydrogel is designed in such as way that inhibitors are released from the hydrogel only on demand. Thus, when heart damage occurs, the secretion of specific enzymes increases and these enzymes break down the cross-linking bonds between the hydrogel and MMPIs, releasing the MMPIs that then inhibit MMPs [67]. The Meis1 homeodomain transcription factor is involved in the embryonic development of several organs, including the heart. Mahmoud *et al.* [68] demonstrated a role of Meis1 in the regeneration of hearts of newborn and adult mice. The authors observed the regeneration of hearts of newborn mice, even after deleting Meis1, suggesting that neonatal hearts have a regenerative capacity. Although the adult mouse heart has lost this regenerative capacity, it can be reactivated without any harmful effects on cardiac function by adding Meis1. Therefore, Meis1 could be a new therapeutic option for adult heart regeneration.

The sarcoplasmic reticulum Ca^{2+} ATPase (SERCA2a) regulates the flow of calcium within heart muscle cells and decreased

TABLE 1

Cardiomyocyte differentiation of different types of induced pluripotent stem cells and adult stem cells[a]

Type of stem cell	Cell density and/or expansion medium	Cell density and/or differentiation medium	Differentiation strategy	Extracellular matrix and/ or biomaterials	Serum	Small molecules	Significant results	Cardiac features	Refs
Human									
iPSC: IMR90 C1 and C4; foreskin C1 and C2; ESCs (H1 and H9)	19,500 cells/cm^2; DMEM/F12 (20% KO serum replacement, 0.1 mmol/L NEAA, 1 mmol/L L-glutamine, 0.1 mmol/L β-ME); 100 ng/ml bFGF for iPS, 4 ng/ml human recombinant bFGF for hESCs	13,000 cells/cm^2; EB20 (80% DMEM/F12, 0.1 mmol/L NEAA, 1 mmol/L L-glutamine, 0.1 mmol/L β-ME, 20% FBS)	Day 1–4, MEFs; day 5–8, ultra-low attachment plates; day 8–18, EB20 medium; from day 19 onwards, EB2 medium	MEFs for 3–4 days, ultra-low attachment plates for 4 days	20% FBS day 1–10; 2% FBS in day 11	bFGF	iPSCs showed similarities to ESCs in upregulation of cardiac genes and electrical activity	RT-PCR: NKX2-5, TNNT2, MYH6 ACTN2, MYL7, MYL2, HPPA, PLN; APs: 33-44 beats per minute; IF staining: cTnT, MLC2v, α-actinin, MLC2a, MF20 antibody	[32]
iPSC (253G1)	MEF-CM with 10 ng/ml bFGF; 6×10^5 cells/cm^2 in DMEM with 10% FBS, 2 mM L-glutamine and 1% NEAA added to tissue culture dishes (with 0.5% gelatin); after 1 day: ESC medium (80% KO DMEM, 20% KO serum replacement, 1% NEAA, 1 mM L-glutamine, 0.1 mM β-mercaptoethanol and 5 ng/ml bFGF)	Bioreactor: 2×10^7 cells resuspended in 100 ml mTeSR1, seeded into 250-ml stirred bioreactor; after 1 day: mTeSR1 without Y27632 StemPro34 medium (50 ng/ml ascorbic acid, 2 mM L-glutamine and 400 μM 1-thioglycerol)	Cardiac differentiation in bioreactor: day 1–3, mTeSR1; from day 4 onwards, StemPro34 medium; day 3–4, 0.5 ng/ml BMP4; day 4–7, 10 ng/ml BMP4, 5 ng/ml bFGF, 3 ng/ml activin A; day 7–9, mikroM IWR-1(Wako); after day 9, 5 ng/ml VEGF and 10 ng/ml FGF; days 4, 7, 9, 11,14: culture medium exchanged in monolayer: hiPSCs in MEF-CM treated with Versene^{TM} for 7–10 min, 1×10^5 cells/cm^2 in MEF-CM with 5 ng/ml bFGF and 10 MM Y27632 3 days before cardiac induction. Cardiac induction: medium changed to RPMI 1640 with B27 supplement without insulin growth factors; day 0–1, 100 ng/ml activin A; day 1–4, 10 ng/ml BMP4 and 10 ng/ml bFGF	Bioreactor: agitation rate, 40 rpm dissolved oxygen 40% with air, oxygen, or nitrogen; pH 7.2 by CO_2 addition, temperature 37°C	100 ml mTeSR1	Activin A; BMP4; bFGF; VEGF	Cardiac differentiation of ~80% hiPSCs; developed suspension culture bioreactor system for myocardial differentiation	Immunocytochemistry: bioreactor: cTnT, Nk x 2.5, SM22, CD31, TRA-1 60. Monolayer culture: cTnT, sarcomeric a-actinin. Electrophysiological analysis: spontaneous and synchronous beating of cardiomyocytes, electrophysiological connections between cardiac cell sheets	[33]
iPSC from human dermal fibroblasts	Maintained on mitomycin C-treated-MEF feeder in hESC medium: 80% KO DMEM, 20% serum replacement, 1% NEAA, 1 mML-glutamine, 0.1 mM beta-ME and 4 ng/ml bFGF	CARM/SB differentiation procedure: CARM (DMEM high glucose 485 ml, L-glutamine 5 ml, NEAA 5 ml, selenium transferrin 5 ml and 2-ME 3.5 ml) completed with SB 203580 (5 mM), a specific p38-MAPK inhibitor; DMEM medium with 2% FBS. EB 20 method: 4% PFA and permeabilised with 0.1% Triton X-100	CARM/SB differentiation procedure: day 1, EBs formed mechanically from hESC/hiPSC colonies, cultured in hESC medium without bFGF for 24 hours; day 2–6, CM differentiation: serum-free and insulin-free medium, CARM; day 6: differentiation medium changed, day 15–21: EBs plated on 0.1% gelatin-coated plate or petri dishes in DMEM medium with 2% FBS. EB 20 method: on day 8, EBs plated before contracting EBs emerged; day 15, EBs fixed with 4% PFA, permeabilised with 0.1% Triton X-100 and co-stained with polyclonal antibody against human cardiac MLC	Gelatine; 4% PFA; 0.1% Triton X-100	2% FBS	Polyclonal antibody against human cardiac MLC	Functionally competent CMs and MSCs co-generated from hiPSCs	IF staining: sarcomeric α-actinin, β-MHC, Titin; percentage of CMs: 22.03%; electrophysiological analysis, whole-cell AP recorded	[35]
iPSCs (201B7)	Undifferentiated iPSCs cultured with a mitomycin C-inactivated MEF feeder layer in DMEM/F-12 medium (with 20% KO serum replacement, 2 mM L-glutamine, 0.1 mM NEAA, 0.11 mM β-ME, 50 U/ml penicillin, 50 mg/ml streptomycin, 4 ng/ml bFGF)	DMEM/F-12 supplemented with 20% FBS, 2 mM L-glutamine, 0.1 mM NEAA, 0.11 mM β-mercaptoethanol, 50 U/ml penicillin, 50 mg/ml streptomycin	hiPSC colonies: dispersed into small clumps using CTK dissociation solution; transferred to suspension culture for 4 days; EBs plated on 0.1% gelatin-coated culture dishes. To start differentiation, DMEM/F-12; medium replaced every 2–4 days	Gelatine	20% FBS	FGF	HiPSCs differentiated into beating CMs; functional cardiac ion channels found in hiPSCCMs; variation in AP waveforms similar to clinically relevant pharmacological responses	RT-PCR: MYH6, MYL2, TNNT2, SCN5A, CACNA1C, CACNA1D, KCNH2, KCND3, KCNQ1, KCNJ2, KCNJ12, HCN4	[36]
iPSCs: IMR90, KS1 (KEVIN-SIU). hESC: H7, HES3	Undifferentiated cells on Matrigel-coated dishes with mTeSR medium	StemPro®-34 medium (with 2 mM glutamine 4 mM monothioglycerol, 50 mg/ml ascorbic acid, 0.5 ng/ml BMP4)	Cells dissociated into clumps using 1 mg/ml dispase; cultured in suspension with low-attachment plates to form EBs; EBs transferred onto gelatin-coated plates in StemPro-34 medium; medium added on post-plating day 1–4, 10 ng/ml BMP4, 5 ng/ml bFGF, 3 ng/ml activin A; day 4–8, 150 ng/ml DKK1, 10 ng/ml VEGF; day 8–21: 150 ng/ml DKK1, 10 ng/ml VEGF, 5 ng/ml bFGF	Gelatine; low attachment plates	mTeSR	BMP4, bFGF, activin A, DKK1, VEGF	HiPSC-derived cardiomyocytes hold functional but immature SR; calcium handling properties of hiPSC-derived CMs relatively immature compared with hESCs	Electrophysiological analysis: spontaneous beating outgrowths, spontaneous rhythmic transients. Immunocytochemical analysis: α-actinin, tropomyosin. RT-PCR: lower expression of α-MHC, β-MHC, Nkx2.5; triadin, junctin, RyR2 and SERCA2a in hiPSCCMs compared with hESCCMs	[37]

TABLE 1 (*Continued*)

Type of stem cell	Cell density and/or expansion medium	Cell density and/or differentiation medium	Differentiation strategy	Extracellular matrix and/or biomaterials	Serum	Small molecules	Significant results	Cardiac features	Refs
hESC: H9; hiPSC	H9 cells in 79% DMEM/F-12 (with 20% KO serum replacement, 2 mM L-glutamine, 1% MEM-NEAA solution, 0.1 mM β-mercaptoethanol and 4 ng/ml bFGF)	DMEM (with 20% foetal bovine serum, 0.1 mM β-mercaptoethanol, 2 mM glutamine, and 1% MEM-NEAA solution)	Human ESC and hiPSC colonies digested by collagenase type IV, EBs formed in suspension in DMEM; after 6 days: 20–30 EBs transferred to 0.1% gelatin-coated 100 mm tissue culture, switched to differentiation medium (DMEM with 10% FBS); day 1–3 after EB attachment: cells treated with 10 mM 5-Aza in DMEM with 10% FBS; to test effect of BMP-2: treating EBs with 25 ng/ml BMP-2 in DMEM with 5% FBS; to test effect of DMSO: EBs treated with 0.25% DMSO after 2–3 days in suspension; to dissociate them into single CMs: cultures incubated with 1 mg/ml collagenase A	Gelatin	20% FBS; 10% FBS after 6 days in suspension; 5% FBS	bFGF; collagenase type IV; 5-AZA; BMP-2 DMSO; collagenase A	Functional differentiated cardiomyocytes from hiPSCs under spontaneous and reagent-induced conditions; adequate response to cardiac drugs; 5-Aza good inducer of cardiomyocyte differentiation	FACS: 4.7% of dissociated cells TnT-positive, treated with 5-AZA: 23.7% of cells TnT-positive; RT-PCR: α-MHC, β-MHC, MLC-2a, MLC2v, ANF, GATA-4, NKx2.5	[38]
iPSCs	iPSCs from clones 1 and 2: grown on inactivated MEF feeders	80% DMEM, 20% FBS, 1 mmol/l L-glutamine and 1% NEAA stock	To induce EB formation: iPSCs detached (using 0.2% type IV collagenase), suspended in Petri dishes; EBs grown in 80% DMEM, 20% FBS, 1 mmol/l L-glutamine and 1% NEAA stock; EBs cultured in suspension for 7 days; plated on 0.1% gelatin-coated plates	Gelatin; NEAA	20% FBS	Type IV collagenase; L-glutamine	iPSCCMs: cardiac-specific RNA and proteins identified; negative force–frequency relations and mild (compared with adult) post-rest potentiation; responded to ryanodine and caffeine; expressed SR-Ca^{2+} handling proteins ryanodine receptor and calsequestrin	RT-PCR: Tbx5, Tbx20, cardiac troponin T, α-cardiac actin. IF staining: α-sarcomeric actinin, cardiac troponin I, myosin heavy chain. Electrophysiological analysis: negative force–frequency relations, positive post-rest potentiation	[40]
hDMSCs	DMEM, with 10% FBS, 1% penicillin-streptomycin, 1 μl/ml insulin, 2 μl/ml glutamine; cultured at 37°C with 5% CO_2 in CO_2 incubator, fresh media fed daily	1×10^4 cells in 65-mm culture dishes	Start of cardiac differentiation: 1×10^4 cells in 65-mm culture dishes; three batches: two treated with 10 μM and 20 μM of 5-Aza, third untreated as control group; three sets of treatments: 48-h treatment, 4 days, and 8 days treatment; after set time period: cells maintained in normal growth media	–	10% FBS	10 μM and 20 μM of 5-Aza; 1% penicillin streptomycin, 1 μl/ml insulin	hDMSCs differentiated into cardiomyocytes using 5-Aza	PCR: 5-Aza-treated hDMSCs: α-cardiac actin, β-MHC, cardiac troponin T; untreated cells: α-cardiac actin. Phase-contrast micrographs: day 14 after hDMSCs treated with 10 μM 5-Aza for 48 hours: long elongated tube-like cells; day 14 of hDMSCs treated with 20 μM 5-Aza for 48 hours: CM-like cell elongations and cytoplasmic granularity	[42]
MiPSCs	hESC culture media containing KO DMEM (with 20% KO serum, 1 mM L-glutamine, 0.1 mM mercaptoethanol, 1% NEAA solution, 10 ng/ml bFGF)	RPMI-1640-based serum-free induction media	MiPSCs dissociated using TryLE Express, adapted onto a 1:400 Geltrex-coated culture surface; single cells passaged every 3 days; EB-formation in 96-well plate with 25 ng/ml BMP4, 5 ng/ml bFGF in a RPMI-1640-based serum-free induction media for 2 days, then in 10% FBS in ultra-low cluster plates; on day 4, EBs adhered on Matrigel-coated plate, fed with 1% FBS in RPMI-1640-based media; medium changed every 3 days	Geltrex-coated culture surface, ultra-low cluster plates, Matrigel-coated plates	20% KO serum; 10% FBS, 1% FBS	L-Glutamine, medium NEAA solution, bFGF, BMP4	MiPSCs differentiated into cardiomyocytes; high expression of cardiac genes	Immunohistology: cTnT, connexin 43, a-sarcomeric actin. Atomic force microscopy: maximal contractile force of each beat comparable to that of native cardiomyocytes ($10^{-0.4} \times 10^{-0.6}$ nN). FACS: MiPSCs retained c-kit (CD117) cell surface marker (MiPSCs+)	[47]

Human ASCs	DMEM-lg, 10% FCS, 1% antibiotic/antimycotic solution	50,000 cells/well modified cardiomyogenic medium (DMEM-lg, 10% FCS, 1% antibiotics, 1.0 mg/ml insulin, 0.55 mg/ml transferrin, 0.5 mikrog/ml sodium selenite, 50 mg/ml BSA, 0.47 mikrog/ml linoleic acid, 10^{-4} M ascorbate, 10^{-9} M dexamethasone)	Day 1, seeding; day 2, cells washed with PBS twice; 5-Aza treatment: incubated in media containing 5-Aza at 10 mmol/l for 1 day, washed three times with PBS; cultured in control medium for 3 weeks. Medium changed 2–3 times/week; modified cardiomyogenic medium: cultured in MCM for 3 weeks; TSA treatment: in first group, ASCs cultured for 1, 2 and 3 weeks after 24-hour exposure to TSA at beginning or with continuous exposure; second group, cells treated with 100 ng/ml TSA for 1 week, washed three times with PBS, cultured in control medium or CCM for 2 weeks. Co-culture system with neonatal rat CMs: (i) ASCs and neonatal rat CMs co-cultured 1:10; semi-permeable membranes allowed diffusion of secreted factors; control group: ASCs co-cultured with ASCs; (ii) direct co-culture: ASCs and neonatal rat CMs co-cultured 1:5 or 1:10 with direct cell interactions between two cell populations; neonatal CMs seeded 1 day before ASCs and co-cultured in CCM. control group: ASCs cultured in CCM	–	10% FCS	5-Aza, antibiotics, insulin, transferrin, sodium selenite, BSA, linoleic acid, ascorbate dexamethasone, TSA	No success in using 5-Aza to induce cardiomyogenic gene and protein expression; MCM and TSA induced partial differentiation to CLCs, but no spontaneous contraction identified. Only direct co-culture system induced ASCs to contract spontaneously, some hASCs formed gap junctions with CM and showed spontaneous Ca^{2+} oscillations from sarcoplasmic reticulum	RT-PCR: TSA treatment: cardiac actin mRNA, cardiac proteins (cMHC, α-actin, cTnI). Immunocytochemistry: MCM treatment: Nkx2.5, α-actin, TnI, cMHC, MyoD; TSA treatment: α-actin, cTnI, Cx43. Co-culture with direct cell-to-cell contact: GATA4, Nkx2.5, α-actin, TnI, cMHC, no MyoD. Calcium imaging with fluorescent Ca^{2+} indicator Fluo-4 AM: hASC showed synchronous Ca^{2+} transient and contraction synchronous with surrounding rat cardiomyocytes	[48]
ASCs	1×10^5 cells/cm^2 DMEM (10% FBS, 100 U/ml penicillin, 100 mg/ml streptomycin, 2 mM L-glutamine)	50,000 cells per well, each coated with 2.5 mg/cm fibronectin or 0.12 mg/cm laminin or left uncoated, in normal culture medium. DMEM 1 (15% FBS) DMEM 2 (15% FBS, 100 U/ml penicillin, 100 mg/ml streptomycin, 2 mM L-glutamine and 1% ITS + premix)	Culture-expanded cells plated into culture dishes, cultured in DMEM 1, when 50–60% confluent, stimulated with 5-Aza-2-deoxycytidine (9 mM) for 24 hours in DMEM 2	Fibronectin-coated culture dishes, laminin-coated culture dishes	10% FBS, 15% FBS	Penicillin, streptomycin, L-glutamine, 1% ITS + premix, 5-Aza-2-deoxycytidine	High percentage of human ASCs differentiated towards cardiomyocytes; laminin encouraged late ASC differentiation	RT-PCR: MLC-2α, α-actinin, desmin, Serca-2α. Immunocytochemical staining: MLC-2α, α-actinin, desmin, Troponin	[50]
Human BM mononuclear cells (MNCs)	a-MEM (20% FBS)	a-MEM (10% FBS) 20,000 cells/100 ml; RPMI 1640 medium (10% FBS, antibiotics, 2 mM $CaCl_2$); EX (1 mg/ml) containing ATP-regenerating system (1 mM ATP,10 mM creatine phosphate, 25 mg/ml creatine kinase)	5-Aza treatment: hMSCs treated with different concentrations of 5-Aza at 3, 5 or 10 mM in a-MEM (10% FBS) for 24 hours; medium changed every 3 day; 10 mM 5-AZA and hMSCs (3000/cm^2) from third passage (12 day) optimal conditions for inducing differentiation; SLO + EX treatment: (a) cell permeabilisation: hMSCs washed in cold PBS, resuspended in cold Ca^{2+}-and Mg^{2+}-free HBSS; cells placed in 1.5-ml tubes and centrifuged for 5 min; sedimented cells suspended in 15.5-ml HBSS, tubes placed in H_2O bath for 2 min, 4.5 Ml SLO added to yield final SLO concentration of 57.5, 115, and 230 ng/ml; samples incubated for 50 min, SLO diluted with 200 Ml HBSS, cells sedimented for 5 min. (b) Incubation of hMSCs with EX: cells in 20 ml EX (1 mg/ml),100 MM GTP, 1 mM of each NTP; cells incubated for 1 hour; cells diluted with RPMI 1640 medium; cells transferred to culture flasks; medium changed to remove $CaCl^2$; cells cultured with a-MEM (20% FBS)	–	20% FBS, 10% FBS	5-AZA, HBSS, neonatal rat cardiomyocytes extract containing an ATP-regenerating system, GTP, NTP; SLO	Upregulation of cardiomyocyte-related genes, EX+ SLO-treatment is possible riskless alternative to 5-Aza	IF staining: sarcomeric α-actinin, connexin-43, GATA-4, SERCA-2, cardiac Troponin I, β-MHC, Nkx2.5, cardiac desmin, MLC-2v, MLC-2a; RT-PCR: β-actin, β1-adrenergic receptor, hemi-nested β1-adrenergic receptor, MLC-2a, hemi-nested MLC-2a, cardiac Troponin T	[52]
hUMSCs	Culturing medium (500 ml basal medium, 25 ml FBS, 5 ml mesenchymal stem cell growth supplement, 5 ml penicillin/streptomycin solution)	1×10^3 cells/cm^2 DMEM + 10% FBS CMCM	hUMSCs plated on polylysine-coated coverslips in DMEM + 10% FBS, grown to adherence; cultured in different conditional mediums including CMCM plus 1 mM S1P or CMCM or DMEM + 10% FBS plus 1 mM S1P; medium changed every 3 days	Polylysine-coated coverslips	25 ml FBS, 500 ml basal medium 10% FBS	MSC growth supplement, penicillin/streptomycin, S1P	S1P amplified differentiation of hUMSCs towards functional cardiomyocytes	Immunocytochemical analysis and patch clamping: MHC, sarcomeric α-actinin; only cells in CMCM + S1P culture condition presented cardiomyocyte-like AP and voltage-gated currents	[53]

TABLE 1 (*Continued*)

Type of stem cell	Cell density and/or expansion medium	Cell density and/or differentiation medium	Differentiation strategy	Extracellular matrix and/or biomaterials	Serum	Small molecules	Significant results	Cardiac features	Refs
ASCs	DMEM (with 10% FBS)	DMEM (with20% FBS and 20 ng/ml IGF-1) 50,000 cells/ml	Indirect co-culture: for 2 weeks: ADSCs and CMs vaccinated at 1:5 in 2 chambers separated by cell culture inserts with semipermeable membrane (pore size 0.4 lm); CMs in upper chamber, ADSCs in the lower; media replaced every 3 days direct co-culture: ADSCs labelled with CFSE; labelled human ADSC and CMs mixed at ratio of 1:5 in DMEM for 2 weeks	–	10% FBS, 20% FBS	20 ng/ml IGF-1, carboxy-fluorescein succinimidyl ester	ADSCs differentiated into CLCs; specific cardiac markers more highly expressed in direct co-culturing compared with indirect co-culturing	Immunocytochemical analysis: MHC, troponin-I, connexin 43. Flow cytometry: expression ratios of MHC, TnI, and Connexin 43, 30–40% in direct co-culturing, 18-25% in indirect co-culturing. Western blot: connexin43, TnI. RT-PCR: a-skA, β-MHC, TnI, Cx43, ANP, GATA-4, and Nkx2.5	[54]
hFib2-iPSCs	Cultured on mitotically inactivated MEF feeder layer; 80% KO high-glucose glutamine-free DMEM with sodium pyruvate (with 20% serum replacement, 1 mmol/L L-glutamine, 0.1 mmol/L mercaptoethanol, 4 ng/ml human recombinant bFGF, 1% NEAA acid stock)	–	HiPSCs dispersed into small clumps with collagenase IV (1 mg/ml for 20 min); transferred to plastic Petri dishes, cultured in suspension for 10 days; EBs plated on 0.1% gelatin–coated culture dishes	Gelatin-coated culture dishes, MEF feeder layer	20% serum replacement	Sodium pyruvate, L-glutamine, L-ME, human recombinant bFGF, NEAA stock, collagenase IV	Differentiated cells had molecular, structural and functional features specific to cardiac cells	RT-PCR: Isl-1, Nkx2.5, Mef-2c, Gata-4, α-MHC, β-MHC, cardiac troponin-I, ion channel proteins (Cav1.2, Cav1.3, KCNH2, HCN-2) Immunostaining: cardiac troponin-I, sarcomeric α-actinin. Semiquantitative RT-PCR: NKX2.5, MEF-2c, and GATA-4, MLC-2v, MYH6, MYH7, cTNNI, ion channel proteins (Cav1.2, Cav1.3, KCNH2, HCN-2). Chronotropic responses and pharmacological studies: hiPSC-derived cardiac tissue can respond appropriately to adrenergic and muscarinic signals	[60]
Human iPSCs (6-9-9 and 19-9-11), lentiviral integrated human iPSC (IMR90C4), hESCs (H9, H13, H14)	Cells maintained on MEF feeders in hESC medium: DMEM/F12 culture medium (with 20% (vol/vol) KO serum replacer, 0.1 mM nonessential amino acids, 1 mM L-glutamine, 0.1 mM β-mercaptoethanol, 10 ng/ml human bFGF, conditioned medium (hESC medium conditioned by MEFs for 24 hours), feeder-free culture: hiPSCs maintained on Matrigel or Synthemax plates in mTeSR1 medium	Cardiac differentiation via EBs: ~13,000 cells/cm^2 hESC medium, RPMI plus 20% (vol/vol) KO serum replacer, RPMI20 (RPMI plus 20% FBS), RPMI2 (RPMI plus 2% FBS), cardiac-directed differentiation using activin A and BMP4: mTeSR1, 100,000–200,000 cell/cm^2, Matrigel-coated cell-culture dish at 100,000–200,000 cell/cm^2 in mTeSR1 [with 5 mM ROCK inhibitor (Y-27632)]	Cardiac differentiation via EBs: hiPSCs passaged onto MEFs, hESC medium for 2 days, another 3 days in hESC medium (with BIO or CHIR99021) to form EBs, hiPSC cell aggregates (dispase treatment) cultured in low-attachment plates overnight in RPMI plus 20% (vol/vol) KO serum replacer; EBs cultured in RPMI20 for 4 days in suspension; EBs plated onto 0.1% (wt/vol) gelatin-coated plates at 50–100 EBs per well, cultured in RPMI20 medium; after 10 days, FBS concentration reduced to 2% (vol/vol) RPMI2 cardiac-directed differentiation using activin A and BMP4: hiPSCs on Matrigel in mTeSR1 dissociated into single cells with Accutase, seeded onto Matrigel-coated cell-culture dish (day 5) for 24 hours; cultured in mTeSR1, changed daily. Day 0: treated with 100 ng/ml activin A in RPMI/B27-insulin; after 24 hours, medium changed to RPMI/B27-insulin (with 5 ng/ml BMP4) for 4 days; day 5: medium changed to RPMI/B27-insulin; day 7: cells transferred to RPMI/B27, medium changed every 3 days; When Gsk3 inhibitors used to stimulate CM differentiation, cells cultured in mTeSR1 containing BIO or CHIR99021; cardiac-directed differentiation via small molecules: cells dissociated, plated as in activin/BMP4 protocol; when hiPSCs achieved confluence, cells treated with CH in RPMI/B27-insulin for 24 hours (day 0 to day 1); medium changed to RPMI/B27-insulin, treated with 2 mg/ml dox at different times between day 1 and day 5 for transgenic cell lines; for genetically unmodified lines, 5 mM IWP2 or IWP4 added at day 3, removed during medium change on day 5; cells maintained in RPMI/B27 starting from day 7, medium changed every 3 days	Low-attachment plates	20% KO serum replacer, 20% FBS, 2% FBS	NEAA, L-glutamine, β-ME, human bFGF, Accutase, ROCK inhibitor (Y-27632), activin A, RPMI/B27-insulin, BMP4, dox, IWP2 or IWP4	Generation of cardiomyocytes from various hiPSC lines possible only by using regulatory elements of Wnt/β-catenin signalling and when applied at correct time	IF staining: Isl1 and Nkx2.5. Flow cytometry and immunofluorescence: cTnT. RT-PCR: ACTB, POU5F1, NANOG, MIXL1, T, ISL1, NKX2-5, GATA4, MEF2C, TBX5, TBX2, TNNI2, TNNI3, PLN, MYL7, MYL2, WT1	[61]

H1 and RUES2 human ESCs; L1 iPS and L2 iPS6 hiPSC lines	Cells maintained on mouse embryonic fibroblasts	Basal differentiation medium, EGM2 and SmGM2 medium	To generate CMs and SMCs: day 6 EBs pre-induced with VEGF A (10 ng/ml) and DKK1 (150 ng/ml) from day 4, dissociated and the low-KDR, c-kit-neg. multipotent cardiovascular progenitors isolated, cultured as a monolayer for 14 day with VEGF (10 ng/ml) and DKK1 (150 ng/ml) before FACS selection; CD166(+) population cultured with basal differentiation medium. CD166(-) population cultured with SmGM2 medium. To generate ECs and SMCs: day 6 EBs pre-induced with VEGF (10 ng/ml) and bFGF (10 ng/ml) from day 4, dissociated, MCPs isolated and cultured as a monolayer for 14 days with VEGF (20 ng/ml) and bFGF (20 ng/ml) before FACS selection. CD31(+) and CD31(-) populations cultured with EGM2 and SmGM2 medium	–	–	VEGF A, DKK1, bFGF	Cardiovascular cell types with high efficiency and high pureness	Quantitative PCR: NKX2.5, cTNT, MLC2A,IRX4, SMA, calponin, CD31, CD166. Immunostaining: CTNT, α-actinin, and gap junction protein CX43), CD166 and SIRPA. Electrophysiological analysis: AP dynamics and intracellular Ca^{2+} handling in hiPSCCMs functionally similar to that of primary cardiomyocytes and suggest potential of iPSCCMs for drug toxicity testing and patient-specific drug screening. FACS: cardiomyocytes with high purity (>90%) by FACS selection of mitochondrial fluorescent dye-labelled cardiomyocytes	[62]
HiPSC line (253G1), murine ESCs	Maintained on feeder layer of mitomycin-C-treated mouse embryonic fibroblasts in primate ES medium (with 4 ng/ml recombinant human bFGF)	StemPro34 (with 2 mM glutamine, 4×10^{-4} M monothioglycerol, 50 mg/ml ascorbic acid)	To induce differentiation: colony isolated in dissociation solution, formed EBs in suspension culture in low cell binding dishes in basic media StemPro34; following cytokines used at relevant differentiation stage: day 0–1, BMP4 (0.5 ng/ml); day 1–4, BMP4 (10 ng/ml), bFGF (5 ng/ml), and activin A (3 ng/ml); day 4–8, DKK1 (150 ng/ml), VEGF (10 ng/ml); and after d 8, VEGF (10 ng/ml), DKK1 (150 ng/ml), bFGF (5 ng/ml); medium replaced every 3–4 days, hiPSCCMs cultured until day 20–30, 50–60, and 80–90 of differentiation (d30CMs, d60CMs, and d90CMs, respectively)	–	–	bFGF glutamine, monothioglycerol, ascorbic acid, BMP4, activin A, DKK1, VEGF	Murine ESCs and human iPSCs differentiate into cardiomyocytes; thin glass pipette used to preserve cardiomyocyte-rich beating cell clusters	RT-PCR: OCT3/4 in undifferentiated hiPSCs but not in d30-CMs, d60-CMs, or d90-CMs; Nkx2.5, MYH6 in d30-CMs, d60-CMs, and d90-CMs but not in undifferentiated hiPSCs. IF staining: GATA4, cardiac actin, cTnT, MYH6, MLC2. Electrophysiological analysis: beating rate 20-60/min; β-adrenergic function comparable in all stages of differentiation. EM myofibrillar structures at days 60 and 90 similarly distributed and more mature than that at day 30	[63]
iPSCs	iPSCs washed in DMEM/F12 basal media	Stem Pro-34medium [with 2 mM L-glutamine, 1% PenStrep (PAA), 400 μM monothioglycerol, 50 μg/ml ascorbic acid]	IPSCs differentiated as a monolayer, in Stem Pro-34 medium, Stem Pro-34 basal media further supplemented with 50 ng/ml activin A for 4 hours; 10 ng/ml BMP4, 5 ng/ml bFGF and 5 ng/ml activin A for 44 hours; full media change with fresh cytokines made on day 2 for 48 hours; cells incubated in Stem Pro 34 basal media alone, with no added cytokines, from day 4 to 14	–	–	L-Glutamine, PenStrep (PAA), monothioglycerol, ascorbic acid, activin A, BMP4, bFGF	Efficient cardiac differentiation after just 14 days	RT-PCR: Goosecoid, Brachyury, Mix1, and Mesp1. IHC: troponin I, α-actinin, and SMA. FACS: ~40% positive for troponin I, 36% for α-actinin, SMA ~6%, CD31 ~1.6%	[20]
Human and mouse								
iPSCs: iPSC-MEF-S-6 (mouse); hESC D3-ES (human)	Cells cultured on mitomycin C-treated STO cells in DMEM medium (20% FBS, 1000 U/ml leukaemia inhibitory factor, 1% NEAA, and 0.55 mM β-mercaptoethanol)	1×10^6 cells/10 ml, microvascular EBM-2 20% DMEM medium	4–5 days: cultured ES or iPSC colonies trypsinised (0.025%), suspended at 1×10^6 cells in 10 ml 20% DMEM in bacteriological dish to induce EB formation; After 4 days: EBs transferred to EBM-2 medium for 4 day; day 8: EBs plated onto 0.1% gelatin-coated tissue culture dishes, 20% DMEM medium for 12 day; in each culture condition, medium replaced every 2 days; preparation of single CMs: treatment with collagenase B	Gelatin	20% FBS	Collagenase B	Improved efficiency of cardiomyocyte differentiation from iPSCs using EBM-2 medium during late EB stage; presence of Ca^{2+} channels, K^+ or Na^+ currents in single iPSCCMs	RT-PCR: GATA4, GATA-binding protein 4; ANF, α1S, L-type calcium channel α1S; α1C, L-type calcium channel α1C; α-MHC; β-MHC. Immunocytochemistry: sarcomeric α-actinin, myosin heavy chain, troponin 1. Electrophysiological analysis: 44.8% contracting EBs from iPS-S-6 cells, D3-ES-cells only 33.3%	[39]
Mouse $ES^{Isl1\text{-}Cre;\ Rosa\text{-}YFP}$, $ES^{Isl1\text{-}Cre;\ Rosa\text{-}RFP}$ cells harbouring $Isl1^{Cre}$; $Rosa^{YFP}$ or $Rosa^{RFP}$; human ESCs (H9), mouse $iPS^{Isl1\text{-}Cre;\ Rosa\text{-}YFP}$ cells	Mouse ES: derived on irradiated MEF in KO DMEM (with 15% FBS, 0.1 mM NEAA, 2 mM GlutaMAX, 0.1 mM sodium pyruvate, 0.1 mM 2-ME, 100 U/ml LIF, 3 MM CHIR99021, 1 MM PD0325901; human ESCs: on Matrigel-coated cell culture plastic, MEF-conditioned KO DMEM (with 20% KO serum replacement, 8 ng/ml human bFGF)	IMDM/Ham-F12 (3:1) with N2, B27, penicillin/streptomycin, 2 mM GlutaMAX, 0.05% BSA, 5 ng/ml L-ascorbic acid, α-monothioglycerol; 75,000 cells/ml. StemPro34 (with 10 ng/ml L-ascorbic acid, penicillin/streptomycin and 2 mM GlutaMAX)	ESC/iPSCs and End2 cells dissociated to single cells, plated on ultra-low attachment plastic surface in IMDM/Ham-F12 (3:1), final concentration: 75,000 cells/ml; medium changed after 3 days of co-culture; for human ESCs, Rock inhibitor (Y27632) added to enable survival of cells in single cell suspension; for cardiac differentiation: CPCs from co-cultures purified by FACS, plated on gelatin-coated cell-culture plastic in StemPro34	Irradiated MEF Matrigel-coated cell culture plastic, ultra-low attachment plastic, gelatin-coated cell-culture plastic	15% FBS, 20% KO serum replacement, 0.05% BSA	Amino acids, GlutaMAX, sodium pyruvate, 2-ME, LIF, CHIR99021, PD0325901, human bFGF, N2, B27, penicillin, L ascorbic acid,α-monothioglycerol, Rock inhibitor (Y27632)	Co-aggregation method is simple and efficient alternative to induce cardiac progenitor cells	Quantitative PCR: H9 hES: *TBX5*, *GATA4*, *NKX2.5*, *ISL*, *ETV2*, *ACTC1*, *MYH6*; mouse ES and iPSC lines: Nkx2.5, Isl1	[58]

TABLE 1 (*Continued*)

Type of stem cell	Cell density and/or expansion medium	Cell density and/or differentiation medium	Differentiation strategy	Extracellular matrix and/ or biomaterials	Serum	Small molecules	Significant results	Cardiac features	Refs
Mouse									
iPSCs	SC-Medium (DMEM/high glucose, 15% foetal bovine serum, NEAA, sodium pyruvate, Glutamax-I, β-mercaptoethanol, gentamicin, and LIF)	10^7 iPSCs differentiation medium (same formula as SC-Medium without LIF)	10^7 iPSCs in 30 ml differentiation medium; day 2: ascorbic acid (100 mg/ml) added; day 6–9: puromycin added for selection of iPSC-derived cardiac progenitors	–	15% FBS	Puromycin (5 mg/ml, Invivogen)	Significant upregulation of cardiac markers	Electrophysiological analysis: synchronous spontaneous beating at 1–2 Hz. IF staining: Actn2, Tnnt2, Myh6, Myl2, cKit positive cells, Myl7, Myh7, Nkx2-5, Tbx5, Mef2c, Myocd; late but significant upregulation in expression levels of ATP2a2, Cacna1c, Casq2, Hcn4, Kcnj2, Kcnj3, Pln, Ryr2, and Slc8a1	[34]
BMSC	3×10^3 cells/cm^2 in 100 mm dish; cells cultured in MesenCult® MSC basal medium	Cells cultured in MesenCult® MSC basal medium	Cardiomyogenic differentiation: 1 mM ATRA added to culture medium every 3 days for 21 days	All-trans retinoic acid	–	–	BMSCs altered morphologically, similar to cardiomyocytes	IF staining: cardiac MHC protein. RT-PCR: α-MHC and MLC-2v, NIS protein; Sca-1 downregulated	[41]
Mature DFAT cells	1×10^5 cells/cm^2 DMEM with 10% FBS, 100 U/ml penicillin, and 100 mg/ml streptomycin	CM-conditioned medium: DMEM/M199 (4:1) medium (10% FBS, 5% horse serum) sc methylcellulose medium: basic 1% methylcellulose in IMDM with 1% BSA, 15% FBS, 2-ME (0.1 mM), L-glutamine (2 mM), recombinant human insulin (10 mg/ml), human transferrin (200 mg/ml), recombinant murine interleukin 3 (IL-3; 10 ng/ml), recombinant human IL-6 (10 ng/ml), recombinant mouse SCF (50 ng/ml)	Four experiments: (i) Co-culture method: 1×10^4 DFAT cells co-cultured with 2×10^4 neonatal cardiomyocytes with DMEM/M199 (4:1) medium with 10% FBS and 5% horse serum; (ii) conditioned medium method: 1×10^5 DFAT cells cultured in cardiomyocyte-conditioned medium; (iii) Transwell culture method: DFAT cells cultured on transwell insert in DMEM (10% FBS) using cardiomyocytes as feeder cells; (iv) stem cell medium method: 1×10^5 DFAT cells cultured in stem cell methylcellulose medium	–	10% FBS, 5% horse serum, 1% BSA, 15% FBS	Penicillin/streptomycin, basic 1% methylcellulose, 2-ME, L-glutamine recombinant human insulin, human transferrin, recombinant murine IL-3, recombinant human IL-6, recombinant mouse SCF	Mature adipocyte-derived DFAT cells converted into cardiomyocyte phenotype *in vitro* and *in vivo*	Immunostaining: GFP-positive DFAT cells showed GATA4, Nkx2.5, cardiac sarcomeric actin, troponin-T. RT-PCR: Nkx2.5, troponin-T, GATA4, cardiac actin. Electrophysiological analysis: no spontaneous beating activity in DFAT cells	[49]
CD117(+)-BMSCs	Isolated CD117+ cells from BMSCs suspended in RPMI 1640 medium (with 15% FBS and 1% penicillin/ streptomycin)	RPMI 1640 medium (with 15% FBS and 1% penicillin/ streptomycin)	Myogenic differentiation of BMSC induced by 24-h stimulation with 5 ng/ml TGF-β1	–	15% FBS	Penicillin/streptomycin, TGF-β1	TGF-β induced morphological differentiation of CD117+ BMSCs into CLCs, but were immature	RT-PCR: GATA-4 and Nkx2.5, cardiac myosin, heavy chain, troponin T, troponin I, connexin-43. Electrophysiological analysis: no spontaneous beating and weak Ca^{2+} transient. Microarray: genes from TGF-β1 signal transduction pathway upregulated: *TGFB1*, *ACVR2B*, *ALK5*, *c-fos*, TSC22	[51]
ADSCs	DMEM (with 10% FBS)	–	ADSCs in lower chamber, CMs in upper chamber of transwell plates (preventing intercellular communication) ADSCs and CMs cultured three ways: (i) two cell types indirectly co-cultured in two separate chambers (non-ICA group); ii) ADSCs (24 hours after 10^{-7} mol/L ICA treatment) co-cultured with CMs as above (ICA group); (iii) both ICA and a specific ERK inhibitor (PD98059) added before co-culture, PD98059 then added to indirectly co-cultured cells	Transwell plates comprising two chambers separated by semipermeable membrane	10% FBS	ICA, ERK inhibitor PD98059	Mouse ADSCs can differentiate into cardiomyocytes when treated with ICA	Immunofluorescence analysis: cTnT expression in ICA-treated cells; RT-PCR: NKX-2.5, GATA-4, MLC-2v, α-actinin, cTnT	[56]
Nanog-iPSC lines (38C2, 20D17) [Myc(−)iPS] (256H18), ESC line (ht7)	DMEM (15% FCS), 0.1 mmol/L 2ME, 1000 U/ml LIF)	DMEM (15% FCS), 0.1 mmol/L 2ME, 1000 U/ml LIF); α-minimum essential medium (with 10% FCS, 0.05 mmol/L 2ME); 3×10^4 cells/well	All cell lines maintained in gelatinised 100 mm dishes in DMEM; puromycin added to medium with Nanog-iPSC lines, hygromycin to medium with ESC line; for differentiation: day 0: cells treated with 0.25% trypsin/EDTA, transferred to gelatinised plates in α-minimum essential medium, concentration of 3×10^4 cells/ well. Medium change on days 3, 5, and 8	Gelatin	15% FCS, 10% FCS	ME, LIF, 2ME, puromycin, hygromycin, trypsin, EDTA	Both Nanog-iPS and Myc(−)iPSCs differentiated into CMs; TSA evoked cardiac differentiation; 20D17 iPSCs did not differentiate into cardiomyocytes after day 5, perhaps because of high expression of Oct3/4	Electrophysiological analysis: 38C2 and 256H18: spontaneous myogenic contractions, few in 20D17; IHC: c-MHC, c-TNT. RT-PCR: Nkx2.5, α-MHC, ANF in 38C2, 256H18. Beating activities: number of beating clusters per well: fewest in 20D1; FACS: c-MHC-positive cells: 11.4% in 38C2, 3.6% in 20D17, 20.2% in 256H18	[57]

iPSC lines O9 and N10; ESC line D3-αPIG44 as control	On MEFs in DMEM (with 15% FCS, 100 U/ml penicillin, 100 mg/ml streptomycin, 1% NEAA, 0.1 mM β-mercaptoethanol, and 1000 IU/ml LIF)	1×10^6 cells in 10 ml IMDM (20% FCS, 100 U/ml penicillin, 100 mg/ml streptomycin, 1% NEAA, and 0.1 mM β-mercaptoethanol)	iPSCs and ESCs passaged every 2 days; cells trypsinised (0.05%) and counted, then 5×10^5 cells added to dish with preplated MEFs (0.8×10^5 feeder cells/6-cm dish); for differentiation cells suspended in IMDM, placed on horizontal shaker for 7 days to allow EB formation; on day 2, cells diluted to 1000 EB/dish. On day 7, EBs plated onto 0.1% gelatin-coated bacterial dishes for further differentiation in 20% IMDM	Dish with preplated MEFs, gelatin-coated bacterial dishes	15% FCS, 20% FCS	Penicillin, streptomycin, NEAA, β-ME, LIF	Cardiac development of N10 and O9 iPSC lines decelerated compared with ESCs	RT-PCR: Nkx2.5, αMHC, Mlc2v, and cTnT; immunocytochemical stainings: Mlc2v, ANF, sarcomeric α-actinin; Electrophysiological analysis: Na^+, L-type Ca^{2+}, depolarisation-activated outward K^+ channels recorded in N10 and O9 iPSCCMs; iPSCCMs at EDS displayed atrial and ventricular APs	[59]
Murine iPSC clone O9, murine ESC line E14.1, 129/Ola	DMEM (with 15% FCS, 0.2 mmol/L L-glutamine, 0.1 mmol/L β-mercaptoethanol, 0.1 mmol/L NEAA stock, 0.1% human leukaemia inhibitory factor-conditioned medium)	IMDM (with 15% FCS, 0.2 mmol/L L-glutamine, 0.1 mmol/L β-mercaptoethanol, 0.1 mmol/L NEAA stock)	iPSC and ESC colonies passaged up to four times without feeder cells on culture dishes coated with 0.1% gelatin to eliminate contaminating MEFs; colonies detached with 0.2% collagenase IV, dissociated into single cells with 0.025% trypsin and 0.1% chicken serum. To initiate EB formation: 'hanging drops' (600 cells in 20 ml of differentiation medium generated (day 0). differentiation medium based on IMDM; day 3: EBs transferred onto nonadherent 1% agarose-coated culture dishes with 1 EB per well, cultivated for 2 days; day 5: ten EB/well seeded on 0.1% gelatin-coated culture dish or three EBs/well on a gelatin-coated culture dish for IF analyses; day 5–24: medium replaced every second or third day	Gelatin 1%, agarose-coated culture; MEFs	15% FCS; 0.1% chicken serum	L-Glutamine, β-ME, NEAA stock, human LIF, collagenase IV, trypsin	Created cells similar to ESCCMs. In most tests, iPSCCMs were almost equivalent to ESCCMs	RT-PCR: GATA4, FOG-2, (Nkx2.5, Tbx5), (Tbx5), (Tbx20), ANF, MLC2a, MLC2v, β–MHC; IF analyses, sarcomeric α-actinin, titin, cardiac troponin T, and MLC2v, connexin 43; electrophysiological analysis, iPSCCs more spontaneous rhythmic intracellular Ca^{2+} fluctuations with amplitudes of Ca^{2+} transients comparable to ESCCMs; functionality and presence of β-adrenergic and muscarinic signalling cascade	[65]
Rat								
BMSCs	DMEM-low glucose medium (with 10% FBS, 100 U/ml penicillin, 100 lg/ml streptomycin, 300 mg/l L-glutamine, 10 mmol/l HEPES)	1×10^5 cells/ml DMEM-low glucose medium (with 10% FBS, 100 U/ml penicillin, 100 lg/ml streptomycin, 300 mg/L L-glutamine, 10 mmol/L HEPES), PBS	Differentiation of CLCs: BMSCs into four groups: Ang II group (0. 1 mmol/L) (group A), 5-Aza group (10 mmol/L) (group B), Ang II combined 5-Aza group (0.1 and 10 mmol/L, respectively) (group C), and untreated group as control; corresponding induction solutions added to each group; incubated for 24 hours; cells washed three times with PBS; medium changed to DMEM-low glucose medium; medium changed every 3 days	PBS, HEPES [4-(2-hydroxyethyl)-1-piperazineethanesulfonic acid]	10% FBS	Penicillin, streptomycin, L-glutamine	Induction period using Ang II and 5-Aza shortened to 3 weeks compared with induction using only 5-Aza; Ang II encourages differentiation of BMSCs induced by 5-Aza	IF staining: cells in groups A, B, and C, but not in control group: cTnI, sarcomeric α-actin; western blot analysis: cTnI protein level in group C higher than in group A or B; FACS analysis: differentiation ratio groups A, B, C 25–31%, control group 0.9%; TEM: induced cells contained myofilaments, z line-like substances, desmosomes, gap junctions	[43]
	DMEM-low glucose medium (with 10% FBS at 37°C in humid air with 5% CO_2)	DMEM-low glucose medium (with 10% FBS at 37°C in humid air with 5% CO_2)	BMSCs and neonatal rat ventricular myocytes co-cultured at 1:10 ratio in two chambers with semipermeable membrane; first contraction of single cells, day 7; synchronous contractions of cell clusters, day 10	Cardiac microenvironment *in vitro* by co-culturing myocardial cells with BMSCs using semipermeable membranes	10% FBS	–	BMSCs differentiate into CLCs under myocardial environment; for BMSC differentiation, physical contact not required when co-cultured with neonatal rat myocytes	RT-PCR: SERCA2 and RyR2 mRNA increased from week 1 to 3; IHC: some cells positive for: desmin (6.8%) sarcomeric α-actinin (9.4%), cTnI (8.5%) and cTnT (10.4%); western blot analysis: cTnI protein level increased from 1 to 3 weeks after treatment. Electrophysiology recordings of IK1: in MC and CLCs group, but not in BMSC group. TEM: $9.8 \pm 1.2\%$ of CLCs displayed cardiac-like myofilaments and sarcomeres	[44]
	MesenCult medium with 20% supplement, 1% penicillin–streptomycin solution in 5% CO_2 incubator at 37°C	Low-glucose DMEM (20% FBS, 1% penicillin–streptomycin)	Two groups: (i) differentiation induced on day 9 of culture; (ii) differentiation induced on day 14. To start differentiation: cells incubated with 10 mmol/L 5-Aza for 24 hours, cells washed, expanded for another 14 days with low-glucose DMEM	–	20% FBS	Penicillin-streptomycin, 5-Aza	MSCs from adult rat bone marrow differentiated into CMLCs as early as 9 days after isolation and expansion after being induced by 5-Aza; culture time for MSCs shortened by nearly 5 days	RT-PCR: cardiac-specific troponin 1, sarcomeric α-actinin, MEF2D expression increased after 5-Aza induction; intracellular Ca^{2+} measurement: no response to caffeine, KCl application: small Ca^{2+} increase; responded to ATP: cytoplasmic Ca^{2+} increase; IHC: CD90	[45]

TABLE 1 (*Continued*)

Type of stem cell	Cell density and/or expansion medium	Cell density and/or differentiation medium	Differentiation strategy	Extracellular matrix and/ or biomaterials	Serum	Small molecules	Significant results	Cardiac features	Refs
Adipose tissue-derived MSCs	5×10^6 in 75-mm^2 culture flasks; DMEM (with 10% FBS and PSA)	1×10^4 cells, in 6-well plates covered by 22-mm diameter coverslips; G1 (control): DMEM media + FBS 10%; G2 (Planat-Benard): DMEM media + FBS 15% + BSA 1% + 10^{-4}mol/L 2-ME + 2 mmol/L L-glutamine + 10 mg/ml human recombinant insulin + 200 mg/ml human transferrin + 10 ng/ml of recombinant IL-3 + 10 ng/ml of recombinant IL-6 + 50 ng/ml of recombinant SCF G3 (Planat-Benard + 5-Aza): G2 + 5 mM 5-Aza G4 (5-Aza) DMEM media + FBS 10% + 5 mM 5-Aza	G1: maintained in same media, changed every 3–4 days; G2: maintained in same media, changed every 3–4 days; G3: maintained in Planat-Benard media with 5-Aza for 24 hours, then maintained in Planat-Benard media; G4: maintained in media for 24 hours, then in complete DMEM	–	10% FBS, 15% FBS, BSA 1%	Penicillin-streptomycin, 5-Aza 2-ME, L-glutamine, human recombinant insulin, human transferrin, recombinant IL-3, recombinant IL-6, recombinant stem cell factor	5-Aza induces cardiomyogenic differentiation in similar way to using Planat-Benard media	Cardiomyocyte markers connexin 43, sarcomeric α-actinin and gap junctions: in G2, G3, G4; no spontaneous contraction in any group	[46]
BMMSCs	1×10^9/L L-DMEM complete medium (with 10% FBS, 100 U/ml penicillin, 100 mg/l streptomycin, and 300 mg/l glutamine)	L-DMEM complete medium	BMMSCs cultured for 24 hours; cells divided into four groups: (i) control: cells untreated; (ii) PFT-α: treated with PFT-α dissolved in DMSO at 20 mmol/L for 24 hours; (iii) 5-AZA: treated with 5-AZA at 10 mmol/L for 24 hours; (4) PFT-α + 5-AZA: treated with PFT-α at 20 mmol/l, and 5-AZA at 10 mmol/L for 24 hours.	–	10% FBS	Penicillin, streptomycin, glutamine; BMMSCs culture: DMSO, 5-AZA at 10 PFT-α	PFT-α decreased BMMSC apoptosis, promoted BMMSC proliferation, and induced BMMSCs to differentiate into CLCs	Immunofluorescence staining: cTnI and CX-43 western blot analysis: cTnI; PFT-α led to downregulation of p53 and p21 expression. Flow cytometry: differentiation rate of CM-like cells in 5-AZA group, PFT-α group, and 5-AZA + PFT-αgroup significantly higher than in control group	[55]

[a] *Abbreviations:* ACVR2B, activin A receptor, type IIB; ACTB, Beta-actin; ACTC1, actin, alpha, cardiac muscle 1; ACTN2, Actinin alpha 2; AFM, atomic force microscopy; ALK-5, Activin receptor-like kinase 5; ANF, atrial natriuretic factor; ANP, atrial natriuretic peptide; ATP2A2, ATPase, Ca^{2+} transporting, cardiac muscle, slow twitch 2; Beta-ME, beta-mercaptoethanol; CACNA1C/D, calcium channel, voltage-dependent, L type, alpha 1C subunit; Casq2, Calsequestrin-2; Cav1.2/3, calcium channel, voltage-dependent, L type, alpha 1C/1D subunit; CD31/90/117/166, cluster of differentiation 31/90/117/166; c-fos, FBJ murine osteosarcoma viral oncogene homolog; CFSE, carboxy-fluorescein succinimidyl ester; DKK1, Dickkopf homologue 1; EDS, early developmental stage; ETV2, ETS variant gene 2; FOX-2, F-box containing protein; HBSS, Hanks' balanced salt solution; Hcn2, Potassium/sodium hyperpolarisation-activated cyclic nucleotide-gated ion channel 2; Hcn4, hyperpolarisation activated cyclic nucleotide-gated potassium channel 4; HEPES, 4-(2-Hydroxyethyl)-1-piperazineethanesulfonic acid; IHC, immunohistochemistry; HPPA, atrial natriuretic factor; IF staining, immunofluorescence staining; IRX4, Iroquois homeobox 4; Kcnd3, potassium voltage-gated channel, Shal-related subfamily, member 3; Kcnh2, potassium voltage-gated channel, subfamily H; Kcnj2/3/12, potassium inwardly rectifying channel, subfamily J, member 2/3/12; Kcnq1, potassium voltage-gated channel, KQT-like subfamily, member 1; LIF, leukaemia inhibitor factor; MCPS, multipotent cardiovascular progenitors; MEF, mouse embryonic fibroblasts; Mef2c, Myocyte enhancer factor 2C; MEF2D, myocyte enhancer factor 2D; Mesp1, mesoderm posterior 1 homolog; MF20, anti-myosin antibody; Mix1, Mix paired-like homeobox; MIXL1, Mix1 Homeobox-like 1; MLC(2), myosin light chain (2); MNCs, mononuclear cells; Mycd, myocardin; MYH6, myosin heavy chain 6; MYL2/7, Myosin regulatory light chain 2/7; MyoD, Myogenic differentiation protein; NEAA, nonessential amino acid; PFA, paraformaldehyde; PBS, phosphate buffer solution; PLN, phospholamban; POU5F1, POU domain, class 5, transcription factor 1; PRP, positive post-rest potentiation; Ryr2, ryanodine receptor 2; SCF, stem cell factor; SCN5A, sodium channel, voltage-gated, type V, alpha subunit; SIRPA, signal-regulatory-protein alpha; Slc8a1, solute carrier family 8 (sodium/calcium exchanger), member 1; SM22, smooth muscle 22; T, T brachyury homolog; TEM, transmission electron microscopy; TNNI, troponin I; TRA-1-60, tumour rejection antigen-1-60; TSC-22, TGF beta-stimulated clone 22 gene; WT1, Wilms tumour 1.

activity of SERCA2a leads to weak contraction of the heart and enlargement of heart muscle cells, resulting in heart failure. Wahlquist *et al.* [69] reported that the miRNA miR-25 blocks the SERCA2a gene. By injecting into mice a small length of RNA that inhibited the action of miR-25, the authors halted the progress of heart failure and showed improved cardiac function and survival in the treated mice. This suggests that identifying miRNAs as new potential therapeutic targets for heart failure could be a useful new research avenue.

CCNA2 (cyclin A2) is a protein-coding prenatal gene that is usually turned during the prenatal period and turned off in humans after birth. Shapiro *et al.* [70] delivered *Ccna2* directly into pig heart and showed improved cardiac function and cellular cardiac regeneration. However, further research is needed to be able to turn on the gene for heart regeneration; if successful, CCNA2 could be another therapeutic target for cardiovascular drug development. On the basis of the fact that neonatal mouse heart can regenerate without scarring, Aurora *et al.* [71] investigated the role of cardiac macrophages from regenerating and nonregenerating hearts. MI often occurs as a result of the death of cardiomyocytes during ischaemic cardiac injury. The authors found that cardiac macrophages of regenerative hearts have a polarisation phenotype and secrete several soluble factors that are essential for the formation of new myocardium. Thus, the isolation of such regenerating macrophages would also be a new therapeutic target for heart regeneration.

All biological fluids, such as blood and urine, as well as the medium of cell cultures, contain bubble-shaped nano-sized (30–100 nm) cell-derived vesicles called exosomes, which are usually formed from plasma membrane. Ibrahim *et al.* [72] showed that exosomes contain signalling information that is necessary for reducing cardiomyocyte death, stimulating the growth of new heart muscle cells, and regenerating healthy blood vessels. The authors isolated exosomes from specialised human CSCs and observed the same beneficial effects of stem cells as seen with exosomes alone. Exosomes are also known to decrease the level of inflammation during a heart attack. miRNAs present in exosomes enable cells to communicate with neighbouring cells to stimulate cardiomyocyte regeneration. In particular, CSCs contain abundant miRNA, which could efficiently provide a regenerative signal to neighbouring cells for the development of healthy blood vessels. Targeting such nano-sized exosomes from specialised CSCs could be a new challenge for instigating heart regeneration.

Mitochondrial targets

Increased mitochondrial fragmentation often leads to cardiac tissue damage under ischaemic conditions. Kim *et al.* [73] discovered that protein seven in absentia homolog (Siah2) causes mitochondrial fragmentation under low oxygen conditions. The authors reported that no mitochondrial fragmentation and no cell death occurred in cells and mice lacking Siah2 [73]. Thus, Siah2 could also be a target for pharmaceutical research.

Rita *et al.* [74] targeted the mitochondria of cardiomyocytes and demonstrated that physical exercise is beneficial for cardiovascular health in mice. They showed that higher levels of two protein kinases (RAF and p38) were secreted into the mitochondria of cardiomyocytes in mice that exercised for 54 weeks on a treadmill-running regimen, whereas no such proteins were found in mice that did not exercise.

G protein-coupled receptor kinase 2

Generally, patients with heart failure have high expression of G protein-coupled receptor kinase 2 (GRK2), which decreases myocardial contractility. Paroxetine is a US Food and Drug Administration (FDA)-approved drug that is a selective serotonin reuptake inhibitor (SSRI) and has been used clinically as such for over three decades. However, the dosages prescribed do not inhibit GRK2 efficiently in patients with heart failure. David *et al.* [75] showed a direct link between GRK2 and its protein target and suggested that it would be necessary to modify the chemical structure of paroxetine to improve its efficiency for such patients.

GRK2 is normally present in the plasma membrane of cardiomyocytes and is involved in the pathological development of certain types of chronic heart failure. The increased activity of GRK2 results in cardiomyocyte death by turning off some of the necessary signals between blood and the surrounding tissues. Therefore, it is unsurprising that patients with heart failure have high levels of GRK2. Chen *et al.* [66] reported the movement of GRK2 from the cell membrane to mitochondria overseen by heat-shock protein 90 (Hsp90) in ischaemic heart cells. The authors suggested that blocking the ability of Hsp90 to bind to GRK2, thus preventing its delivery to mitochondria, would be a new therapeutic target for preventing cardiomyocyte death. The authors went on to show in preclinical studies that beta adrenergic receptor kinase 1 (bARKct) inhibited GRK2 in failing hearts and protected the heart from death. They reported that bARKct can block the movement of GRK2 from the plasma membrane to mitochondria after ischaemia, an important finding for drug development for the treatment of heart failure [66].

Migration inhibitory factor-related protein 14 (MRP14) is considered to be a 'heart attack protein' in that it acts to form clots that can result in heart attack or stroke in both humans and mice [76]. This finding also provides a new therapeutic target in the form of MRP14 for more effective and safer anticlotting agents for the treatment of pathological clotting in heart attack and stroke. This is important given that current anticlotting drugs are associated with a high bleeding risk along with increased mortality.

A high level of fats circulating in the bloodstream (hyperlipidaemia) is risk factor for heart complications. Hyperlipidaemia occurs as a result of a fatty diet that contributes to high levels of lipids such as cholesterol and triglycerides and also to the overproduction of lipoproteins that is independent of food intake but dependent on microsomal triglyceride transfer protein (MTP). James *et al.* [77] demonstrated that miRNA-30c (miR-30c), a genetic regulator, reduces MTP activity and even induces MTP degradation, thus lowering lipoprotein production. It provides a new target for the development of molecules that mimic miR-30c and that could be a safer and more effective treatment for reducing hyperlipidaemia in humans.

Transcription factors and oxygenation

Von Gise *et al.* [78] demonstrated that the role of Yes-associated protein isoform 1 (Yap1) in cardiomyocyte proliferation, cardiac morphogenesis, and myocardial trabeculation. Activation of Yap1 in postnatal cardiomyocytes using pharmaceutical agents could be a new strategy to stimulate cardiomyocyte expansion in diseased hearts for therapeutic myocardial regeneration. A protein called Erbin acts as a brake against this excessive and pathological growth

of heart muscle. Rachmin *et al.* [79] demonstrated that a significant decrease in the synthesis of Erbin leads to severe pathological and excessive growth of heart muscle and a decrease in heart function, resulting in heart failure. Thus, Erbin is viewed as a negative modulator of cardiac hypertrophy. Moreover, the induction of hypertrophy in mice lacking Erbin led to the early death all of these mice, compared with only a 30% mortality in the control group. Histological examination showed that heart failure was the main reason for early cardiac death [79].

Previously, it was thought that local fibroblasts were irrelevant to the healthy functioning of the heart. However, Furtado *et al.* [80] showed that local fibroblasts could be an alternative to a heart transplant for patients with heart disease. They found that local cardiac fibroblasts were similar to cardiomyocytes in terms of the cardiogenic genes expressed [80]. Courties *et al.* [81] silenced the transcription factor interferon regulatory factor 5 (IRF5) *in vivo* to reprogram the macrophage phenotype and showed improved infarct healing. It was thought that the neonatal animal heart can heal completely, whereas the adult heart lacks this ability. Puente *et al.* [82] reported that oxygen has a key role in the regenerative capacity of the heart. The authors showed that cardiomyocytes from oxygen-rich adult mouse hearts were unable to proliferate because of cell cycle arrest, whereas they could do so in neonatal mouse hearts, in which oxygen levels are lower This might appear surprising given that the main function of the heart is circulate oxygen throughout body. However oxygen is a highly reactive, oxidising agent that can form toxic compounds with other endogenous substances. Therefore, creating a low-oxygen microenvironment in a diseased heart could be a possible cardiomyocyte proliferation-based therapeutic approach.

Behfar *et al.* [83] summarised extensively the clinical trial experience of stem-cell-based therapies targeting cardiovascular disease. They described their therapeutic value and highlighted barriers to successful clinical application. Inagawa *et al.* [84] used three cardiac transcription factors, Gata4, myocyte enhancer factor 2C (Mef2c), and T-box 5 (Tbx5), to reprogram fibroblasts for direct conversion into functional cardiomyocytes *in vitro* and evaluated the resulting cells in a mouse model. They found that immunosuppressed mouse hearts expressed cardiac markers. Qian *et al.* [85] also demonstrated *in vivo* reprogramming of cardiac fibroblasts into CLCs using direct retroviral delivery of the same cardiac-specific transcription factors. Thal *et al.* [75] reprogrammed mouse Lin-Sca1(+)CD31(+) EPCs and human CD34(+) cells epigenetically by treated them with inhibitors of DNA methyltransferases (5-Aza), histone deacetylases (valproic acid), and G9a histone dimethyltransferase, and evaluated the effectiveness of the resulting cells for ischaemic myocardial repair. They found a significant improvement in ventricular function along with increased capillary density and reduced fibrosis, and reported that intramyocardial transplantation of reprogrammed mouse and human EPCs was safe and did not result in the formation of teratomas. Recently, Hou *et al.* [86] generated mouse iPSC using only seven chemicals. Senyo *et al.* [87] demonstrated that adult cardiomyocytes are responsible for the generation of new cardiomyocytes in heart and that this potential is lost in aged hearts. Russell *et al.* [88] targeted native progenitors with 3,5-disubstituted isoxazoles (Isx) to direct cell fate decisions towards cardiomyocytes; this could be an attractive approach for regenerative medicine. The authors showed promising *in vivo* efficacy of this approach for regenerative heart repair. Ott *et al.* [89] used a decellularised matrix to build a bioartificial heart, whereas Lu *et al.* [90] used a variety of agents to remove all the cells from a mouse heart. After this decellularisation process, which took approximately 10 hours, the authors repopulated the decellularised mouse heart with hiPSC-derived cardiovascular progenitor cells. The mouse heart began contracting with a speed of 40–50 beats per minute after a few weeks. Bolli *et al.* [91] reported that intracoronary infusion of autologous CSC was effective in improving post-infarction LV systolic function and reducing infarct size in patients with heart failure. Ellison *et al.* [92] found that adult Ckit+ CSCs are necessary for cardiac regeneration and repair.

Synthetic modified RNA

Zhangi *et al.* [93] targeted triggers of cardiovascular regeneration in a mouse MI model. They injected synthetic modified RNA (modRNA) encoding human VEGF-A for expansion and directed differentiation of native endogenous heart stem cells, which could be innovative step towards treatment for patients having a heart attack. The normal defence system of the body is unable to degrade modRNA but can degrade and reject non-modified mRNA. Zhang *et al.* [94] visually monitored cellular cardiac regeneration events in a zebrafish heart. They tracked both atrial and ventricular cardiomyocytes during cardiac ventricular injury using fluorescent proteins. They observed that cardiomyocytes in the atrium of the heart converted into ventricular cardiomyocytes by transdifferentiation. It is generally the ventricle that is primarily affected during a heart attack. Zhang *et al.* [94] showed that atrial cardiomyocytes can regenerate and repair ventricle cardiomyocytes, suggesting this as a possible therapeutic approach for future research.

Numb and Numbl

Shenje *et al.* [95] determined the role of two genes, *Numb* and *Numbl* in the conversion of cardiac progenitor cells into fully mature, specialised cardiomyocytes. When Numb and Numbl were disabled in early cardiac progenitor cells during mouse embryo development, the mouse embryos were unable to develop normal hearts and eventually died. This result highlights *Numb* and *Numbl* as potential new targets for instigating normal heart formation. Anand *et al.* [96] showed that bromodomain and extraterminal domain (BET) activated a broad set of genes involved in heart failure and stimulated heart-wall thickening, the formation of scar tissue, and pump failure. A potent BET inhibitor, JQ1, is already in use as an anticancer therapy but the authors used it to inhibit BET in a mouse model of cardiac disease, resulting in less thickening of the heart wall, reduction of scar tissue, and stimulation of pumping. Given that improper blood flow is also a main factor in heart failure, target BET to inhibit its activation could be an innovative target for heart drug development.

Blocking of the Hippo signalling pathway

Some fish and amphibians have the potential to regenerate their heart during both the embryonic and adult stage, whereas such an ability has been lost in adult mammals, including humans, although it is retained during embryonic development. Thus, it is likely that this ability has been lost during evolution. Heallen *et al.* [97] showed that the Hippo signalling pathway blocks the regenerative capacity of the adult heart. Research should now focus on finding chemical agents that will inhibit the Hippo signalling pathway to enable regeneration in the adult heart.

Watson *et al.* [98] used 5-Aza-2′-deoxycytidine as an inhibitor of DNA methyltransferase (DNMT) to suppress the profibrotic effects of TGF-β. Ischaemic conditions create a high degree of hypoxia and cause increased expression of collagen 1 and α-smooth muscle actin (ASMA), resulting in a myofibroblast-like phenotype. Watson *et al.* also used small interfering RNA (siRNA) to block DNMT 3B expression to reduce collagen 1 and ASMA expression. Therefore, inhibition or blocking of DNMT could be a valuable therapeutic target approach for ischaemic heart disease.

Insulin growth factor 2 and histone deacetylase inhibitors

Huang *et al.* [99] found that insulin-like growth factor 2 (IGF2) is crucial for cardiomyocyte proliferation and heart growth during embryonic heart development in mice. They also showed upregulation of *igf2b* during heart regeneration in zebrafish. Stimulation of Igf1 receptor (Igf1r) signalling is also required for cardiomyocyte proliferation during heart development and regeneration. Using fluorescent ubiquitylation-based cell cycle indicator technology, Choi *et al.* [100] found several small molecules that increase or reduce cardiomyocyte proliferation during heart development. All small molecules act via signalling pathways, including Hedgehog, IGF, or TGF-β. Zhao *et al.* [101] demonstrated that notch signalling is essential for cardiomyocyte division and heart regeneration in zebrafish, and showed that cardiomyocyte division occurred following heart injury. Therefore, it might be possible to stimulate uninjured cardiomyocytes for cell division for significant regeneration of adult zebrafish hearts following injury.

Zhang *et al.* [102] targeted inhibition of histone deacetylases (HDACs) for myocardial repair and cardiac function via c-kit signalling in mouse myocardial infarction models. Xie *et al.* [103] investigated the role of suberoylanilide hydroxamic acid (SAHA) in a large animal MI model and showed a significant reduction in MI size. SAHA is an FDA-approved anticancer HDAC inhibitor, but could prove useful for treating patients with heart disease. Kao *et al.* [104] evaluated the effects of MPT0E014, a novel HDAC inhibitor, on systolic heart failure and found improved cardiac contractility and attenuated structural remodelling. Recently, Aune *et al.* [105] targeted specific HDAC isoforms for cardiac protection from ischaemia reperfusion. Possible molecular and cellular targets for the *in vivo* regeneration of cardiomyocytes are given in Fig. 1.

Cardiac diseases modelling and drug screening

Long-QT syndrome

Moretti *et al.* [106] produced patient-specific PSCCMs from members of a family affected by long-QT syndrome type 1 (LQTS) and recapitulated the electrophysiological characteristics of this genetic disorder, such as prolongation of the AP, altered IKs channel activation and deactivation properties, and an abnormal response to catecholamine stimulation *in vitro*. The team displayed the pathogenesis of the R190Q mutation of long-QT syndrome on patient-specific PSCCMs and tested the ability of two drugs (propranolol and isoprenaline) to repair the pathology of long-QT syndrome type 1. Egashira *et al.* [107] generated iPSCCMs from a patient with sporadic LQTS, which is caused by a heterozygous mutation of the potassium voltage-gated channel, KQT-like subfamily, member 1 (*KCNQ1*) gene. Ventricular tachyarrhythmia is associated with sudden death in patients with LQTS. Egashira *et al.* [107] showed IKs channel dysfunction in LQTS-iPSCCMs and confirmed a significantly prolonged corrected field potential duration (FPD) in LQTS cardiomyocytes compared with control. The team tested the effects of the IKr blocker E4031 and found significantly prolonged FPD in control- and LQTS-iPSC-derived EB. They found that ventricular arrhythmias were frequently observed in LQTS-iPSC-derived but not in control-iPSC-derived beating EBs. Itzhaki *et al.* [108] generated LQTS hiPSCCMs from a patient with LQTS type 2 (LQTS2), which results from a missense mutation in *KCNH2*. The authors were able to reproduce the characteristic LQTS phenotype in LQTS hiPSCCMs. They showed significant prolongation of AP duration, reduction of cardiac potassium current IKr in LQTS hiPSCCMs compared with healthy control cells. Marked arrhythmogenicity and triggered arrhythmias were also seen in LQTS hiPSCCMs. The authors tested the ability of pharmacological agents to repair the disease phenotype of LQTS hiPSCCMs, including drugs acting as potassium-channel blockers, drugs able to improve calcium-channel blockers, KATP-channel openers and late sodium-channel blockers. When the authors added a Ca^{2+}-channel blocker (nifedipine) to LQTS hiPSCCMs, they found complete elimination of all early afterdepolarisations (EADs) and of all arrhythmic activity in these cells. Matsa *et al.* [109] generated LQTS2-derived cardiomyocytes from a patient with LQTS2 and showed the characteristic features of the syndrome in the cells (i.e. prolonged field and AP duration). It was possible to reverse the disease by using the beta-blockers, propranolol, and nadolol. Impaired glycosylation and channel transport to the cell surface via the IKr ion-channel pore results from a KCNH2c G1681A mutation in LQTS2. The same group were able to knockdown the KCNH2 c.G1681A mutation in LQTS 2-derived cardiomyocytes using RNA interference (RNAi) and showed normalised AP duration and K^+ currents [110]. Lahti *et al.* [111] created LQTS2-derived cardiomyocytes from a patient with LQTS2 and were able to correct the disease pathophysiology using a panel of drugs, including erythromycin, sotalol and cisapride, and a non-drug compound, E-4031 [111]. Increased arrhythmogenicity was found in control cardiac cells, but more frequently in LQT2 cardiomyocytes treated with E-4031. Interestingly, it was possible to elicit arrhythmogenicity in LQT2 cardiomyocytes by exposing cells to sotalol, an anti-arrhythmic drug with both beta-blocker and class III activity [111]. Davis *et al.* [112] showed recapitulation of the complex of ion channel disorders of an overlapping syndrome of cardiac sodium channel disease in mice iPSCCMs.

Timothy syndrome

Yazawa *et al.* [113] showed disease pathophysiology (i.e. irregular contractions, excess Ca^{2+} influx, prolonged APs, irregular electrical activity, and abnormal calcium transients in ventricular-like cells) in Timothy syndrome iPSCCMs. The authors reported the ability of roscovitine to reverse the cellular disease phenotype of electrical and Ca^{2+} signalling properties of these cardiomyocytes to a non-diseased state [113]. Fatima *et al.* [114] created catecholaminergic polymorphic ventricular tachycardia type 1 (CPVT1)-derived cardiomyocytes from a patient with CPVT1, as did Jung *et al.* [115]. Interestingly, the latter authors corrected the disease phenotype in CPVT iPSCCMs using the drug dantrolene. Itzhaki *et al.* [108] also generated CPVT-iPSCCMs from a patient with CPVT1 and

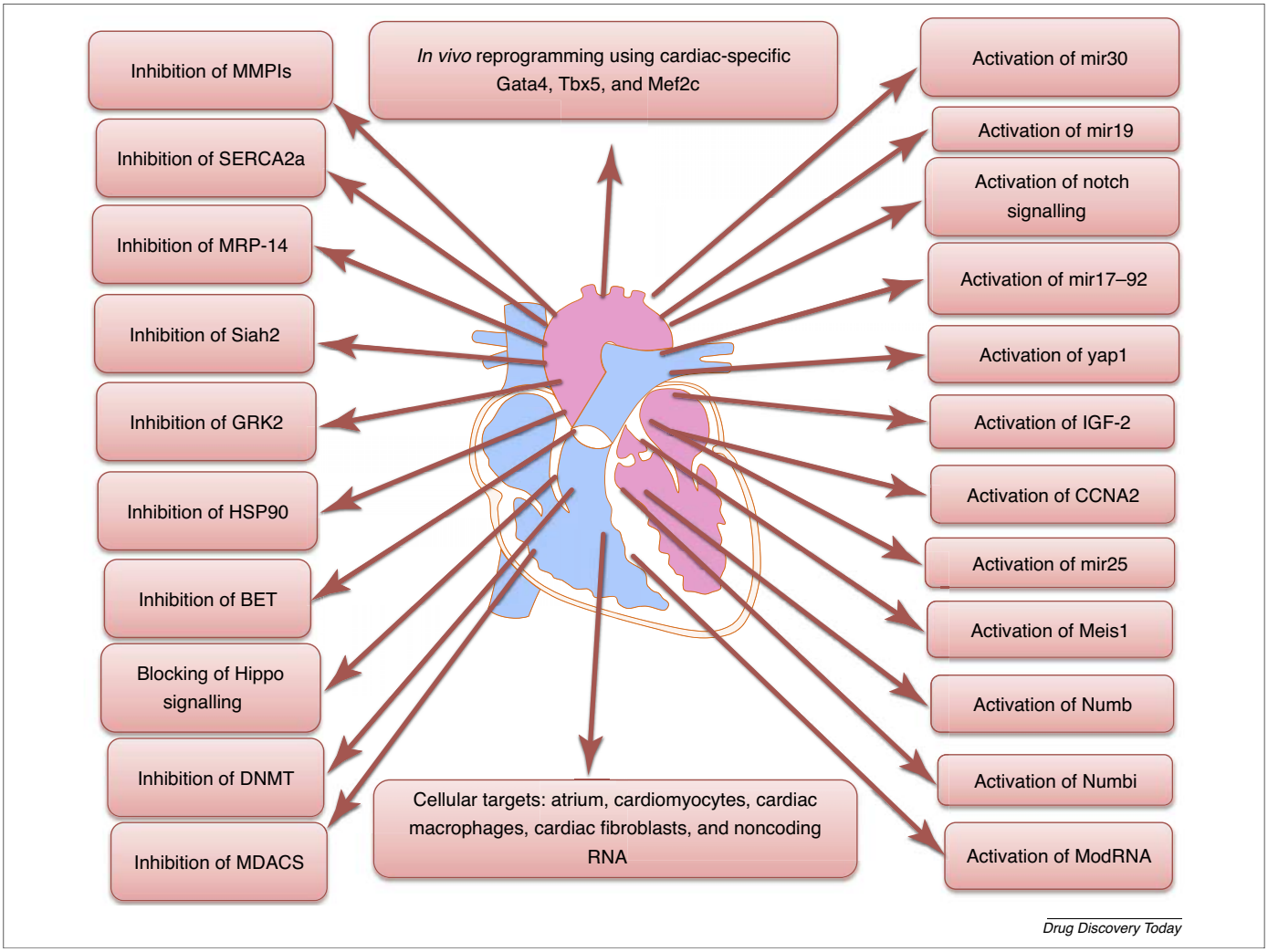

FIGURE 1

Possible molecular and cellular targets for the *in vivo* regeneration of cardiomyocytes. For more details and definitions of abbreviations, please see the main text.

compared the disease pathology with healthy control cardiomyocytes. They found delayed afterdepolarisations in 69% of the CPVT iPSCCMs compared with 11% of healthy control cardiomyocytes. The magnitude of afterdepolarisations was increased CPVT iPSCCMs upon addition of isoproterenol or forskolin. Novak *et al.* [116] generated cardiomyocytes from two patients with CPVT and two healthy controls. The authors showed that the more immature phenotypes had less-organised myofibrils, enlarged sarcoplasmic reticulum cisternae and a reduced number of caveolae in CPVT iPSCCMs.

Dilated cardiomyopathy and hypertrophic cardiomyopathy

Sun *et al.* [117] generated cardiomyocytes from a patient with diseased dilated cardiomyopathy carrying a point mutation (R173W) of the Troponin T type 2 (*TNNT2*) gene. Dilated cardiomyopathy iPSCCMs exhibited altered Ca^{2+} handling, decreased contractility, and an abnormal sarcomeric-actinin distribution. The team tested the effect of metoprolol, a beta-blocker, on dilated cardiomyopathy iPSCCMs and found that it resulted in normalisation of the sarcomeric organisation and improved Ca^{2+} handling. The authors also observed complete degeneration of myofilaments after prolonged norepinephrine treatment in dilated cardiomyopathy iPSCCMs, but not in healthy controls. Recapitulation of the disease phenotype of dilated cardiomyopathy was shown [117]. Lan *et al.* [118] generated patient-specific iPSCCMs from a patient with familial hypertrophic cardiomyopathy carrying a missense mutation in the *MYH7* gene. The hypertrophic cardiomyopathy disease phenotype includes cellular enlargement and contractile arrhythmia at the single-cell level. Dysregulation of Ca^{2+} cycling and an elevation in intracellular Ca^{2+} ($[Ca^{2+}]_i$) were shown in diseased iPSCCMs. The authors tested 12 drugs that are used clinically to treat patients with hypertrophic cardiomyopathy for the correction of hypertrophy and electrophysiological irregularities. They showed that verapamil prevented cellular hypertrophy, whereas lidocaine, mexiletine, and ranolazine had the potential to restore normal beat frequency in diseased cardiomyocytes. The Ca^{2+} channel blockers nifedipine and diltiazem were able to correct Ca^{2+}-handling abnormalities and arrhythmia in diseased cardiomyocytes, whereas myocyte hypertrophy, Ca^{2+}-handling abnormalities, and arrhythmia were corrected by the continuous addition of verapamil to single diseased cardiomyocytes for 10–20 days.

Multiple lentigines syndrome

Carvajal-Vergara *et al.* [119] created iPSCCMS from two patients with multiple lentigines syndrome. Key features of the phenotype of this disease, such as larger cardiomyocytes, more sarcomeric organisation and different localisation of nuclear factor of activated T cells, cytoplasmic 4 (NFATC4) in the nucleus, were seen when compared with control cardiomyocytes from a healthy sibling of one of the patients. Furthermore, increased phosphorylation of certain proteins was found in iPSCCMs derived from the two patients.

Arrhythmogenic right ventricular dysplasia and cardiomyopathy

Ma *et al.* [120] generated patient-specific iPSCCMs from a patient with arrhythmogenic right ventricular cardiomyopathy (ARVC) carrying a plakophilin 2 (*PKP2*) gene mutation. Desmosomal proteins (i.e. PKP2 and plakoglobin) were significantly lower in diseased cardiomyocytes compared with control cardiomyocytes. Diseased cardiomyocytes were larger and contained darker lipid droplets compared with control cardiomyocytes. Spontaneous cell contraction and contraction amplitude were decreased by treatment with a calcium channel antagonist, whereas the contraction rate was increased in the presence of a beta agonist. Kim *et al.* [121] created patient-specific iPSCCMs from patients with arrhythmogenic right ventricular dysplasia. The authors showed the induction of adult-like metabolic energetics from a glycolytic state and abnormal peroxisome proliferator-activated receptor gamma (PPAR-γ) activation in those diseased cardiomyocytes. Caspi *et al.* [122] also generated patient-specific iPSCCMs from two patients with ARVC. The abnormal desmosomal phenotype was seen in diseased cardiomyocytes from both patients. 6-Bromoindirubin-3′-oxime (BIO) application did not reverse the desmosomal abnormalities in the ARVC hiPSCCMs, but significantly reduced lipid droplet accumulation in treated cells. Adequate chronotropic responses to adrenergic and cholinergic stimuli were also noted.

Hypoplastic left heart syndrome and Barth syndrome

Jiang *et al.* [123] generated hypoplastic left heart syndrome (HLHS)-derived cardiomyocytes from a patient with HLHS and from an unaffected healthy control and reported a lower level of myofibrillar organisation, persistence of a foetal gene expression pattern, and changes in commitment to ventricular versus atrial lineages in the HLHS-derived cardiomyocytes. In addition, calcium transient patterns and electrophysiological responses to caffeine and β-adrenergic antagonists were also different compared with unaffected healthy control-derived cardiomyocytes. Recently, Wang *et al.* [124] created cardiomyocytes from two patients with Barth syndrome (BTHS), which is a rare X-linked cardiac disorder caused by mutation of a single gene (*Tafazzin*, or *TAZ*) that is currently untreatable. The mutation disrupts the normal activity of mitochondria and produces an excess amount of reactive oxygen species (ROS). Weaker contractions and irregular sarcomere assembly were observed in BTHS iPSCCMs. Interestingly, the researchers were able to correct the genetic defect of BTHS iPSCCMs *in vitro* using modified RNA transfection. Using iPS technology, approximately 20 genetic heart diseases have already been modelled and remaining heart diseases are likely to be modelled in the near future. Such efforts will be valuable to screen compounds for safer and more effective drugs, and also to predict the cardiotoxicity of candidates during drug development.

Concluding remarks

Previously, it was thought that the adult heart was unable to regenerate following injury, ageing or a pathological effect, unlike that of human neonates or embryos. However, recent discoveries have shown that the adult heart can regenerate under some specific conditions, including: (i) the inhibition of MMPIs, SERCA2a, MRP-14, Siah2, GRK2, HSP90, BET, Hippo signalling, DNMT, and MDACS; (ii) activation of mir19, notch signalling, mir 17–92, yap1, IGF-2, CCNA2, Mir-25, Meis1, Numb, Numbl, Mir30, and ModRNA; (iii) *in vivo* reprogramming using cardiac-specific transcription factors, such as GATA 4, Mef2c, and Tbx5, and cell organelles, such as atrium cardiomyocytes, cardiac macrophages, exosomes, noncoding miRNA, and cardiac fibroblasts; and (iv) cardiac differentiation of primary adult stem cells and iPSCs. Approximately 20 currently untreatable human cardiac genetic diseases have been modelled *in vitro* and attempts to treat them have focussed mainly on the use of drugs. However, it might be that iPSCCMs could offer a new, more affordable approach to treating such diseases. Although more research is required, both preclinically and in clinical trials, the use of iPSCCMs holds the promise of personalised treatments for CVD in the future.

Conflict of interest

None declared.

Acknowledgement

We thank Priya Giri for her technical assistance with the figure and text.

References

1 Maron, B.J. *et al.* (2006) Contemporary definitions and classification of the cardiomyopathies: an American Heart Association Scientific Statement from the Council on Clinical Cardiology, Heart Failure and Transplantation Committee; Quality of Care and Outcomes Research and Functional Genomics and Translational Biology Interdisciplinary Working Groups; and Council on Epidemiology and Prevention. *Circulation* 113, 1807–1816

2 Smits, J. *et al.* (2010) Considerations for patients awaiting heart transplantation. *Thorac. Cardiovasc. Surg.* 58, S179–S184

3 Stehlik, J. *et al.* (2011) The Registry of the International Society for Heart and Lung Transplantation: Twenty-eighth Adult Heart Transplant Report 2011. *J. Heart Lung Transplant.* 30, 1078–1094

4 Hoffman, F.M. (2005) Outcomes and complications after heart transplantation: a review. *J. Cardiovasc. Nurs.* 20, S31–S42

5 Aliabadi, A. *et al.* (2012) Current strategies and future trends in immunosuppression after heart transplantation. *Curr. Opin. Organ Transplant.* 17, 540–545

6 Stiefel, P. *et al.* (2013) Symptom experiences in patients after heart transplantation. *J. Health Psychol.* 18, 680–692

7 Løgstrup, S. and O'Kelly, S. (2012) *ESC European Cardiovascular Disease Statistics 2012.* European Heart Network

8 Sheng, C. *et al.* (2013) Current stem cell delivery methods for myocardial repair. *Biomed. Res. Int.* 2013, 1–15

9 Templin, C. *et al.* (2010) Stamm- und progenitorzellbasierte Therapieansätze. *Herz* 35, 445–457
10 Hare, J.M. and Chaparro, S.V. (2008) Cardiac regeneration and stem cell therapy. *Curr. Opin. Organ Transplant.* 13, 536–542
11 Murry, C.E. *et al.* (2005) Cell-based cardiac repair: reflections at the 10-year point. *Circulation* 112, 3174–3183
12 Takahashi, K. and Yamanaka, S. (2006) Induction of pluripotent stem cells from mouse embryonic and adult fibroblast cultures by defined factors. *Cell* 126, 663–676
13 Nelson, T.J. *et al.* (2009) Repair of acute myocardial infarction by human stemness factors induced pluripotent stem cells. *Circulation* 120, 408–416
14 Li, X. *et al.* (2013) Intramyocardial injection of pig pluripotent stem cells improves left ventricular function and perfusion: a study in a porcine model of acute myocardial infarction. *PLOS ONE* 8, e66688
15 Gu, M. *et al.* (2012) Microfluidic single-cell analysis shows that porcine induced pluripotent stem cell-derived endothelial cells improve myocardial function by paracrine activation. *Circ. Res.* 111, 882–893
16 Zhang, Y. *et al.* (2011) Intramyocardial transplantation of undifferentiated rat induced pluripotent stem cells causes tumorigenesis in the heart. *PLoS ONE* 6, e19012
17 Halbach, M. *et al.* (2013) Electrophysiological integration and action potential properties of transplanted cardiomyocytes derived from induced pluripotent stem cells. *Cardiovasc. Res.* 100, 432–440
18 Miki, K. *et al.* (2012) Bioengineered myocardium derived from induced pluripotent stem cells improves cardiac function and attenuates cardiac remodeling following chronic myocardial infarction in rats. *Stem Cells Transl. Med.* 1, 430–437
19 Zwi-Dantsis, L. *et al.* (2013) Derivation and cardiomyocyte differentiation of induced pluripotent stem cells from heart failure patients. *Eur. Heart J.* 34, 1575–1586
20 Carpenter, L. *et al.* (2012) Efficient differentiation of human induced pluripotent stem cells generates cardiac cells that provide protection following myocardial infarction in the rat. *Stem Cells Dev.* 21, 977–986
21 Chong, J.J. *et al.* (2014) Human embryonic-stem-cell-derived cardiomyocytes regenerate non-human primate hearts. *Nature* 510, 273–277
22 Kawamura, M. *et al.* (2012) Feasibility, safety, and therapeutic efficacy of human induced pluripotent stem cell-derived cardiomyocyte sheets in a porcine ischemic cardiomyopathy model. *Circulation* 126 (Suppl. 1), 29–37
23 Kawamura, M. *et al.* (2013) Enhanced survival of transplanted human induced pluripotent stem cell-derived cardiomyocytes by the combination of cell sheets with the pedicled omental flap technique in a porcine heart. *Circulation* 128 (Suppl. 1), 87–94
24 Pecha, S. *et al.* (2014) Human iPS-cell-derived engineered heart tissue for cardiac repair. *Thorac. Cardiovasc. Surg* 62, OP48
25 Barile, L. *et al.* (2007) Endogenous cardiac stem cells. *Prog. Cardiovasc. Dis.* 50, 31–48
26 Choi, S.H. *et al.* (2012) Perspectives on stem cell therapy for cardiac regeneration. *Circ. J.* 76, 1307–1312
27 Zhao, X. and Huang, L. (2013) Cardiac stem cells: a promising treatment option for heart failure. *Exp. Ther. Med.* 5, 379–383
28 Clifford, D.M. *et al.* (2012) Stem cell treatment for acute myocardial infarction. *Cochrane Database Syst. Rev.* 2, CD006536
29 Templin, C. *et al.* (2011) Cell-based cardiovascular repair and regeneration in acute myocardial infarction and chronic ischemic cardiomyopathy current status and future developments. *Int. J. Dev. Biol.* 55, 407–417
30 Chugh, A.R. *et al.* (2012) Administration of cardiac stem cells in patients with ischemic cardiomyopathy: the SCIPIO trial: surgical aspects and interim analysis of myocardial function and viability by magnetic resonance. *Circulation* 126 (Suppl. 1), S54–S64
31 Donndorf, P. *et al.* (2013) Stem cell therapy for the treatment of acute myocardial infarction and chronic ischemic heart disease. *Curr. Pharm. Biotechnol.* 14, 12–19
32 Zhang, J. *et al.* (2009) Functional cardiomyocytes derived from human induced pluripotent stem cells. *Circ. Res.* 104, e30–e41
33 Matsuura, K. *et al.* (2012) Creation of human cardiac cell sheets using pluripotent stem cells. *Biochem. Biophys. Res. Commun.* 425, 321–327
34 Christoforou, N. *et al.* (2013) Induced pluripotent stem cell-derived cardiac progenitors differentiate to cardiomyocytes and form biosynthetic tissues. *PLOS ONE* 8, e65963
35 Wei, H. *et al.* (2012) One-step derivation of cardiomyocytes and mesenchymal stem cells from human pluripotent stem cells. *Stem Cell Res.* 9, 87–100
36 Honda, M. *et al.* (2011) Electrophysiological characterization of cardiomyocytes derived from human induced pluripotent stem cells. *J. Pharmacol. Sci.* 117, 149–159
37 Lee, Y.-K. *et al.* (2011) Calcium homeostasis in human induced pluripotent stem cell-derived cardiomyocytes. *Stem Cell Rev. Rep.* 7, 976–986
38 Gai, H. *et al.* (2009) Generation and characterization of functional cardiomyocytes using induced pluripotent stem cells derived from human fibroblasts. *Cell Biol. Int.* 33, 1184–1193
39 So, K.H. *et al.* (2011) Generation of functional cardiomyocytes from mouse induced pluripotent stem cells. *Int. J. Cardiol.* 153, 277–285
40 Germanguz, I. *et al.* (2011) Molecular characterization and functional properties of cardiomyocytes derived from human inducible pluripotent stem cells. *J. Cell. Mol. Med.* 15, 38–51
41 Kim, M.H. *et al.* (2012) *In vitro* monitoring of cardiomyogenic differentiation of mesenchymal stem cells using sodium iodide symporter gene. *Tissue Eng. Regen. Med.* 9, 304–310
42 Potdar, P.D. and Prasannan, P. (2013) Differentiation of human dermal mesenchymal stem cells into cardiomyocytes by treatment with 5-azacytidine: concept for regenerative therapy in myocardial infarction. *ISRN Stem Cells* 2013, 1–9
43 Xing, Y. *et al.* (2012) The combination of angiotensin II and 5-azacytidine promotes cardiomyocyte differentiation of rat bone marrow mesenchymal stem cells. *Mol. Cell. Biochem.* 360, 279–287
44 Li, X. *et al.* (2007) Bone marrow mesenchymal stem cells differentiate into functional cardiac phenotypes by cardiac microenvironment. *J. Mol. Cell. Cardiol.* 42, 295–303
45 Tokcaer-Keskin, Z. *et al.* (2009) Timing of induction of cardiomyocyte differentiation for *in vitro* cultured mesenchymal stem cells: a perspective for emergencies. *Can. J. Physiol. Pharmacol.* 87, 143–150
46 Carvalho, P.H. *et al.* (2013) Differentiation of adipose tissue-derived mesenchymal stem cells into cardiomyocytes. *Arq. Bras. Cardiol.* 100, 82–89
47 Ge, X. *et al.* (2012) Human amniotic mesenchymal stem cell-derived induced pluripotent stem cells may generate a universal source of cardiac cells. *Stem Cells Dev.* 21, 2798–2808
48 Choi, Y.S. *et al.* (2010) Differentiation of human adipose-derived stem cells into beating cardiomyocytes. *J. Cell. Mol. Med.* 14, 878–889
49 Jumabay, M. *et al.* (2009) Dedifferentiated fat cells convert to cardiomyocyte phenotype and repair infarcted cardiac tissue in rats. *J. Mol. Cell. Cardiol.* 47, 565–575
50 Dijk, A. *et al.* (2008) Differentiation of human adipose-derived stem cells towards cardiomyocytes is facilitated by laminin. *Cell Tissue Res.* 334, 457–467
51 Li, T.-S. *et al.* (2008) TGF-β induces the differentiation of bone marrow stem cells into immature cardiomyocytes. *Biochem. Biophys. Res. Commun.* 366, 1074–1080
52 Labovsky, V. *et al.* (2010) Cardiomyogenic differentiation of human bone marrow mesenchymal cells: role of cardiac extract from neonatal rat cardiomyocytes. *Differentiation* 79, 93–101
53 Zhao, Z. *et al.* (2011) Sphingosine-1-phosphate promotes the differentiation of human umbilical cord mesenchymal stem cells into cardiomyocytes under the designated culturing conditions. *J. Biomed. Sci.* 18, 37
54 Zhu, Y. *et al.* (2009) ADSCs differentiated into cardiomyocytes in cardiac microenvironment. *Mol. Cell. Biochem.* 324, 117–129
55 Yan, X. *et al.* (2011) Inhibition of p53-p21 pathway promotes the differentiation of rat bone marrow mesenchymal stem cells into cardiomyocytes. *Mol. Cell. Biochem.* 354, 21–28
56 Jin, M.-S. *et al.* (2010) Icariin-mediated differentiation of mouse adipose-derived stem cells into cardiomyocytes. *Mol. Cell. Biochem.* 344, 1–9
57 Kaichi, S. *et al.* (2010) Cell line-dependent differentiation of induced pluripotent stem cells into cardiomyocytes in mice. *Cardiovasc. Res.* 88, 314–323
58 Uosaki, H. *et al.* (2012) Direct contact with endoderm-like cells efficiently induces cardiac progenitors from mouse and human pluripotent stem cells. *PLOS ONE* 7, e46413
59 Kuzmenkin, A. *et al.* (2009) Functional characterization of cardiomyocytes derived from murine induced pluripotent stem cells *in vitro*. *FASEB J.* 23, 4168–4180
60 Zwi, L. *et al.* (2009) Cardiomyocyte differentiation of human induced pluripotent stem cells. *Circulation* 120, 1513–1523
61 Lian, X. *et al.* (2012) Robust cardiomyocyte differentiation from human pluripotent stem cells via temporal modulation of canonical Wnt signaling. *Proc. Natl. Acad. Sci. U. S. A.* 109, E1848–E1857
62 Lin, B. *et al.* (2012) High-purity enrichment of functional cardiovascular cells from human iPS cells. *Cardiovasc. Res.* 95, 327–335
63 Shinozawa, T. *et al.* (2012) A novel purification method of murine embryonic stem cell- and human-induced pluripotent stem cell-derived cardiomyocytes by simple manual dissociation. *J. Biomol. Screen.* 17, 683–691
64 Oberwallner, B. *et al.* (2014) Human cardiac extracellular matrix supports myocardial lineage commitment of pluripotent stem cells. *Eur. J. Cardiothorac. Surg.* http://dx.doi.org/10.1093/ejcts/ezu163

65 Mauritz, C. *et al.* (2008) Generation of functional murine cardiac myocytes from induced pluripotent stem cells. *Circulation* 118, 507–517
66 Chen, J. *et al.* (2013) mir-17-92 cluster is required for and sufficient to induce cardiomyocyte proliferation in postnatal and adult hearts. *Circ. Res.* 112, 1557–1566
67 Brendan, P. *et al.* (2014) Injectable and bioresponsive hydrogels for on-demand matrix metalloproteinase inhibition. *Nat. Mater.* 13, 653–661
68 Mahmoud, A.I. *et al.* (2013) Meis1 regulates postnatal cardiomyocyte cell cycle arrest. *Nature* 497, 249–253
69 Wahlquist, C. *et al.* (2014) Inhibition of miR-25 improves cardiac contractility in the failing heart. *Nature* 508, 531–535
70 Shapiro, S.D. *et al.* (2014) Cyclin A2 induces cardiac regeneration after myocardial infarction through cytokinesis of adult cardiomyocytes. *Sci. Transl. Med.* 6, 224ra27
71 Aurora, A.B. *et al.* (2014) Macrophages are required for neonatal heart regeneration. *J. Clin. Invest.* 124, 1382–1392
72 Ibrahim, A.G-E. *et al.* (2014) Exosomes as critical agents of cardiac regeneration triggered by cell therapy. *Stem Cell Rep.* 2, 606–619
73 Kim, H. *et al.* (2011) Fine-tuning of Drp1/Fis1 availability by AKAP121/Siah2 regulates mitochondrial adaptation to hypoxia. *Mol. Cell* 44, 532–544
74 Ferreira, R. *et al.* (2014) Lifelong exercise training modulates cardiac mitochondrial phosphoproteome in rats. *J. Proteome Res.* 13, 2045–2055
75 Thal, D.M. *et al.* (2012) Paroxetine is a direct inhibitor of G protein-coupled receptor kinase 2 and increases myocardial contractility. *ACS Chem. Biol.* 7, 1830–1839
76 Wang, Y. *et al.* (2014) Platelet-derived S100 family member myeloid-related protein-14 regulates thrombosis. *J. Clin. Invest.* 124, 2160–2167
77 Soh, J. *et al.* (2013) MicroRNA-30c reduces hyperlipidemia and atherosclerosis in mice by decreasing lipid synthesis and lipoprotein secretion. *Nat. Med.* 19, 892–900
78 von Gise, A. *et al.* (2012) YAP 1, the nuclear target of Hippo signaling, stimulates heart growth through cardiomyocyte proliferation but not hypertrophy. *Proc. Natl. Acad. Sci. U. S. A.* 109, 2394–2399
79 Rachmin, S. *et al.* (2014) Erbin is a negative modulator of cardiac hypertrophy. *Proc. Natl. Acad. Sci. U. S. A.* 111, 5902–5907
80 Furtado, M.B. *et al.* (2014) Cardiogenic genes expressed in cardiac fibroblasts contribute to heart development and repair. *Circ. Res.* 114, 1422–1434
81 Courties, G. *et al.* (2013) *In vivo* silencing of the transcription factor IRF5 reprograms the macrophage phenotype and improves infarct healing. *J. Am. Coll. Cardiol.* 63, 1556–1566
82 Puente, B.N. *et al.* (2014) The oxygen-rich postnatal environment induces cardiomyocyte cell-cycle arrest through DNA damage response. *Cell* 157, 565–579
83 Behfar, A. *et al.* (2014) Cell therapy for cardiac repair: lessons from clinical trials. *Nat. Rev. Cardiol.* 11, 232–246
84 Inagawa, K. *et al.* (2012) Induction of cardiomyocyte-like cells in infarct hearts by gene transfer of Gata4, Mef2c, and Tbx5. *Circ. Res.* 111, 1147–1156
85 Qian, L. *et al.* (2012) *In vivo* reprogramming of murine cardiac fibroblasts into induced cardiomyocytes. *Nature* 485, 593–598
86 Hou, P. *et al.* (2013) Pluripotent stem cells induced from mouse somatic cells by small-molecule compounds. *Science* 341, 651–654
87 Senyo, S.E. *et al.* (2013) Mammalian heart renewal by pre-existing cardiomyocytes. *Nature* 493, 433–436
88 Russell, J.L. *et al.* (2012) Targeting native adult heart progenitors with cardiogenic small molecules. *ACS Chem. Biol.* 7, 1067–1076
89 Ott, H.C. *et al.* (2008) Perfusion-decellularized matrix: using nature's platform to engineer a bioartificial heart. *Nat. Med.* 14, 213–221
90 Lu, T.Y. *et al.* (2013) Repopulation of decellularized mouse heart with human induced pluripotent stem cell-derived cardiovascular progenitor cells. *Nat. Commun.* 4, 2307
91 Bolli, R. *et al.* (2011) Cardiac stem cells in patients with ischaemic cardiomyopathy (SCIPIO): initial results of a randomised phase 1 trial. *Lancet* 378, 1847–1857
92 Ellison, G.M. *et al.* (2013) Adult Ckit+ cardiac stem cells are necessary and sufficient for functional cardiac regeneration and repair. *Cell* 154, 827–842
93 Zangi, L. *et al.* (2013) Modified mRNA directs the fate of heart progenitor cells and induces vascular regeneration after myocardial infarction. *Nat. Biotechnol.* 31, 898–907
94 Zhang, R. *et al.* (2013) *In vivo* cardiac reprogramming contributes to zebrafish heart regeneration. *Nature* 498, 497–501
95 Shenje, L.T. *et al.* (2014) Precardiac deletion of Numb and Numblike reveals renewal of cardiac progenitors. *eLife* http://dx.doi.org/10.7554/eLife.02164
96 Anand, P. *et al.* (2013) BET bromodomains mediate transcriptional pause release in heart failure. *Cell* 154, 569–582
97 Heallen, T. *et al.* (2013) Hippo signaling impedes adult heart regeneration. *Development* 140, 4683–4690
98 Watson, C.J. *et al.* (2013) Hypoxia-induced epigenetic modifications are associated with cardiac tissue fibrosis and the development of a myofibroblast-like phenotype. *Hum. Mol. Genet.* 23, 2176–2188
99 Huang, Y. *et al.* (2013) Igf signaling is required for cardiomyocyte proliferation during zebrafish heart development and regeneration. *PLOS ONE* http://dx.doi.org/10.1371/journal.pone.0067266
100 Choi, W.Y. *et al.* (2013) *In vivo* monitoring of cardiomyocyte proliferation to identify chemical modifiers of heart regeneration. *Development* 140, 660–666
101 Zhao, L. *et al.* (2014) Notch signaling regulates cardiomyocyte proliferation during zebrafish heart regeneration. *Proc. Natl. Acad. Sci. U. S. A.* 111, 1403–1408
102 Zhang, L. *et al.* (2012) Inhibition of histone deacetylase-induced myocardial repair is mediated by c-kit in infarcted hearts. *J. Biol. Chem.* 287, 39338–39348
103 Xie, M. *et al.* (2014) Histone deacetylase inhibition blunts ischemia/reperfusion injury by inducing cardiomyocyte autophagy. *Circulation* 129, 1139–1151
104 Kao, Y.H. *et al.* (2013) Histone deacetylase inhibition improved cardiac functions with direct antifibrotic activity in heart failure. *Int. J. Cardiol.* 168, 4178–4183
105 Aune, S.E. *et al.* (2014) Selective inhibition of class I but not class IIb histone deacetylases exerts cardiac protection from ischemia reperfusion. *J. Mol. Cell. Cardiol.* 72, 138–145
106 Moretti, A. *et al.* (2010) Patient-specific induced pluripotent stem-cell models for long-QT syndrome. *N. Engl. J. Med.* 363, 1397–1409
107 Egashira, T. *et al.* (2012) Disease characterization using LQTS-specific induced pluripotent stem cells. *Cardiovasc. Res.* 95, 419–429
108 Itzhaki, I. *et al.* (2012) Modeling of catecholaminergic polymorphic ventricular tachycardia with patient-specific human induced pluripotent stem cells. *J. Am. Coll. Cardiol.* 60, 990–1000
109 Matsa, E. *et al.* (2011) Drug evaluation in cardiomyocytes derived from human induced pluripotent stem cells carrying a long QT syndrome type 2 mutation. *Eur. Heart J.* 32, 952–962
110 Matsa, E. *et al.* (2013) Allele-specific RNA interference rescues the long-QT syndrome phenotype in human induced pluripotent stem cell cardiomyocytes. *Eur. Heart J.* 35, 1078–1087
111 Lahti, A.L. *et al.* (2012) Model for long QT syndrome type 2 using human iPS cells demonstrates arrhythmogenic characteristics in cell culture. *Dis. Model. Mech.* 5, 220–230
112 Davis, R.P. *et al.* (2012) Cardiomyocytes derived from pluripotent stem cells recapitulate electrophysiological characteristics of an overlap syndrome of cardiac sodium channel disease. *Circulation* 125, 3079–3091
113 Yazawa, M. *et al.* (2011) Using induced pluripotent stem cells to investigate cardiac phenotypes in Timothy syndrome. *Nature* 471, 230–234
114 Fatima, A. *et al.* (2011) *In vitro* modeling of ryanodine receptor 2 dysfunction using human induced pluripotent stem cells. *Cell. Physiol. Biochem.* 28, 579–592
115 Jung, C.B. *et al.* (2012) Dantrolene rescues arrhythmogenic RYR2 defect in a patient-specific stem cell model of catecholaminergic polymorphic ventricular tachycardia. *EMBO Mol. Med.* 4, 180–191
116 Novak, A. *et al.* (2012) Cardiomyocytes generated from CPVTD307H patients are arrhythmogenic in response to beta-adrenergic stimulation. *J. Cell. Mol. Med.* 16, 468–482
117 Sun, N. *et al.* (2012) Patient specific induced pluripotent stem cells as a model for familial dilated cardiomyopathy. *Sci. Transl. Med.* 4, 130ra147
118 Lan, F. *et al.* (2013) Abnormal calcium handling properties underlie familial hypertrophic cardiomyopathy pathology in patient-specific induced pluripotent stem cells. *Cell Stem Cell* 12, 101–113
119 Carvajal-Vergara, X. *et al.* (2010) Patient-specific induced pluripotent stem-cell-derived models of LEOPARD syndrome. *Nature* 465, 808–812
120 Ma, D. *et al.* (2013) Generation of patient-specific induced pluripotent stem cell-derived cardiomyocytes as a cellular model of arrhythmogenic right ventricular cardiomyopathy. *Eur. Heart J.* 34, 1122–1133
121 Kim, C. *et al.* (2013) Studying arrhythmogenic right ventricular dysplasia with patient-specific iPSCs. *Nature* 494, 105–110
122 Caspi, O. *et al.* (2013) Modeling of arrhythmogenic right ventricular cardiomyopathy with human induced pluripotent stem cells. *Circ. Cardiovasc. Genet.* 6, 557–568
123 Jiang, Y. *et al.* (2014) An induced pluripotent stem cell model of hypoplastic left heart syndrome (HLHS) reveals multiple expression and functional differences in HLHS-derived cardiac myocytes. *Stem Cells Transl. Med.* 3, 416–423
124 Wang, G. *et al.* (2014) Modeling the mitochondrial cardiomyopathy of Barth syndrome with induced pluripotent stem cell and heart-on-chip technologies. *Nat. Med.* 20, 616–623

frontiers in Genetics

ORIGINAL RESEARCH
published: 06 March 2018
doi: 10.3389/fgene.2018.00072

Qualitative and Quantitative Analysis of Cardiac Progenitor Cells in Cases of Myocarditis and Cardiomyopathy

Marie Gerisch[1], Jan Smettan[2], Sabine Ebert[1], Maria Athelogou[3], Beate Brand-Saberi[4], Nick Spindler[5], Wolf C. Mueller[6], Shibashish Giri[1,7†] and Augustinus Bader[1*†]*

[1] Applied Stem Cell Biology and Cell Technology, Biomedical and Biotechnological Center, University of Leipzig, Leipzig, Germany, [2] Division of Cardiology and Angiology, Department of Internal Medicine, Neurology and Dermatology, University Hospital Leipzig, Leipzig, Germany, [3] Definiens AG, Munich, Germany, [4] Department of Anatomy and Molecular Embryology, Institute of Anatomy, Faculty of Medicine, Ruhr-University Bochum, Bochum, Germany, [5] Department of Orthopedics, Trauma and Plastic Surgery, University Hospital Leipzig, Leipzig, Germany, [6] Department of Neuropathology, University Hospital Leipzig, Leipzig, Germany, [7] Department of Plastic and Hand Surgery, University Hospital Rechts der Isar, Munich Technical University, Munich, Germany

OPEN ACCESS

Edited by:
Elena G. Pasyukova, Institute of Molecular Genetics (RAS), Russia

Reviewed by:
Federico Quaini, Università degli Studi di Parma, Italy
Georgina May Ellison-Hughes, King's College London, United Kingdom

***Correspondence:**
Shibashish Giri
shibashish.giri@bbz.uni-leipzig.de
Augustinus Bader
Augustinus.bader@bbz.uni-leipzig.de

† These authors have contributed equally to this work.

Specialty section:
This article was submitted to Genetics of Aging, a section of the journal Frontiers in Genetics

Received: *12 September 2017*
Accepted: *16 February 2018*
Published: *06 March 2018*

Citation:
Gerisch M, Smettan J, Ebert S, Athelogou M, Brand-Saberi B, Spindler N, Mueller WC, Giri S and Bader A (2018) Qualitative and Quantitative Analysis of Cardiac Progenitor Cells in Cases of Myocarditis and Cardiomyopathy. Front. Genet. 9:72. doi: 10.3389/fgene.2018.00072

We aimed to identify and quantify $CD117^+$ and $CD90^+$ endogenous cardiac progenitor cells (CPC) in human healthy and diseased hearts. We hypothesize that these cells perform a locally acting, contributing function in overcoming medical conditions of the heart by endogenous means. Human myocardium biopsies were obtained from 23 patients with the following diagnoses: Dilatative cardiomyopathy (DCM), ischemic cardiomyopathy (ICM), myocarditis, and controls from healthy cardiac patients. High-resolution scanning microscopy of the whole slide enabled a computer-based immunohistochemical quantification of CD117 and CD90. Those signals were evaluated by Definiens Tissue Phenomics® Technology. Co-localization of CD117 and CD90 was determined by analyzing comparable serial sections. $CD117^+/CD90^+$ cardiac cells were detected in all biopsies. The highest expression of CD90 was revealed in the myocarditis group. CD117 was significantly higher in all patient groups, compared to healthy specimens ($*p < 0.05$). The highest co-expression was found in the myocarditis group (6.75 ± 3.25 $CD90^+CD117^+$ cells/mm^2) followed by ICM (4 ± 1.89 cells/mm^2), DCM (1.67 ± 0.58 cells/mm^2), and healthy specimens (1 ± 0.43 cells/mm^2). We conclude that the human heart comprises a fraction of local $CD117^+$ and $CD90^+$ cells. We hypothesize that these cells are part of local endogenous progenitor cells due to the co-expression of CD90 and CD117. With novel digital image analysis technologies, a quantification of the CD117 and CD90 signals is available. Our experiments reveal an increase of CD117 and CD90 in patients with myocarditis.

Keywords: local cardiac stem/progenitor cells, c-Kit$^+$ (CD117$^+$) cells, CD90$^+$ cells, myocarditis, cardiomyopathy, human myocardium biopsy

INTRODUCTION

The World Health Organization reports cardiovascular diseases as the main cause of 29% of global death each year (Lozano et al., 2012). There are approximately 17.3 million cardiovascular-related deaths per year worldwide (Townsend et al., 2015). Particularly in the European region, cardiovascular diseases cause 4 million deaths; which is, 45% of death per year (Townsend et al., 2015). In all countries of Europe, the primary cause of death in women is cardiovascular diseases,

estimated to be 51% of all-cause mortality in women. For men, 42% of deaths are caused by cardiovascular diseases (Townsend et al., 2015).

Due to the profound importance of cardiovascular diseases, the natural endogenous regenerative capacity of the human heart has been a topic of debate for decades. Accumulating evidence over the last decade has suggested that the human heart has the potential to undergo natural regeneration. Locally resident cardiac progenitor or stem cells might play a vital role toward the natural regeneration capacity of the heart. Myocyte proliferation happens to a low extent in the human heart, while enhanced proliferation was observed following injuries of the heart such as myocardial infarction (Beltrami et al., 2001). In addition, the muscle cells of the whole human heart are replaced every 4.5 years (Anversa et al., 2006). Cardiac progenitor cells (CPCs) can replicate in response to some pathological conditions, and they are also able to play an active role in the regeneration of injured parts of the heart (Gonzalez et al., 2008).

Of particular interest are cells with the c-Kit receptor (CD117 or SCFR-stem cell factor receptor) on the surface. Beltrami and colleagues reported the existence of $CD117^+$ cells with characteristics of CPCs (Beltrami et al., 2003). In addition, other researchers described that cardiac $CD117^+$ cells are potential local stem cells, which reside in the human heart (Castaldo et al., 2008; Di Meglio et al., 2010; Sandstedt et al., 2012). Bearzi and colleagues also described the typical stem cell features of the $CD117^+$ cells: they are clonogenic, multipotent, and self-renewing (Bearzi et al., 2007). An increase in the number of cardiac $CD117^+$ cells was observed in several cardiovascular diseases such as heart failure, cardiac hypertrophy, ischemic cardiomyopathy (ICM), acute cardiac injury, and pressure overload (Urbanek et al., 2003, 2005; Castaldo et al., 2008; Kubo et al., 2008; Altarche-Xifró et al., 2009; Itzhaki-Alfia et al., 2009; Rupp et al., 2012).

Nurzynska and colleagues conducted a comparative study of human CPCs in normal and pathological conditions (ischemic heart disease) and confirmed that the differentiation potential of $CD117^+$ CPCs of the adult human pathological heart is weak in comparison to healthy cardiac tissue (Nurzynska et al., 2013). Bolli et al. conducted a phase I clinical trial for the clinical implication of $CD117^+$ stem cells, and interestingly they found an increased cardiac functional capacity, reduced left ventricle scar size, and improved quality of life due to these cells (Bolli et al., 2011). They isolated $CD117^+$ cells from 1 g myocardial tissue during cardiac surgery. They showed that the infusion of 1 million autologous $CD117^+$ stem cells is not associated with noticeable adverse or significant positive effects. Therefore, the study of the anatomy of the human heart and the manner in which pathological states and micro-environmental conditions correlate with the availability of resident CPCs for cardiac tissue regeneration is required to further confirm the presence of local resident progenitor cells as well as for potential clinical strategies for novel forms of cardiac cell therapy by endogenous recruitment. Nevertheless, for progenitor cell detection, additional stem cell markers must be proven. Herein, we focus on the existence of $CD90^+$ and $CD117^+$ cells as regenerative precursor cells in the human healthy and diseased heart, that are responsible for the activation of endogenous resident progenitor cells toward tissue or cell injury. Previous investigations focused on the detection of $CD90^+$ and $CD117^+$ progenitor cells in the human heart along with additional information about biopsy location, diagnosis, patient age, and experimental structure are shown in **Table 1**. A schematic representation of the human heart provides an overview about biopsy locations used for previous identifications of $CD90^+$ and $CD117^+$ endogenous CPCs (**Figure 1**).

In the current study, we obtained myocardium biopsies from 23 patients with the following diagnoses: dilatative cardiomyopathy (DCM), ICM, myocarditis, and controls from cardiac healthy. The collected material was characterized by immunohistochemistry. Currently, paraffin-based histopathological tissue analysis represents the main conventional method for confirmation of presence or absence of histological markers, grading, or the quantification of stem cells markers in ready tissue sections. Additional quantification of these histopathological slides using an automated image analysis perspective, though providing with more sensitive and qualitative information on the presence of local CPCs in myocardium biopsies, represents a new set of challenges. In our previous studies, we compared immunohistochemical data with an automated image analysis method of digitized slides by Definiens Tissue Studio software (Abraham et al., 2005; Kaemmerer et al., 2014; Neubauer et al., 2016). In several cases, we quantified tissue morphology, staining distribution and intensity of staining, using both automated image analysis and manually performed slides (Abraham et al., 2005; Kaemmerer et al., 2014; Neubauer et al., 2016). Interestingly, in this image analysis, the digital image processing is performed by digitized histological slides, which results in numerous advantages over the conventional immunohistochemical method.

In the present study, we combined a fully automated digital image analysis with conventional histological slides to more sensitively confirm the presence of potential local endogenous CPCs and to perform a quantitative analysis of the cardiac cell signals in human myocardium biopsies from patients with various cardiac diseases.

MATERIALS AND METHODS

Patients and Tissue Samples

Ready sections ($n = 69$) of paraffin-embedded human endomyocardial biopsies from 23 different patients were generously provided after the patient's consent by Prof. K. Klingel (Department of Molecular Pathology, University of Tuebingen, Germany). These biopsies were obtained from cardiac healthy subjects ($n = 3$), patients with myocarditis ($n = 3$), DCM ($n = 7$), or ICM ($n = 10$). The biopsies were derived from the right as well as from the left ventricular myocardium and septum. The mean age of the patients with DCM was 44 years, the average duration of illness amounted 18 years. Patients with ICM had a mean age of 58 years and an average duration of illness of 10 years. In addition, patients with myocarditis had a mean age of 24 years with duration of illness of 1–6 months.

TABLE 1 | Previous identifications of CD117 and CD90 in human along with patient age, diagnosis, and additional major details.

Stem cell marker	Biopsy location	Diagnosis	Patient age in years	Culture/biopsy	*In vivo/in vitro* expansion	Quantitative/qualitative analysis of CD117/CD90	Findings/comments	References
CD117	Outflow tract	Aortic stenosis ($n = 36$) Control hearts ($n = 12$)	73 ± 10 71 ± 8	Formalin-fixed tissue	–	IHC	Increased number of stem-like cells in aortic stenosis	Urbanek et al., 2003
CD117	Right ventricle	DCM ($n = 19$) Idiopathic DCM ($n = 10$) Control hearts ($n = 7$)	73 ± 2 61 ± 4 76 ± 4	Tissue sections from biopsies with a size of nearly 3 mm^3	–	IHC; Confocal microscopy	Cellular senescence and death of $CD117^+$ cells leads to HF and premature cardiac aging	Chimenti et al., 2003
CD117	Left ventricular wall	Acute infarcts ($n = 20$) End-stage post-infarction CM ($n = 20$) Control hearts ($n = 12$)	62 ± 13 56 ± 7 60 ± 20	Formalin-fixed tissue	–	IHC	Increased number of CPCs in acute and chronic infarcts	Urbanek et al., 2005
CD117	Right ventricle; Right atrial appendage	Heart transplant recipients ($n = 32$) Chronic ICM ($n = 18$)	45.8 ± 11 65.3 ± 8.1	Formalin-fixed, paraffin-embedded tissue; Culture of right atrial appendage specimens	*In vitro*	IHC; Immuno-fluorescence; Confocal laser microscopy; Flow cytometry	Higher number of $CD117^+$ cells in right ventricle than in atrial appendage; small number of $CD117^+$ cells in cultured right atrial appendages	Pouly et al., 2008
CD117	Right + left ventricle; Left atrium; Left atrio-ventricular junction; Apex	End-stage HF with ICM ($n = 20$) Control hearts ($n = 11$)	55 ± 5.5 41 ± 12	Formalin-fixed, paraffin-embedded tissue; Isolation and culture from fragments of left ventricular myocardium	*In vitro*	Immuno-fluorescence	Increased number of $CD117^+$ cells in ICM; Higher number of $CD117^+$ cells in the atrial subepicardium than in the myocardium	Castaldo et al., 2008
CD117 CD90	Ventricle	Endomyocardial biopsy ($n = 160$) Heart transplant ($n = 59$) Unexplained CM ($n = 12$)	Recipients: 52 ± 14 Donors: 32 ± 12 CM: 49 ± 15	Direct culture and expansion of CPCs from myocardial tissue	*In vitro*	IHC; Confocal microscopy; Flow cytometry	Expansion and proliferation of CPCs is simple	Davis et al., 2009
CD117	Right atrium	Coronary artery disease ($n = 30$)	38–72	Culture of biopsy tissue, non-enzymatic isolation of CSCs	*In vitro*	Flow cytometry	Number of CSCs is not influenced by disease severity or risk factors for coronary artery disease	Aghila Rani et al., 2009
CD117	Left ventricular walls	Hearts from patients who died from non-cardiovascular diseases ($n = 5$)	<1–75	Formalin-fixed, paraffin-embedded tissue	–	IHC	A subpopulation of $CD117^+$ cardiac cells may be authentic stem/progenitor cells	Zhou et al., 2010
CD117	Atrium	Coronary artery disease, Valvular disease, Atrial fibrillation ($n = 43$)	47–84	Directly isolated cells, monolayer and explant cultured cells	*In vitro*	Flow cytometry; RT-PCR	Number of CD117+ cells in directly isolated cells is lower than in monolayer culture	Sandstedt et al., 2010
CD117	Atrial appendage; Left ventricle	ICM ($n = 20$) Control hearts ($n = 11$)	55 ± 5.5 41 ± 12	Formalin-fixed, paraffin-embedded tissue; Epicardial cell culture from fragments of the appendages	*In vitro*	IHC; Immuno-fluorescence	Number of $CD117^+$ cells increased in ICM, higher number in epicardium than in myocardium; EDCs partially express CD117	Di Meglio et al., 2010

(Continued)

TABLE 1 | Continued

Stem cell marker	Biopsy location	Diagnosis	Patient age in years	Culture/biopsy	*In vivo/in vitro* expansion	Quantitative/qualitative analysis of CD117/CD90	Findings/comments	References
CD117	Left ventricle	Hearts from patients who died from non-cardiovascular diseases (n=74)	19–104	Formalin-fixed, paraffin-embedded tissue	–	ICC; Spectral Analysis	The female myocardium possesses more CSCs and younger myocytes than the male myocardium.	Kajstura et al., 2010
CD117 CD90	Atrium	ICM, Idiopathic CM, HCM, Valvular disease, Acromegaly ($n = 23$) Donor hearts ($n = 18$)	39–65 45.8 ± 15.7	Formalin-fixed, paraffin-embedded tissue; Isolation and expansion of CSCs	*In vitro*	Flow cytometry; Immunolabeling; RT-PCR; Spectral analysis	Number of $CD117^+$ cells was higher in explanted hearts than in donor hearts	Cesselli et al., 2011
CD117	Right atrial appendage	Patients with postinfarction LV dysfunction, treated ($n = 16$) Controls ($n = 7$)	56 ± 8.8 57.3 ± 8.9	Isolation, expansion and intracoronary re-infusion of autologous CSCs	*In vivo*	Immunolabeling; Confocal microscopy; Flow cytometry	No adverse effects after infusion of CSCs; Improvement in left ventricular systolic function; Increased functional capacity; Reduced left ventricular scar size	Bolli et al., 2011
CD117	Right atrial appendage	During routine procedure ($n = 30$)	–	Fixed tissue sections, freshly isolated or cultured CSCs	*In vitro*	IHC; ICC; Flow cytometry; RT-PCR	Tissue sections and freshly isolated cells contain CD117	He et al., 2011
CD117 CD90	Atrial appendages	Patients undergoing aorto-coronary bypass grafting	–	Atrial appendage tissue specimens and cultured cells	*In vitro*	Immuno-fluorescence; Confocal analysis; Flow cytometry; qRT-PCR	$CD117^+$ cardiac progenitors are primitive stem cells with multilineage differentiation potential; Possible relationship between $CD117^+$cells and a heart-specific MSC population	Gambini et al., 2011
CD117 CD90	Right portion of the septum; Apex of the left ventricle	Patients undergoing cardiac transplantation LVAD implantation ($n = 20$)	23–67	Collection and expansion of CSCs	*In vitro*	Flow cytometry	Successful isolation and expansion to a clinically relevant number for autologous delivery	D'Amario et al., 2011
CD117	Left ventricle; Atrial appendages	Patients undergoing cardiac surgery	67 ± 2	Isolation of mononuclear cells; Analysis of formalin-fixed, paraffin-embedded tissue	–	Flow cytometry; IHC	Number of CSCs is higher in atria than in left ventricle	Arsalan et al., 2012
CD117	Endo-myocardium	Pressure overloaded single right ventricles ($n = 8$) DCM ($n = 4$) Heart transplant ($n = 14$)	<1–19	Formalin-fixed, paraffin-embedded tissue;	–	IHC; Confocal microscopy	Number of $CD117^+$ cells is increased in human hearts exposed to pressure overload	Rupp et al., 2012
CD117	Right and left atrium	Patients undergoing cardiac surgery ($n = 17$)	32–79	Isolation and differentiation of side population cells	*In vitro*	Flow cytometry; RT-PCR	Identification of side population cells in left atrial biopsies	Sandstedt et al., 2012
CD117 CD90	Right atrium; Left ventricular epicardium	Chronic IHD ($n = 22$)	67 ± 2	Isolation and culture of explant- and CDCs	*In vitro*	Flow cytometry; Immuno-fluorescence	No routine culture of CDCs from ventricular epicardial biopsies; atrial and ventricular epicardial CDCs comprise few $CD117^+$ cells & a various number of $CD90^+$ cells	Chan et al., 2012

(Continued)

TABLE 1 | Continued

Stem cell marker	Biopsy location	Diagnosis	Patient age in years	Culture/biopsy	*In vivo/in vitro* expansion	Quantitative/qualitative analysis of CD117/CD90	Findings/comments	References
CD117	Atrial appendages	Oncologic patients with CHF ($n = 6$) and without CHF ($n = 2$) Control hearts ($n = 6$)	53 ± 6 63, 61 50 ± 9	Isolation and culture of CPCs and treatment with doxorubicin	*In vitro*	Immuno-fluorescence	Doxorubicin exposure adversely affects the population of CPCs and their function	Piegari et al., 2013
CD117	Atrial appendage	Patients with end-stage HF due to ICM undergoing heart transplants ($n = 9$) Control hearts ($n = 9$)	55.8 ± 3.1 50.4 ± 4.1	Isolation and proliferation of $CD117^+$ cells	*In vitro*	Immuno-fluorescence	$CD117^+$ cells do not reach terminal differentiation and functional competence in pathological conditions	Nurzynska et al., 2013
CD117	Atrium	Patients undergoing CABG surgery ($n = 3$)	52–65	Isolation and expansion of CSCs	*In vitro*	ICC; Flow cytometry	Characterization of ion-channels in $CD117^+$ cells from all patients	Zhang et al., 2014
CD117 CD90	Ventricle	DCM; ICM; CHD ($n = 32$)	<1–59	Enzymatic processing of heart tissue, Culture and differentiation of cardiospheres	*In vitro*	Immuno-fluorescence; Confocal microscopy; Flow Cytometry; RT-PCR	$CD117^+$ cells also expressed CD34, CD90, CD31, or CD144; $CD90^+$ cells expressed mesenchymal cell markers and showed incomplete differentiation into cardiomyocyte—like cells	Gago-Lopez et al., 2014
CD117 CD90	Right and left ventricle; Intra-ventricular septum, Atrium, Apex	Explanted hearts removed during heart transplant surgery, including IHD, DCM, HCM, congenital heart defect ($n = 26$)	3–65	Formalin-fixed, paraffin-embedded tissue; Isolation and primary cardiac cell culture from tissue fragments	*In vitro*	IHC; Flow cytometry	Identification of $CD117^+$ cells directly in myocardial tissue and $CD117^+$ and $CD90^+$ cells in cell culture	Matuszczak et al., 2014
CD117	Appendages	Patients undergoing cardiac surgery ($n = 105$)	1–78 (55.6 ± 17.0)	Isolation and culture of CSCs	*In vitro*	Flow cytometry	The percentage of $CD117^+$ CSCs decreases with age, DM and CHD	Hu et al., 2014
CD117	Right atrium; Left ventricle	Patients undergoing left ventriculoplasty due to ICM ($n = 10$)	65.1 ± 9.1	CSC isolation and culture	*In vitro*	ICC; Fluorescent microscopy	Successful preparation of $CD117^+$ CSCs	Hayashi, 2015
CD90	Atrium	Hypoplastic left heart syndrome ($n = 14$)	1.8 ± 1.5	Isolation and expansion of autologous CDCs followed by intracoronary infusion	*In vivo*	Flow cytometry	Intracoronary infusion of autologous CDCs is safe and practicable	Ishigami et al., 2015
CD117	Left ventricle	ICM and end-stage HF submitted to LVAD implantation ($n = 4$)	–	Formalin-fixed, paraffin-embedded tissue	–	IHC	CSCs are present in left ventricular apical segment of patients with LVAD implantation	Cameli et al., 2016
CD90	Right atrium	Patients who underwent heart surgery ($n = 26$)	2–83	Isolation and culture of CDCs	*In vitro*	Flow cytometry	Age has a limited influence on the quantity and quality of CDCs	Nakamura et al., 2016
CD117 CD90	Atrial appendage	Patients who underwent CABG surgery	–	Isolation, culture as CDCs, simulation of HR injury	*In vitro*	Flow cytometry	CDCs showed expression of CD117 and CD90, CDCs have greater resistance to HR injury compared to MSCs	RajendranNair et al., 2017

(Continued)

TABLE 1 | Continued

Stem cell marker	Biopsy location	Diagnosis	Patient age in years	Culture/biopsy	*In vivo/in vitro* expansion	Quantitative/qualitative analysis of CD117/CD90	Findings/comments	References
CD117	Right atrium; Left atrium; Left ventricle	Valvular heart diseases ($n = 8$); Patients receiving left ventriculoplasty ($n = 13$)	66.1 ± 10.0	Isolation and culture of CSCs from fresh and frozen tissue	*In vitro*	ICC	Cryopreservation has no influence on proliferative potential of CSCs	Hosoda et al., 2017
(Ishigami et al., 2015)CD90	Atrium	Single ventricle physiology ($n = 41$)	≤20	Isolation, expansion and intracoronary infusion of autologous CDCs	*In vivo*	Flow cytometry	Intracoronary infusion of CDCs improved cardiac function	Ishigami et al., 2017
CD117 CD90	Right ventricle; Left ventricle; Septum	DCM ($n = 7$) ICM ($n = 10$) Myocarditis ($n = 3$) Control hearts ($n = 3$)	DCM: 44 ICM: 58 Myocarditis: 24 Control hearts: 35 (mean values)	Formalin-fixed, paraffin-embedded tissue	–	IHC; Digital image analysis	Identification of $CD117^+$ and $CD90^+$ cells directly in myocardial tissue, CD117 is increased in ICM, DCM and myocarditis in comparison to control hearts	Present study

CABG, Coronary artery bypass graft; CDC, cardiosphere-derived cell; CHD, Coronary Heart Disease; CHF, congestive heart failure; CM, cardiomyopathy; CPC, cardiac progenitor cell; CSC, cardiac stem cell; DCM, dilatative cardiomyopathy; DM, Diabetes Mellitus; EDC, Epicardially-derived cell; HCM, hypertrophic cardiomyopathy; HF, heart failure; HR, hypoxia–reoxygenation; ICC, Immunocytochemistry; ICM, ischemic cardiomyopathy; IHC, Immunohistochemistry; IHD, ischemic heart disease; LVAD, Left ventricular assist device; MSC, mesenchymal stem cell; RT- PCR, real time polymerase chain reaction.

Control patients had a mean age of 35 years. Human skin tissue (University of Leipzig, Department of Orthopedics, Trauma and Plastic Surgery) was used as positive control, negative control, and IgG–control. The investigations were approved by the local ethics committee (050-2010-08032010) and conducted in accordance with the principles of the Declaration of Helsinki World Medical Association (1975). Control tissues also included human cerebellum (University of Leipzig, Neuropathology Department) and kidney (University of Leipzig, Institute of Pathology).

Immunohistochemistry

Two serial sections of each patient were utilized, one for CD90 staining and the other for CD117 staining, and a partial third one for CD105. The skin specimens were then embedded. The paraffin sections, 8–10 μm in thickness were cut with a rotary microtome (model RM2165; Leica Microsystems). The slides were deparaffinized and rehydrated. Afterwards, cells were blocked with 0.6% H_2O_2 in phosphate-buffered saline (PBS; pH 7.4) and washed in PBS/0.3% Triton-x. For antigen retrieval, the heat-induced epitope retrieval method was used. The slides were incubated in retrieval solution (10 mM citrate buffer) in a water bath set to 60°C overnight. On day 2, the slides were washed in PBS and blocked for 30 min at room temperature with 5% normal goat serum in PBS. Primary antibodies, in specific, CD90 [anti-CD90/Thy-1 antibody, rabbit monoclonal IgG, clone EPR3133, ab 133350 (dilution 1:100) Abcam Cambridge, UK] and CD117 [anti-c-kit/CD117 antibody, rabbit monoclonal IgG, clone YR145, ab 32363 (dilution 1:50) Abcam Cambridge, UK] were added and incubated overnight at 4°C. All primary antibodies are particularly suitable for immunohistochemistry of paraffin sections (IHC-P). For supplementary investigations, a further primary antibody was applied on an additional serial section [anti-CD105 antibody, rabbit monoclonal IgG, clone EPR10145, ab 169545 (dilution 1:200) Abcam Cambridge, UK]. Negative control staining was performed whereby the primary antibody was omitted. As isotype control served rabbit monoclonal IgG [clone EPR25A, ab172730 (dilution 1:100) Abcam Cambridge, UK]. The images of the positive and negative controls can be found in the Supplementary Material.

On day 3, the slides were washed in PBS and incubated with the secondary antibody [secondary horseradish peroxidase conjugated goat anti-rabbit IgG (H + L), 111-035-003 (dilution 1:100 in PBS + 1% goat serum + 1% human serum), Dianova Jackson Immuno-research Hamburg, Germany], for 45 min at room temperature, followed by incubation with 3-amino-9-ethyl-carbazole (AEC) in sodium acetate buffer (0.1 mol/L, pH 5.2) containing hydrogen peroxide. After rinsing, the sections were counterstained with hematoxylin Lillie's modification (ready-to-use formulation; DakoCytomation, Copenhagen, Denmark) and mounted in glycergel (Kaiser's glycerol gelatine; Merck KGaA, Darmstadt, Germany).

Image Analysis

Scanning of the complete slide was performed by Virtual Microscope Olympus VS 120 (Ruhr-University Bochum Faculty

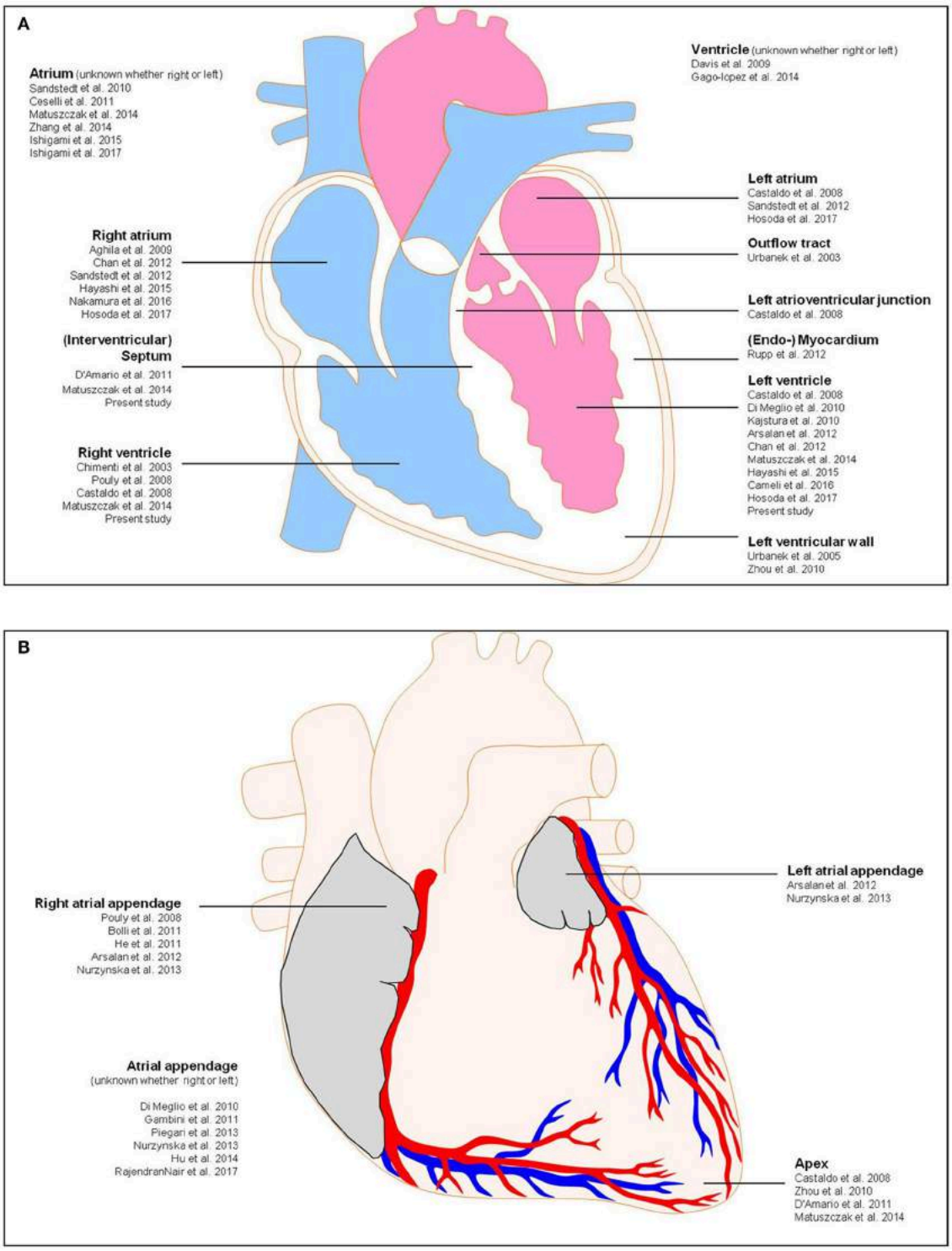

FIGURE 1 | Schematic representation of the human heart showing biopsy locations used for previous identifications of CD117 and CD90. **(A)** Anterior view, **(B)** frontal section. Detailed information about the previous studies is shown in **Table 1**.

of Medicine, Anatomy and Molecular Embryology). Individual image processing and optimization were performed via cellSens Software (OLYMPUS Germany). Fully automatic image analysis using the Definiens Tissue Phenomics® Technology (DEFINIENS AG, Munich, Germany) and the image analysis platform Developer XD enabled a quantitative image analysis

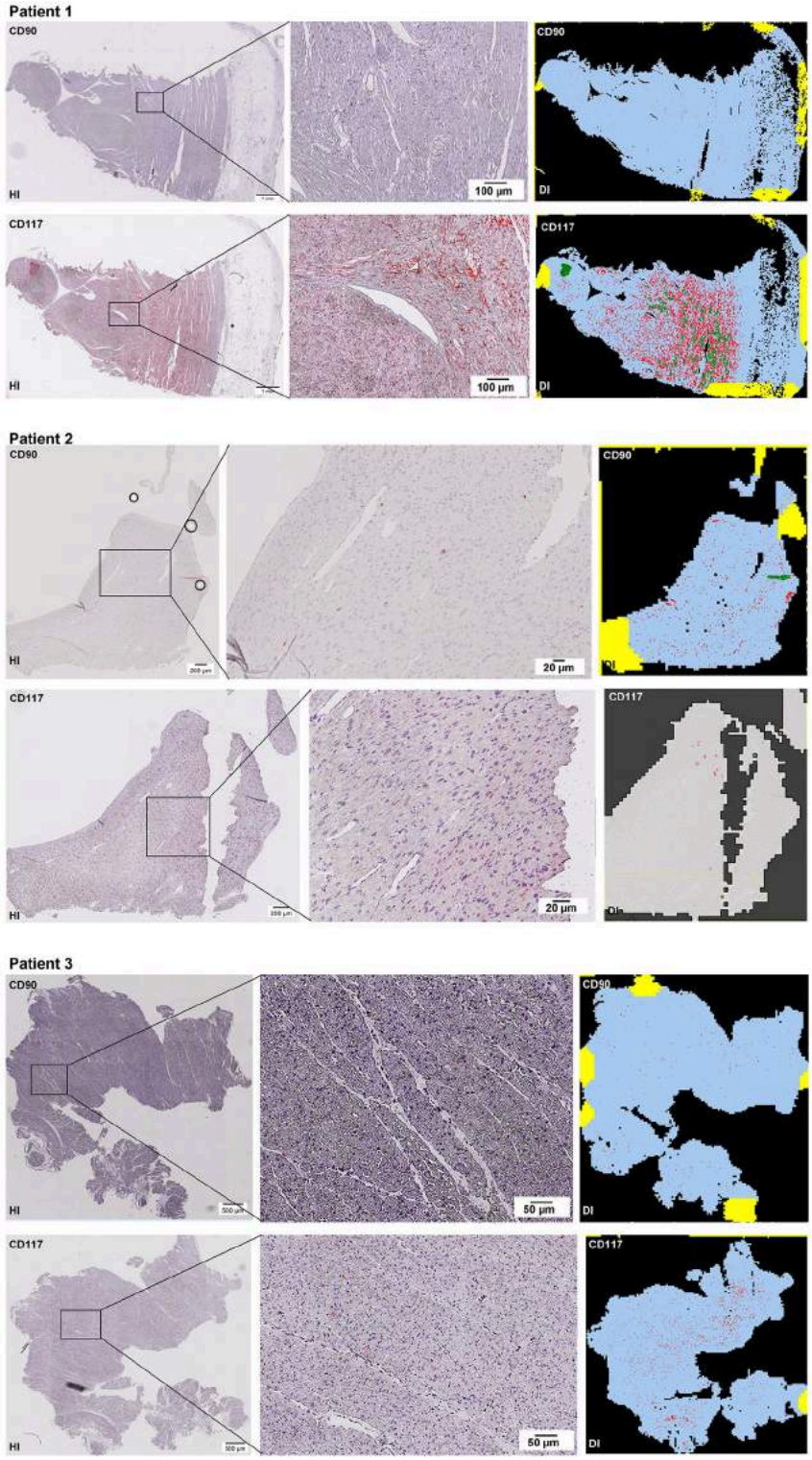

FIGURES 2–10 | Histological and digital images of all tissue sections ($n = 92$). *(HI)* Histological whole slide images scanned with virtual slide microscope VS120 and *(DI)* reprocessed images, resulting from digital image analysis using the Definiens Tissue Phenomics® Technology. **(2)** Healthy cardiac patients, **(3)** patients with Myocarditis, **(4-7)** patients with ICM, **(8-10)** patients with DCM. Full-size images are available for download (https://figshare.com/s/13e838d63dfeac772894).

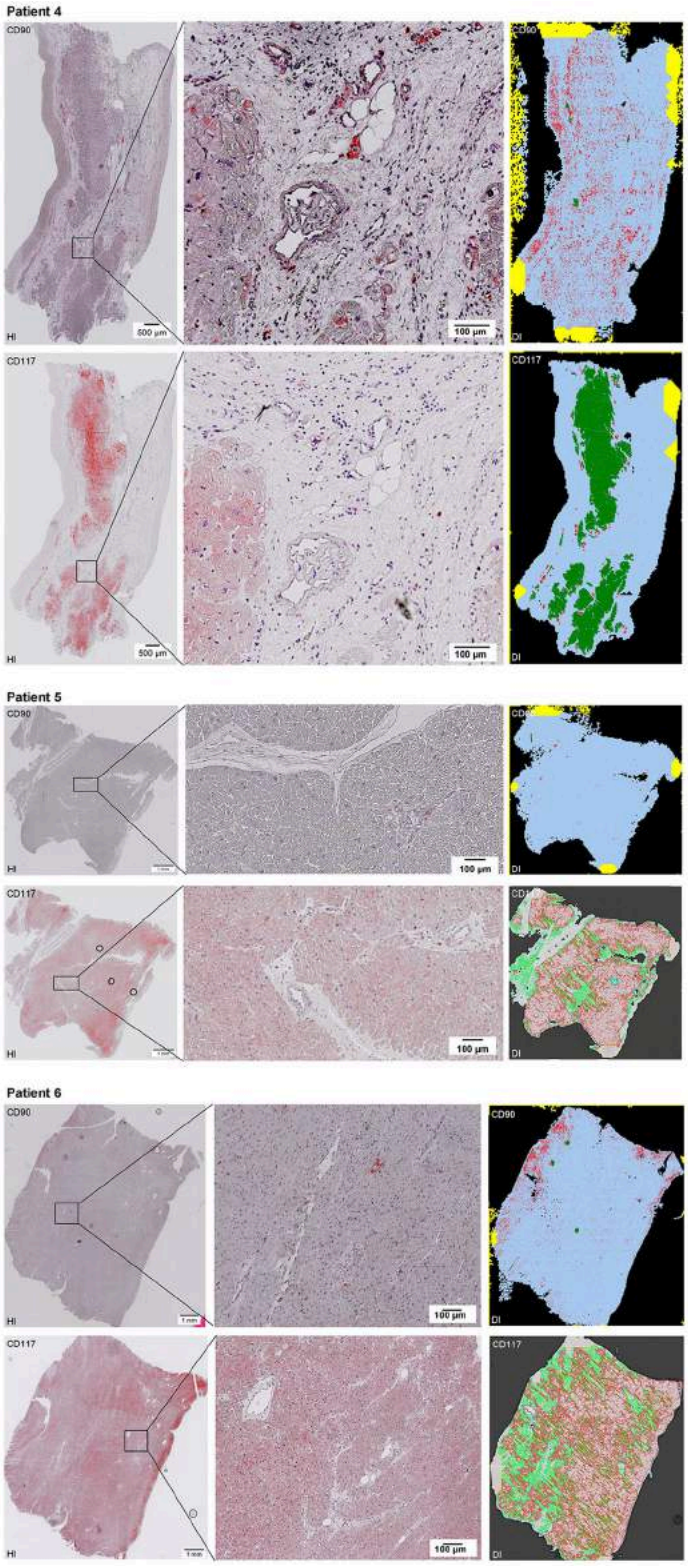

FIGURE 3 | See **Figure 2**.

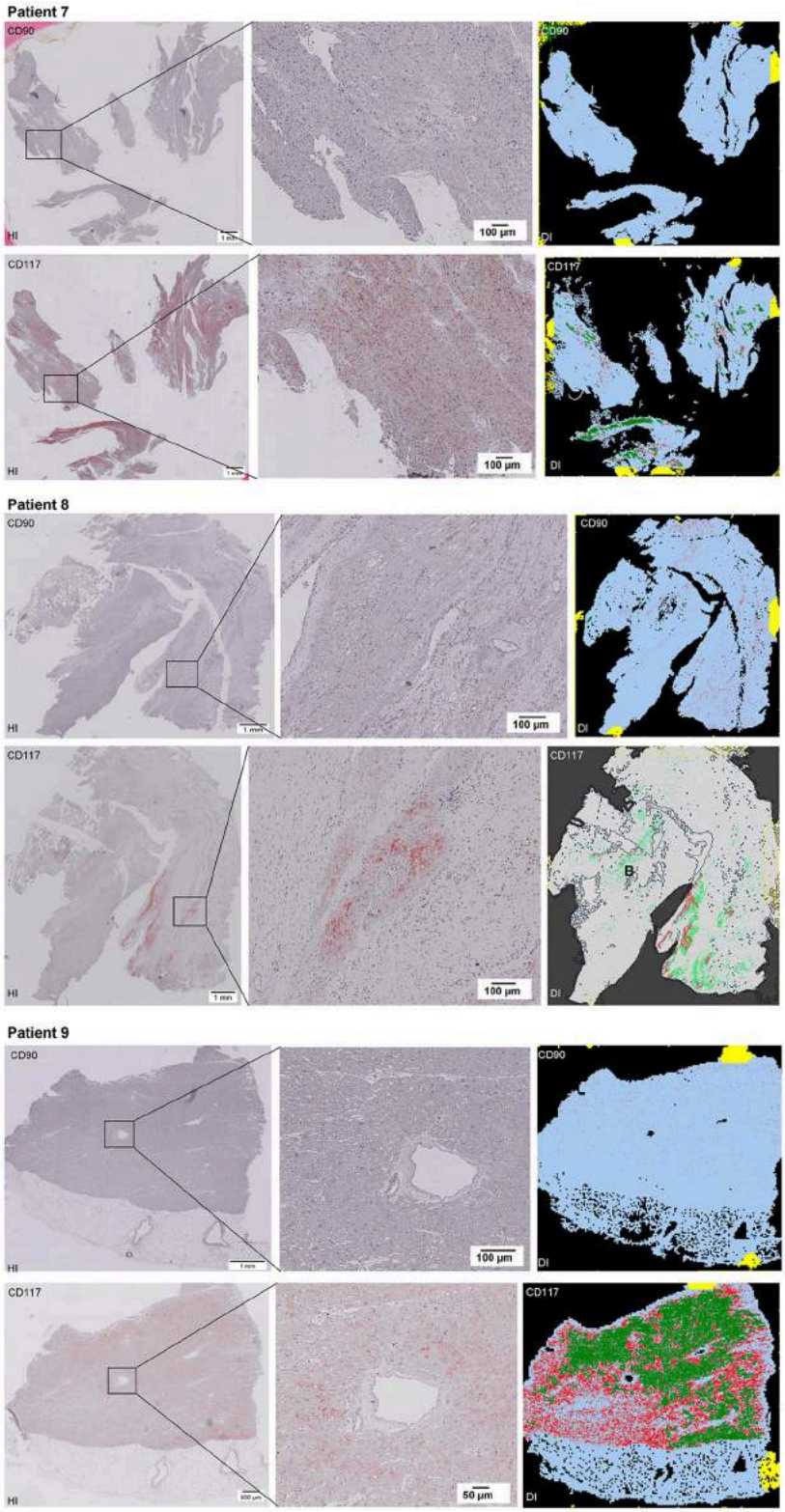

FIGURE 4 | See **Figure 2**.

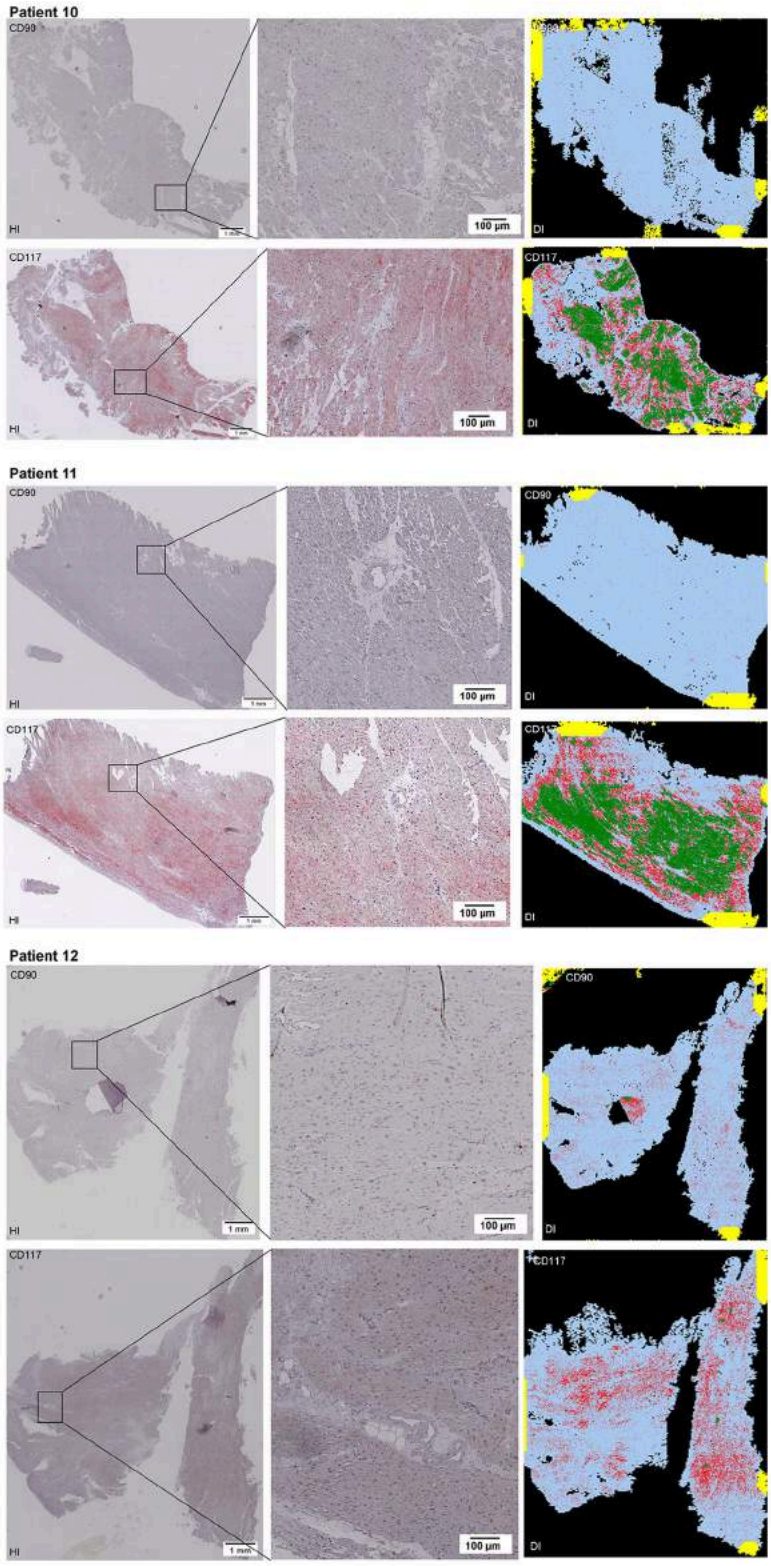

FIGURE 5 | See **Figure 2**.

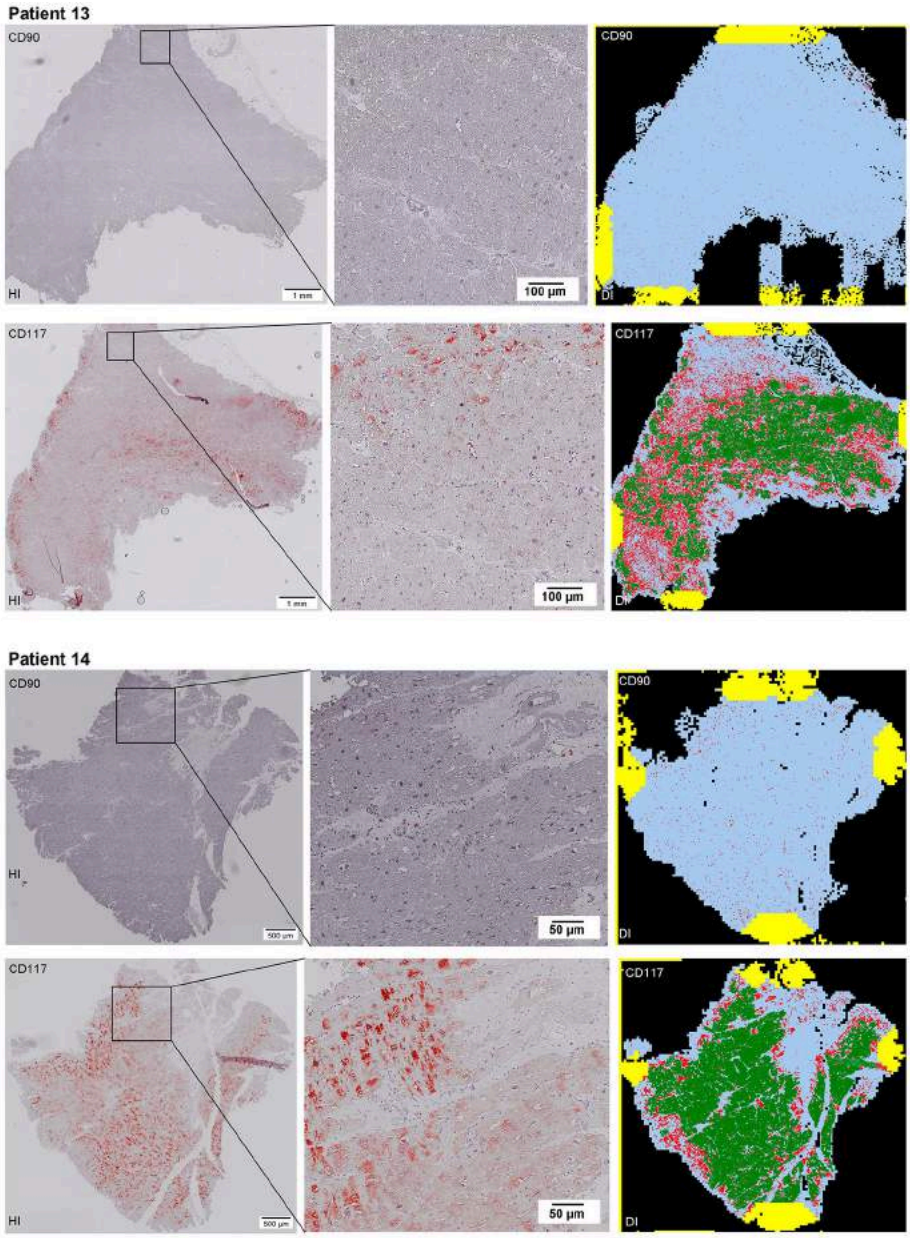

FIGURE 6 | See **Figure 2**.

of the whole slide. The analysis was made with the original image files (*vsi), which were created by the Olympus Virtual Slide Microscope using the 20x objective and have a very high resolution until the cellular level. A tailored image analysis solution (rule set) was developed using Definiens AG Software. The rule set separated first foreground (tissue regions) from the background (image regions without tissue) and excluded tissue along the edge to avoid artifacts. In the next step, the solution segmented and classified signals according to their individual morphology and their relative staining intensity. Afterwards, the solution reclassified the signals into two groups: in single signals and concatenated signals. The relative number of $CD90^+$ signals (total number of signals divided by the total area of tissue section), the relative area of $CD90^+$ signals and relative area of $CD117^+$ signals (total area of signals divided by the total area of tissue section) were calculated.

To classify the cells as local progenitor cells, the detection of several stem cell markers was necessary. As we utilized only one antibody per slide, the identification of cells with co-expression of several markers was done through visual comparison of two or rather three serial sections each. A representative field

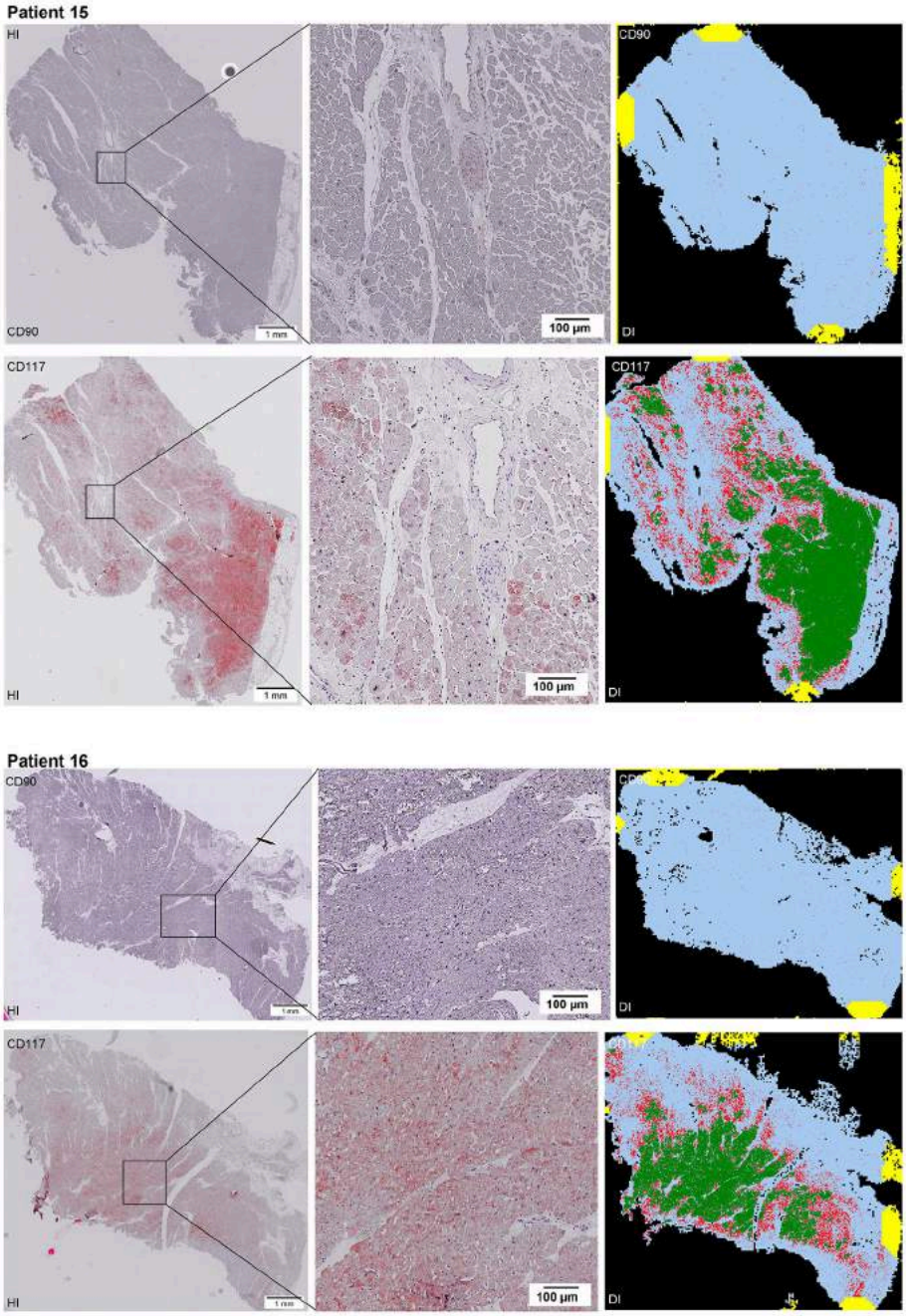

FIGURE 7 | See **Figure 2**.

(4 mm^2) with high histological quality was chosen to account for the variable size of the tissue samples. The total number of cells, which expressed both stem cell markers, CD90 and CD117, was counted and normalized per square millimeter. This procedure was performed in three examples of each group; the ones that had the best histological quality were chosen.

Statistics

The data obtained from digital image analysis are best analyzed on the logit scale [logit $(p) = \log (p/(1 - p))$]. Analyses were performed in Microsoft Excel 2007. The statistical significance of differences between groups was evaluated by ANOVA (analysis of variance, one way), followed up by a *post-hoc* test (Tukey-Kramer method). $P < 0.05$ was considered statistically significant. The

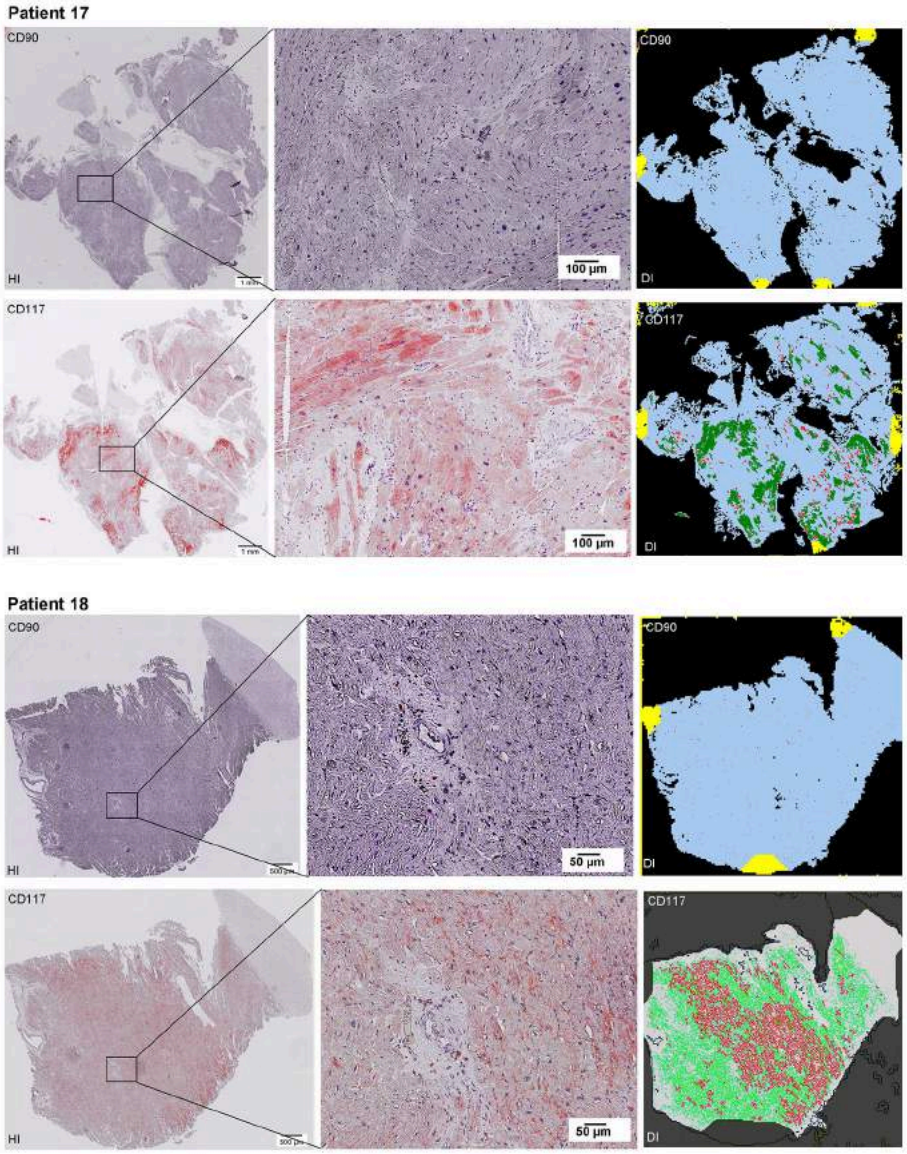

FIGURE 8 | See **Figure 2**.

results from co-expression analysis were expressed as the mean ± standard deviation.

RESULTS

Identification of CD90$^+$ and CD117$^+$ Cells

Scanning of the whole slide enabled a detailed view of the tissue sections in entirety and provided the basis for creating new images for the digital image analysis (**Figures 2–10**; high resolution images are available for download here: https://figshare.com/s/13e838d63dfeac772894). The histological analysis showed positive CD90 and CD117 signals in every group. CD90$^+$ cells were detected as individual signals between the cardiomyocytes. In contrast, the CD117$^+$ signals were identified both in cardiomyocytes and in cells which are located between the muscle cells. In many patients, the CD117 staining of the cardiomyocytes seems to predominate and only few signals in the interstitium were proved.

The digital image analysis facilitated a specialized quantitative analysis of the whole slide to CD90$^+$ and CD117$^+$ signals. The relative *number* of CD90$^+$ signals (total number of signals divided by the total area of tissue section) and the relative *area* of CD90$^+$ signals (total area of signals divided by the total area of the tissue section) were calculated (**Table 2**). On comparison of the acute and chronic disease states of the heart in this study, it is striking to see that the highest expression of CD90$^+$ cells was detected in the myocarditis group (**Figure 11A**). ICM and DCM groups have similar numbers of CD90$^+$ cells or even

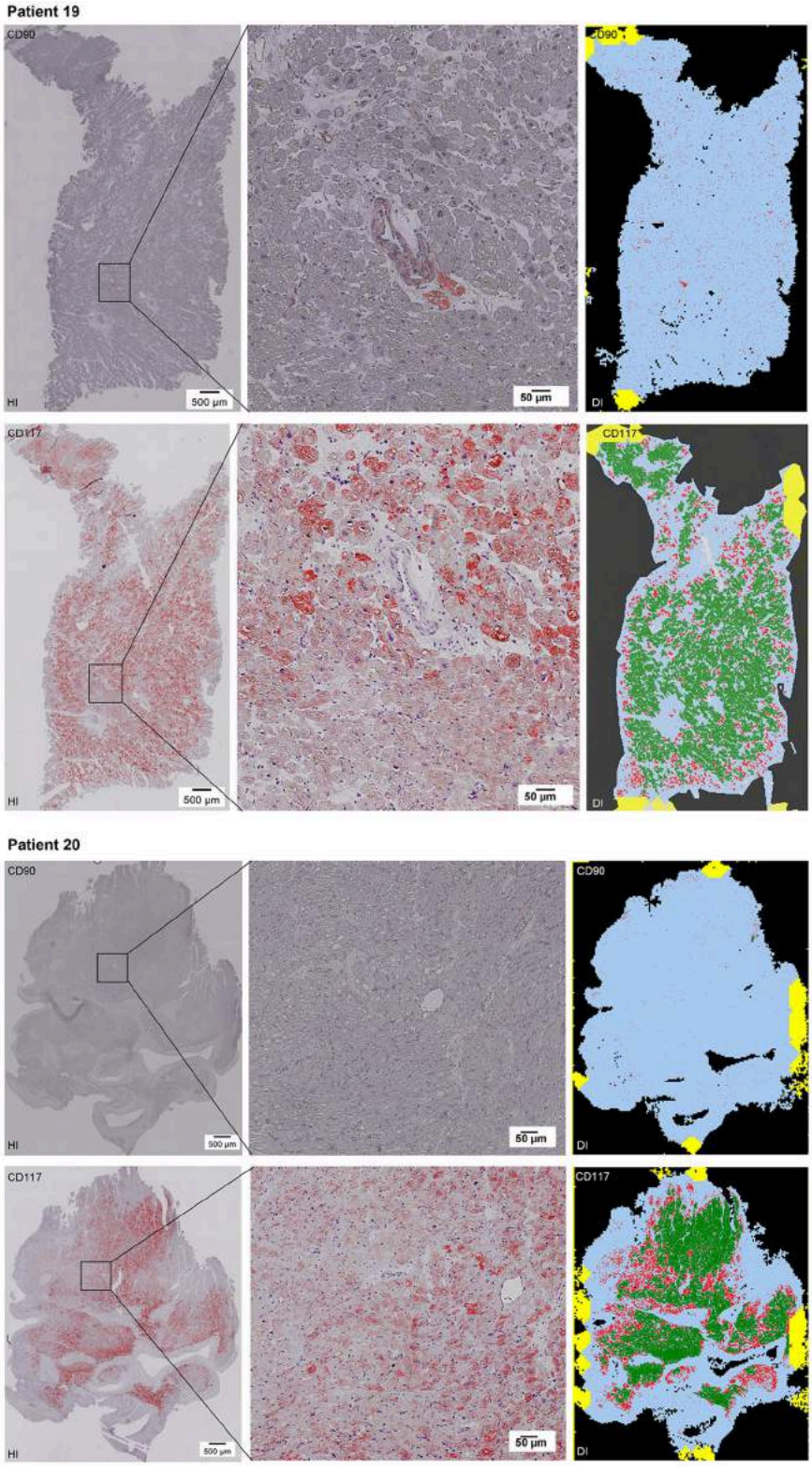

FIGURE 9 | See **Figure 2**.

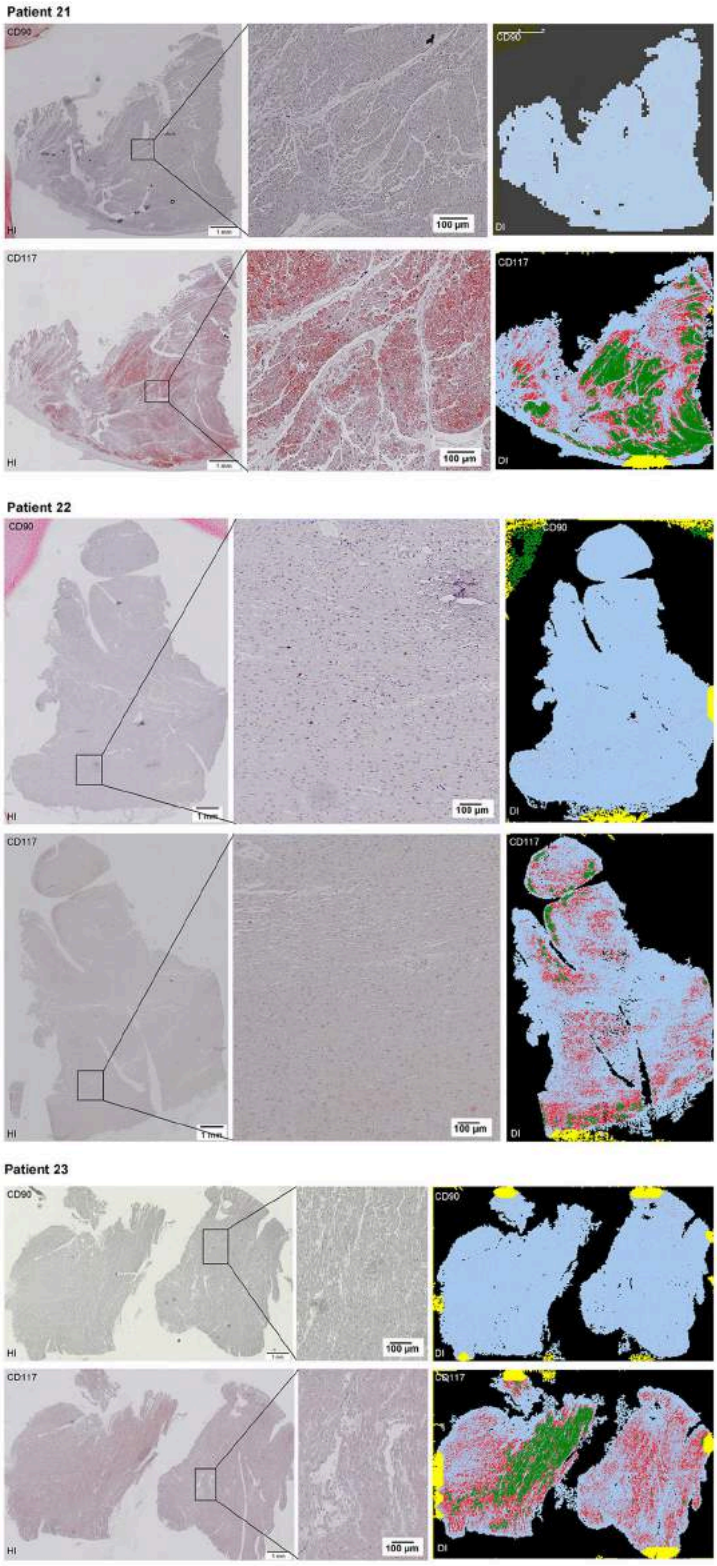

FIGURE 10 | See **Figure 2**.

lower, in comparison to healthy cardiac patients. The relative area of CD90 (**Figure 11B**) correlates with the relative number of $CD90^+$ signals. The greatest relative area of CD90 was found in the myocarditis group, even though no statistical evidence for group differences was detected.

As CD117 staining included not only individual signals but also larger stained areas, the focus was set on the relative area of $CD117^+$ signals (total area of signals divided by the total area of the tissue section) and not on the number of $CD117^+$ signals (**Table 2**). The relative area of $CD117^+$ signals is significantly increased in all three disease states: myocarditis, ICM and DCM, compared to healthy patients ($p < 0.05$; **Figure 12**).

Co-Expression of CD90 and CD117

The co-localized signals were evaluated and counted manually, based on the comparison of the histological images. $CD90^+$ cells, which were co-localized with CD117, were identified in all patient groups (**Figure 13**). The lowest number of cells with co-expression was found in the group of cardiac healthy (1 ± 0.43 $CD90^+CD117^+$ cells/mm^2), followed by DCM group (1.67 ± 0.58 cells/mm^2) and patients with ICM (4 ± 1.89 cells/mm^2; **Figure 14**). Patients with myocarditis had by far the highest number of cells with co-expression (6.75 ± 3.25 cells/mm^2). These results also support our previous described outcome of an increase of CD90 and CD117, especially in myocarditis. The $CD117^+$ signal directly in the cardiomyocytes was not detected in the CD90 stained sections. We conclude that these cells do not belong to the local progenitor cells. Furthermore, on some selected tissue samples we analyzed a third stem cell marker, CD105, and we identified cells with expression of all three stem cell markers (**Figure 15**).

DISCUSSION

Numerous stem cell markers were analyzed especially referring to CPCs. In the present study, the focus was mainly set on the co-expression of CD90 and CD117 in the human heart, which was already demonstrated (Gambini et al., 2011). In general, the CD90 marker is considered as a fibroblast marker but is also known as a mesenchymal stem cell (MSC) marker. Cardiac fibroblast research has been tremendously accelerated in the last decade (Gourdie et al., 2016). The novel therapeutic strategies

TABLE 2 | Detailed patient information including biopsy location, diagnosis, and results of the digital image analysis ($n = 23$).

Patient ID	Biopsy location	Diagnosis	Total number of $CD90^+$ signals per tissue section	Relative number of $CD90^+$ signals per tissue section	Relative area of $CD90^+$ signals per tissue section	Relative area of $CD117^+$ signals per tissue section
Patient 1	Right ventricle	Healthy	1,766	0.00006964	0.00657148	0.15489015
Patient 2	Ventricle	Healthy	986	0.00034775	0.02691154	0.00128155
Patient 3	Ventricle	Healthy	357	0.00003978	0.00351804	0.02040115
Average			1,036	0.00015239	0.012333687	0.058857617
Patient 4	Septum	Myocarditis	14,493	0.00073061	0.08861789	0.28542232
Patient 5	Septum	Myocarditis	870	0.00004446	0.00457649	0.60600118
Patient 6	Septum	Myocarditis	13,860	0.00035446	0.04414038	0.64796254
Average			9,741	0.00037651	0.045778253	0.51312868
Patient 7	Septum	ICM	3,003	0.00009935	0.00788957	0.07027659
Patient 8	Left ventricle	ICM	7,000	0.00021093	0.01858989	0.01535276
Patient 9	Left ventricle	ICM	1,562	0.00008959	0.00703351	0.41275665
Patient 10	Septum	ICM	3,566	0.00013633	0.01256228	0.40487681
Patietn 11	Septum	ICM	1,230	0.00006138	0.00538673	0.48448345
Patient 12	Septum	ICM	12,254	0.00055332	0.04938569	0.13488475
Patient 13	Left ventricle	ICM	1,977	0.00008794	0.00760771	0.48799854
Patient 14	Left ventricle	ICM	1,190	0.0001929	0.01611067	0.57780017
Patient 15	Left ventricle	ICM	781	0.00003774	0.00313921	0.41058415
Patient 16	Left ventricle	ICM	793	0.00004349	0.00341586	0.32906417
Average			3,336	0.000151297	0.013112112	0.332807804
Patient 17	Left ventricle	DCM	1,634	0.00005087	0.00423627	0.15127794
Patient 18	Septum	DCM	626	0.00004535	0.00356114	0.21075096
Patient 19	Septum	DCM	4,203	0.00022521	0.01916202	0.45260291
Patient 20	Left ventricle	DCM	1,388	0.00006808	0.00492588	0.3632407
Patient 21	Septum	DCM	96	0.00000503	0.00120728	0.36082968
Patient 22	Left ventricle	DCM	3,251	0.00008052	0.00644762	0.1610318
Patient 23	Septum	DCM	3,808	0.00011138	0.00938711	0.30622664
Average			2,144	8.37771E-05	0.006989617	0.286565804

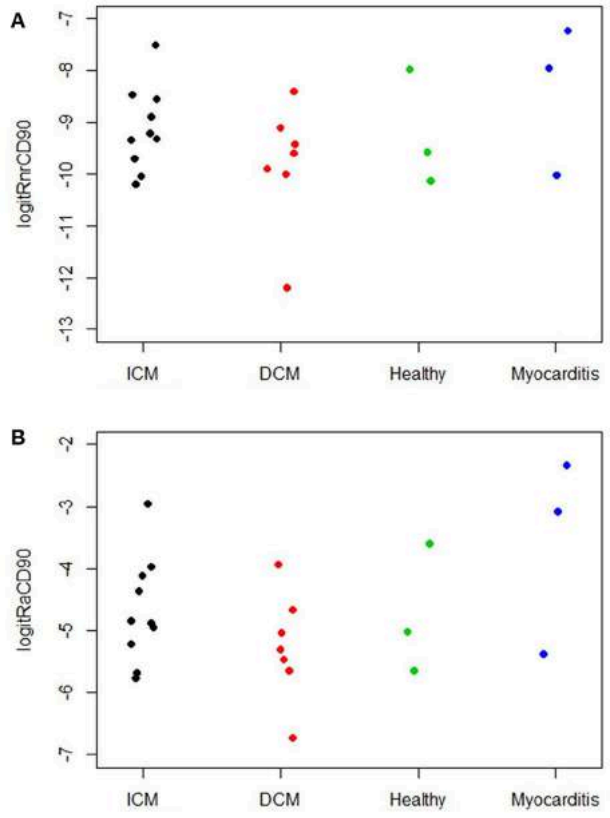

FIGURE 11 | (A) Relative *number* of CD90$^+$ cells per tissue section ($n = 23$). The X axis designates the patient groups: ICM ($n = 10$), DCM ($n = 7$), Healthy ($n = 3$), and Myocarditis ($n = 3$). The Y axis presents the relative number of CD90$^+$ signals (total number of signals divided by total area of tissue section; **Table 2**), converted to the logit scale [logit(p) = log (p/(1 – p))]. Individual values of the patients are presented as spots. **(B)** Relative *area* of CD90 per tissue section ($n = 23$). The X axis designates the patient groups: ICM ($n = 10$), DCM ($n = 7$), Healthy ($n = 3$), and Myocarditis ($n = 3$). The Y axis presents the relative area of CD90$^+$ signals (total area of signals divided by total area of tissue section; **Table 2**), converted to logit scale [logit(p) = log (p/(1 – p))]. Individual values are presented as spots.

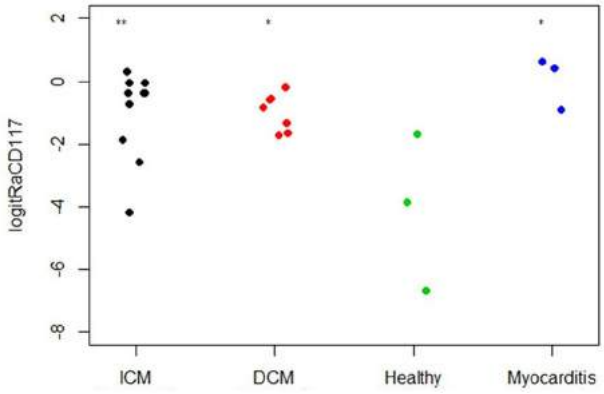

FIGURE 12 | Relative *area* of CD117 per tissue section ($n = 23$). The X axis designates the patient groups: ICM ($n = 10$), DCM ($n = 7$), Healthy ($n = 3$), and Myocarditis ($n = 3$). The Y axis presents the relative area of CD117$^+$ signals (total area of signals divided by total area of tissue section; **Table 2**), converted to logit scale [logit(p) = log (p/(1 – p))]. Individual values are presented as spots. The expression of CD117 is significantly higher in ICM, DCM and Myocarditis, compared to healthy (*$P < 0.05$ vs. healthy, **$P < 0.01$ vs. healthy).

in heart diseases with special focus on fibroblasts are reviewed elsewhere (Gourdie et al., 2016). In our previous studies, we have shown the multilineage potential of skin-derived CD90$^+$ cells (Lorenz et al., 2008). Moreover, we have successfully treated acute and chronic diabetic wounds and skin ulcer of human cases by activation of local progenitor cells (Bader et al., 2011; Günter et al., 2013). In our opinion, it is important to note that the CD90 marker characterizes seemingly opposing states of cells; on the one hand fibroblasts involved in scar formation, but on the other hand, stem or progenitor cells, which could induce functional tissue regeneration. We believe that those CD90$^+$ progenitor cells reside in local organs and are activated after injury. Previously, we have studied CD90 progenitor cells of the skin and shown their dependence toward localized cytokine stimulation for proliferation (Lorenz et al., 2008) and we proved the proliferation of local CD90$^+$ progenitor cells after injury in the liver (unpublished data). Acute myocarditis is a process that is characterized by intense local inflammation as well. Even though the myocarditis group in the present experiments was very small ($n = 3$) due to the limited availability of the samples, the high expression of CD90$^+$ cells corresponds to the fact that myocarditis patients more frequently undergo a complete healing pattern. The progenitor cell activation in myocarditis may explain the better functional outcome with less or no scar presence allowing the localized functional regeneration of cardiac tissue. In contrast, chronic disease states showed a depletion of CD90$^+$ cells, correlating clinically to the unsuccessful healing outcomes.

Moreover, various researchers identified CD117$^+$ cells in human myometrium (Ciontea et al., 2005), human fallopian tube (Popescu et al., 2005), human mammary gland stroma (Radu et al., 2005) as well as in human atrial myocardium (Hinescu et al., 2006), and ventricular myocardium (Popescu et al., 2006). We have proved here, that the number of CD117$^+$ cells is upregulated in the diseased heart, especially in myocarditis. Our results validate the findings of previous studies; the number of CD117$^+$ cells is increased in several cardiac diseases, for instance in advanced heart failure and aortic stenosis (Urbanek et al., 2003; Kubo et al., 2008; Itzhaki-Alfia et al., 2009). The human heart possesses a cardiac stem cell pool (Urbanek et al., 2005). The activation of the local stem cells occurs in response to ischemic injury. The stem cell pool has a crucial role in the regeneration of infarction heart (Urbanek et al., 2005). Matuszczak et al. reported that there are no differences in the number of CD117$^+$ cells between various disease groups (Matuszczak et al., 2014). However, they had not used control tissue from healthy patients.

CD117$^+$ local CPCs had already been used for the treatment of heart diseases in both human cases and animal models (Bolli et al., 2011). The method involves the isolation of autologous CD117$^+$ cells, expansion *in vitro* and injection of those in high numbers (Bolli et al., 2011).

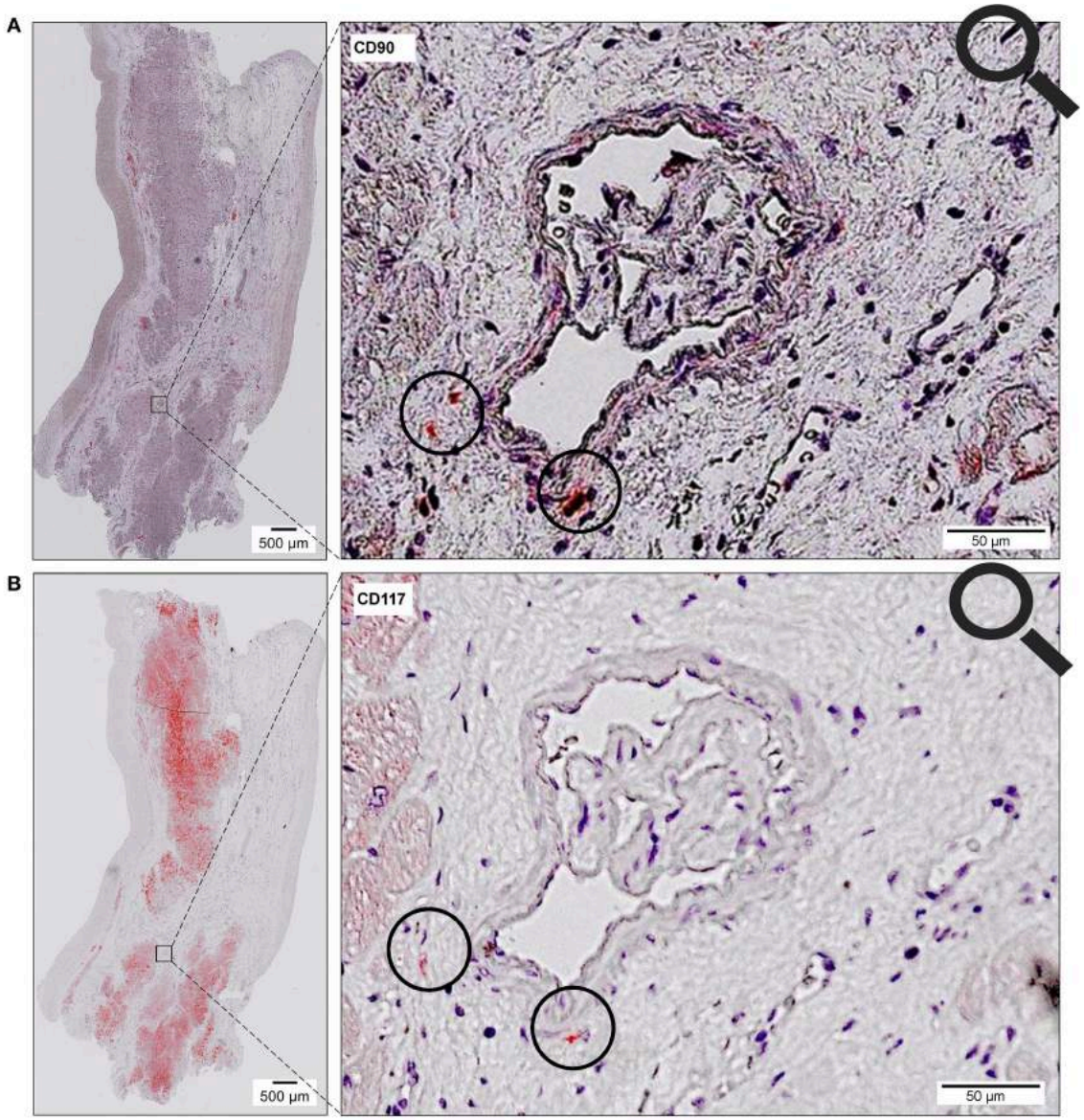

FIGURE 13 | Coexpression of CD90 and CD117. Two serial sections of the same patient (Patient 4) are stained with different antibodies (**A**, CD90; **B**, CD117). The circle shows cells with co-expression of both stem cell markers ($CD90^+$ on 1st slide, $CD117^+$ on 2nd slide).

In comparison with conventional stem cell therapy, the activation of local endogenous progenitor cells is a holistic approach to both preventing and regulating the heart. We are aware that the characterization of progenitor cells requires the identification of various stem cell markers and it is of high importance to exclude unspecific signals. Here, we analyzed the co-expression of CD117, CD90, and partially CD105, also. Previous studies underline our analyses: Gambini and colleagues demonstrated a co-expression of CD117 and CD90 or rather CD105 in human heart auricle primary cultured cells (Gambini et al., 2011). Several other studies also identified $CD117^+$ cells which were positive for CD105 and CD90, too (Li et al., 2012; Matuszczak et al., 2014). CD90 and CD105 were detected on cardiosphere-derived cells (CDCs) (Smith et al., 2007; Davis et al., 2009; Mishra et al., 2011; Chan et al., 2012). A series of other markers was proven on $CD117^+$ cells, including CD29, CD44, CD31, CD34, and Sca1 (Gambini et al., 2011; Fang et al., 2012; Matuszczak et al., 2014). Furthermore, it was already displayed that CD117+ cardiac stem cells are negative for CD45 (Matuszczak et al., 2014) and that not all $CD117^+$ cells are mast cells (Kubo et al., 2008; Zhou et al., 2010).

Vicinanza et al. also showed that cardiac $CD117^+/CD45^-$ cells are clonogenic and multipotent, but they determined that >90% of cardiac $CD117^+$ cells contain endothelial cells and

their precursors (Vicinanza et al., 2017). They demonstrated the myogenic and regenerative potential of $CD117^+/CD45^-$ cells in the damaged myocardium after injection of $CD117^+/CD45^-$ cells into damaged myocardium. Therefore, they conclude that CD117 is still an essential marker for CPCs (Vicinanza et al., 2017).

Nevertheless, future experiments with additional stem cell markers are necessary to prove the progenitor cell identity of $CD117^+$ cardiac cells and to exclude unspecific labeling. We identified many $CD117^+$ stained cardiomyocytes, which do not belong to the local progenitor cells. Other researchers studied $CD117^+$ hematopoietic bone marrow cells and their ability to act as cardiac progenitors and to transdifferentiate into cardiomyocytes (Orlic et al., 2001; Rota et al., 2007). Rota et al. reported that $CD117^+$ bone marrow cells lose their hematopoietic CD45 phenotype and obtain a cardiomyocyte phenotype (Rota et al., 2007). Probably these cells were also enriched in cases of inflammation or other pathological conditions. Further studies would be necessary to analyze this kind of cells.

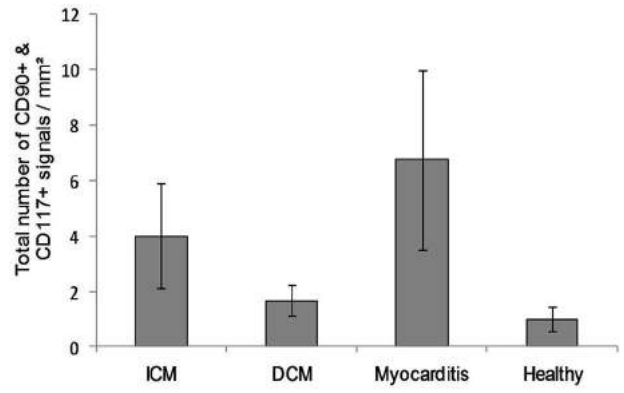

FIGURE 14 | A number of cells with co-expression of CD90 and CD117 per square millimeter ($n = 12$). The data are expressed as mean ± standard deviation. The Myocarditis patient group displayed the most cells with co-expression of both stem cell markers.

In the present study, it was not our purpose to perform a series analysis of cardiac stem cell markers. Rather than that, the present study mainly focuses on investigating the combination of a traditional histological method with a novel digital image analysis technology. This technology enables a quantitative evaluation of two CPC markers in comparison of paraffin–embedded tissue sections of healthy and diseases heart samples. It would be of high interest to complement these experiments with other techniques such as immunofluorescence and high magnification confocal microscopy in the future.

In the present experiment, we identified $CD90^+$ and $CD117^+$ cells in all patient groups: Myocarditis, ICM, DCM, and healthy cardiac patients. With the novel digital image analysis technology, a comparison of differently sized paraffin-embedded tissue sections is available. Taking into consideration that the sample size in the present experiment was limited, we proved an increase of $CD90^+/CD117^+$ cells in acute myocarditis. This finding supports our theory that endogenous cardiac stem or progenitor cell activation is part of the repairing mechanism after acute myocardial damage, as in cases of acute myocarditis. A similar inflammation process is described for acute myocardial infarction. Nevertheless, in most cases, acute myocardial infarction leads to the development of a scar. Further studies may show, how an amplification of the local myocardial stem or progenitor cell activation may contribute to the myocardial regeneration and healing process.

CONCLUSION

This study aimed at the identification and the quantitative analysis of $CD90^+$ and $CD117^+$ cardiac cells from human myocardium biopsies of 23 patients. Besides the conventional histological image analysis, the digital image analysis enabled a computer-based immunohistochemical quantification of some stem cell markers, using whole-slide images created by the virtual slide scanning microscopy. In our experiments, the number of CD90 and CD117 signals in patients with myocarditis was higher than in all other groups. Taking into consideration

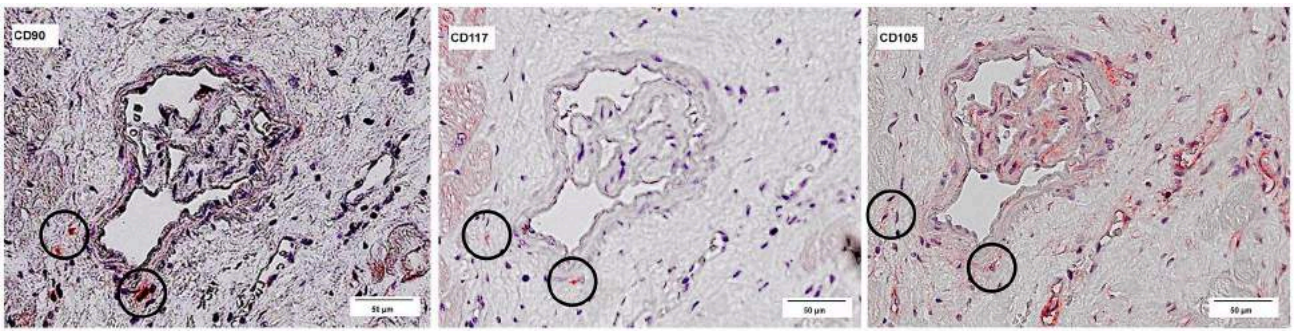

FIGURE 15 | Co-expression of CD90, CD117, and CD105. Three serial sections of the same patient (Patient 4) are stained with different antibodies: CD90, CD117, and CD105. The circles mark cells, which are positive for all three antibodies.

the regenerative healing potential prospects of myocarditis, it is likely that there is a relation between CD90 and CD117 expression and clinical outcome. Future studies with larger sample size are necessary to confirm that theory. The proof on the existence of endogenous resident progenitor cells not only in the healthy but also in the diseased human heart opens up the promising concept of regeneration instead of repair, which has an impressive scope in treating or preventing cardiovascular diseases.

AUTHOR CONTRIBUTIONS

MG, JS, SE, SG, and AB: conceived and designed the experiments; NS, WM, and JS: organized the human tissue samples; MG and SE: performed the experiments; MG, SE, BB-S, and MA: analyzed the data; MG, JS, SE, SG, AB, and MA: wrote the paper; SG and AB: provided guidance on the whole study.

FUNDING

The study is funded by University of Leipzig, Germany.

ACKNOWLEDGMENTS

Special thanks are extended to Prof. Dr. med. K. Klingel (Department of Molecular Pathology, University of Tuebingen, Germany) for providing the human endomyocardial biopsies and Prof. Dr. med. Christian Wittekind (Institute of Pathology, University of Leipzig, Germany) for providing human kidney tissue.

SUPPLEMENTARY MATERIAL

The Supplementary Material for this article can be found online at: https://www.frontiersin.org/articles/10.3389/fgene.2018.00072/full#supplementary-material

REFERENCES

Abraham, B. K., Fritz, P., McClellan, M., Hauptvogel, P., Athelogou, M., and Brauch, H. (2005). Prevalence of $CD44^{+}/CD24^{-/low}$ cells in breast cancer may not be associated with clinical outcome but may favor distant metastasis. *Clin. Cancer Res.* 11, 1154–1159. Available online at: http://clincancerres.aacrjournals.org/content/11/3/1154.long

Aghila Rani, K. G., Jayakumar, K., Sarma, P. S., and Kartha, C. C. (2009). Clinical determinants of ckit-positive cardiac cell yield in coronary disease. *Asian Cardiovasc. Thorac. Ann.* 17, 139–142. doi: 10.1177/0218492309103292

Altarche-Xifró, W., Curato, C., Kaschina, E., Grzesiak, A., Slavic, S., Dong, J., et al. (2009). Cardiac c-kit+AT2+ cell population is increased in response to ischemic injury and supports cardiomyocyte performance. *Stem Cells* 27, 2488–2497. doi: 10.1002/stem.171

Anversa, P., Kajstura, J., Leri, A., and Bolli, R. (2006). Life and death of cardiac stem cells: a paradigm shift in cardiac biology. *Circulation* 113, 1451–1463. doi: 10.1161/CIRCULATIONAHA.105.595181

Arsalan, M., Woitek, F., Adams, V., Linke, A., Barten, M. J., Dhein, S., et al. (2012). Distribution of cardiac stem cells in the human heart. *ISRN Cardiol.* 2012:483407. doi: 10.5402/2012/483407

Bader, A., Lorenz, K., Richter, A., Scheffler, K., Kern, L., Ebert, S., et al. (2011). Interactive role of trauma cytokines and erythropoietin and their therapeutic potential for acute and chronic wounds. *Rejuvenation Res.* 14, 57–66. doi: 10.1089/rej.2010.1050

Bearzi, C., Rota, M., Hosoda, T., Tillmanns, J., Nascimbene, A., and De Angelis, A., et al. (2007). Human cardiac stem cells. *Proc. Natl. Acad. Sci. U.S.A.* 104, 14068–14073. doi: 10.1073/pnas.0706760104

Beltrami, A. P., Barlucchi, L., Torella, D., Baker, M., Limana, F., Chimenti, S., et al. (2003). Adult cardiac stem cells are multipotent and support myocardial regeneration. *Cell* 114, 763–776. doi: 10.1016/S0092-8674(03)00687-1

Beltrami, A. P., Urbanek, K., Kajstura, J., Yan, S. M., Finato, N., Bussani, R., et al. (2001). Evidence that human cardiac myocytes divide after myocardial infarction. *N. Engl. J. Med.* 344, 1750–1757. doi: 10.1056/NEJM200106073442303

Bolli, R., Chugh, A. R., D'Amario, D., Loughran, J. H., Stoddard, M. F., Ikram, S., et al. (2011). Cardiac stem cells in patients with ischaemic cardiomyopathy (SCIPIO): initial results of a randomised phase 1 trial. *Lancet* 378, 1847–1857. doi: 10.1016/S0140-6736(11)61590-0

Cameli, M., Righini, F. M., Sparla, S., Tacchini, D., Dokollari, A., Sassi, C. G., et al. (2016). First evidence of cardiac stem cells from the left ventricular apical tip in patients with left ventricular assist device implantation. *Transplant. Proc.* 48, 395–398. doi: 10.1016/j.transproceed.2015.12.045

Castaldo, C., Di Meglio, F., Nurzynska, D., Romano, G., Maiello, C., Bancone, C., et al. (2008). CD117-positive cells in adult human heart are localized in the subepicardium, and their activation is associated with laminin-1 and alpha6 integrin expression. *Stem Cells* 26, 1723–1731. doi: 10.1634/stemcells.2007-0732

Cesselli, D., Beltrami, A. P., D'Aurizio, F., Marcon, P., Bergamin, N., Toffoletto, B., et al. (2011). Effects of age and heart failure on human cardiac stem cell function. *Am. J. Pathol.* 179, 349–366. doi: 10.1016/j.ajpath.2011.03.036

Chan, H H., Meher Homji, Z., Gomes, R. S., Sweeney, D., Thomas, G. N., Tan, J. J., et al. (2012). Human cardiosphere-derived cells from patients with chronic ischaemic heart disease can be routinely expanded from atrial but not epicardial ventricular biopsies. *J. Cardiovasc. Trans. Res.* 5, 678–687. doi: 10.1007/s12265-012-9389-0

Chimenti, C., Kajstura, J., Torella, D., Urbanek, K., Heleniak, H., Colussi, C., et al. (2003). Senescence and death of primitive cells and myocytes lead to premature cardiac aging and heart failure. *Circ. Res.* 93, 604–613. doi: 10.1161/01.RES.0000093985.76901.AF

Ciontea, S. M., Radu, E., Regalia, T., Ceafalan, L., Cretoiu, D., Gherghiceanu, M., et al. (2005). C-kit immunopositive interstitial cells (Cajal-type) in human myometrium. *J. Cell. Mol. Med.* 9, 407–420. doi: 10.1111/j.1582-4934.2005.tb00366.x

D'Amario, D., Fiorini, C., Campbell, P. M., Goichberg, P., Sanada, F., Zheng, H., et al. (2011). Functionally competent cardiac stem cells can be isolated from endomyocardial biopsies of patients with advanced cardiomyopathies. *Circ. Res.* 108, 857–861. doi: 10.1161/CIRCRESAHA.111.241380

Davis, D. R., Zhang, Y., Smith, R. R., Cheng, K., Terrovitis, J., Malliaras, K., et al. (2009). Validation of the cardiosphere method to culture cardiac progenitor cells from myocardial tissue. *PLoS ONE* 4:e7195. doi: 10.1371/journal.pone.0007195

Di Meglio, F., Castaldo, C., Nurzynska, D., Miraglia, R., Romano, V., Russolillo, V., et al. (2010). Localization and origin of cardiac CD117-positive cells: identification of a population of epicardially-derived cells in adult human heart. *Ital. J. Anat. Embryol.* 115, 71–78.

Fang, S., Wei, J., Pentinmikko, N., Leinonen, H., Salven, P., and Goodell, M. A. (2012). Generation of functional blood vessels from a single c-kit+ adult vascular endothelial stem cell. *PLoS Biol.* 10:e1001407. doi: 10.1371/journal.pbio.1001407

Gago-Lopez, N., Awaji, O., Zhang, Y., Ko, C., Nsair, A., Liem, D., et al. (2014). THY-1 receptor expression differentiates cardiosphere-derived cells with divergent cardiogenic differentiation potential. *Stem Cell Rep.* 2, 576–591. doi: 10.1016/j.stemcr.2014.03.003

Gambini, E., Pompilio, G., Biondi, A., Alamanni, F., Capogrossi, M. C., Agrifoglio, M., et al. (2011). C-kit+ cardiac progenitors exhibit mesenchymal markers and preferential cardiovascular commitment. *Cardiovasc. Res.* 89, 362–373. doi: 10.1093/cvr/cvq292

Gonzalez, A., Rota, M., Nurzynska, D., Misao, Y., Tillmanns, J., Ojaimi, C., et al. (2008). Activation of cardiac progenitor cells reverses the failing heart senescent phenotype and prolongs lifespan. *Circ. Res.* 102, 597–606. doi: 10.1161/CIRCRESAHA.107.165464

Gourdie, R. G., Dimmeler, S., and Kohl, P. (2016). Novel therapeutic strategies targeting fibroblasts and fibrosis in heart disease. *Nat. Rev. Drug Discov.* 15, 620–638. doi: 10.1038/nrd.2016.89

Günter, C. I., Bader, A., Dornseifer, U., Egert, S., Dunda, S., Grieb, G., et al. (2013). A multi-center study on the regenerative effects of erythropoietin in burn and scalding injuries: study protocol for a randomized controlled trial. *Trials* 14:124. doi: 10.1186/1468-6708-14-124

Hayashi, E. (2015). The characterization of cardiac stem cells obtained from patients who have received left ventriculoplasty. *Stem Cell Transl. Invest.* 2:e537. doi: 10.14800/scti.537

He, J. Q., Vu, D. M., Hunt, G., Chugh, A., Bhatnagar, A., and Bolli, R. (2011). Human cardiac stem cells isolated from atrial appendages stably express c-kit. *PLoS ONE* 6:e27719. doi: 10.1371/journal.pone.0027719

Hinescu, M. E., Gherghiceanu, M., Mandache, E., Ciontea, S. M., and Popescu, L. M. (2006). Interstitial Cajal-like cells (ICLC) in atrial myocardium: ultrastructural and immunohistochemical characterization. *J. Cell. Mol. Med.* 10, 243–257. doi: 10.1111/j.1582-4934.2006.tb00306.x

Hosoda, T., Iguchi, N., Cho, Y., Inoue, M., Murakami, T., Tabata, M., et al. (2017). The proliferative potential of human cardiac stem cells was unaffected after a long-term cryopreservation of tissue blocks. *Ann. Transl. Med.* 5:41. doi: 10.21037/atm.2017.01.69

Hu, S., Yan, G., He, W., Liu, Z., Xu, H., and Ma, G. (2014). The influence of disease and age on human cardiac stem cells. *Ann. Clin. Biochem.* 51, 582–590. doi: 10.1177/0004563213511065

Ishigami, S., Ohtsuki, S., Eitoku, T., Ousaka, D., Kondo, M., Kurita, Y., et al. (2017). Intracoronary cardiac progenitor cells in single ventricle physiology: the perseus (Cardiac Progenitor Cell Infusion to Treat Univentricular Heart Disease) randomized phase 2 trial. *Circ. Res.* 120, 1162–1173. doi: 10.1161/CIRCRESAHA.116.310253

Ishigami, S., Ohtsuki, S., Tarui, S., Ousaka, D., Eitoku, T., Kondo, M., et al. (2015). Intracoronary autologous cardiac progenitor cell transfer in patients with hypoplastic left heart syndrome: the TICAP prospective phase 1 controlled trial. *Circ. Res.* 116, 653–664. doi: 10.1161/CIRCRESAHA.116.304671

Itzhaki-Alfia, A., Leor, J., Raanani, E., Sternik, L., Spiegelstein, D., Netser, S., et al. (2009). Patient characteristics and cell source determine the number of isolated human cardiac progenitor cells. *Circulation* 120, 2559–2566. doi: 10.1161/CIRCULATIONAHA.109.849588

Kaemmerer, D., Athelogou, M., Lupp, A., Lenhardt, I., Schulz, S., Luisa, P., et al. (2014). Somatostatin receptor immunohistochemistry in neuroendocrine tumors: comparison between manual and automated evaluation. *Int. J. Clin. Exp. Pathol.* 7, 4971–4980.

Kajstura, J., Gurusamy, N., Ogorek, B., Goichberg, P., Clavo-Rondon, C., Hosoda, T., et al. (2010). Myocyte turnover in the aging human heart. *Circ. Res.* 107, 1374–1386. doi: 10.1161/CIRCRESAHA.110.231498

Kubo, H., Jaleel, N., Kumarapeli, A., Berretta, R. M., Bratinov, G., Shan, X., et al. (2008). Increased cardiac myocyte progenitors in failing human hearts. *Circulation* 118, 649–657. doi: 10.1161/CIRCULATIONAHA.107.761031

Li, T. S., Cheng, K., Malliaras, K., Smith, R. R., Zhang, Y., Sun, B., et al. (2012). Direct comparison of different stem cell types and subpopulations reveals superior paracrine potency and myocardial repair efficacy with cardiosphere-derived cells. *J. Am. Coll. Cardiol.* 59, 942–953. doi: 10.1016/j.jacc.2011.11.029

Lorenz, K., Sicker, M., Schmelzer, E., Rupf, T., Salvetter, J., Schulz-Siegmund, M., et al. (2008). Multilineage differentiation potential of human dermal skin-derived fibroblasts. *Exp. Dermatol.* 17, 925–932. doi: 10.1111/j.1600-0625.2008.00724.x

Lozano, R., Naghavi, M., Foreman, K., Lim, S., Shibuya, K., Aboyans, V., et al. (2012). Global and regional mortality from 235 causes of death for 20 age groups in 1990 and 2010: a systematic analysis for the global burden of disease study 2010. *Lancet* 380, 2095–2128. doi: 10.1016/S0140-6736(12)61728-0

Matuszczak, S., Czapla, J., Jarosz-Biej, M., Wiśniewska, E., Cichon, T., Smolarczyk, R., et al. (2014). Characteristic of c-Kit+ progenitor cells in explanted human hearts. *Clin. Res. Cardiol.* 103, 711–718. doi: 10.1007/s00392-014-0705-3

Mishra, R., Vijayan, K., Colletti, E. J., Harrington, D. A., Matthiesen, T. S., Simpson, D., et al. (2011). Characterization and functionality of cardiac progenitor cells in congenital heart patients. *Circulation* 123, 364–373. doi: 10.1161/CIRCULATIONAHA.110.971622

Nakamura, T., Hosoyama, T., Kawamura, D., Takeuchi, Y., Tanaka, Y., Samura, M., et al. (2016). Influence of aging on the quantity and quality of human cardiac stem cells. *Sci. Rep.* 6:22781. doi: 10.1038/srep22781

Neubauer, E., Wirtz, R. M., Kaemmerer, D., Athelogou, M., Schmidt, L., Sänger, J., et al. (2016). Comparative evaluation of three proliferation markers, Ki-67, TOP2A, and RacGAP1, in bronchopulmonary neuroendocrine neoplasms: issues and prospects. *Oncotarget* 7, 41959–41973. doi: 10.18632/oncotarget.9747

Nurzynska, D., Di Meglio, F., Romano, V., Miraglia, R., Sacco, A. M., Latino, F., et al. (2013). Cardiac primitive cells become committed to a cardiac fate in adult human heart with chronic ischemic disease but fail to acquire mature phenotype: genetic and phenotypic study. *Basic Res. Cardiol.* 108:320. doi: 10.1007/s00395-012-0320-2

Orlic, D., Kajstura, J., Chimenti, S., Jakoniuk, I., Anderson, S. M., Li, B., et al. (2001). Bone marrow cells regenerate infarcted myocardium. Nature 410, 701–705. doi: 10.1038/35070587

Piegari, E., Angelis, A., de, Cappetta, D., Russo, R., Esposito, G., Costantino, S., et al. (2013). Doxorubicin induces senescence and impairs function of human cardiac progenitor cells. *Basic Res. Cardiol.* 108:334. doi: 10.1007/s00395-013-0334-4

Popescu, L. M., Ciontea, S. M., Cretoiu, D., Hinescu, M. E., Radu, E., Ionescu, N., et al. (2005). Novel type of interstitial cell (Cajal-like) in human fallopian tube. *J. Cell. Mol. Med.* 9, 479–523. doi: 10.1111/j.1582-4934.2005.tb00376.x

Popescu, L. M., Gherghiceanu, M., Hinescu, M. E., Cretoiu, D., Ceafalan, L., Regalia, T., et al. (2006). Insights into the interstitium of ventricular myocardium: interstitial cajal-like cells (ICLC). *J. Cell. Mol. Med.* 10, 429–458. doi: 10.1111/j.1582-4934.2006.tb00410.x

Pouly, J., Bruneval, P., Mandet, C., Proksch, S., Peyrard, S., Amrein, C., et al. (2008). Cardiac stem cells in the real world. *J. Thorac. Cardiovasc. Surg.* 135, 673–678. doi: 10.1016/j.jtcvs.2007.10.024

Radu, E., Regalia, T., Ceafalan, L., Andrei, F., Cretoiu, D., and Popescu, L. M. (2005). Cajal-type cells from human mammary gland stroma: phenotype characteristics in cell culture. *J. Cell. Mol. Med.* 9, 748–752. doi: 10.1111/j.1582-4934.2005.tb00509.x

RajendranNair, D. S., Karunakaran, J., and Nair, R. R. (2017). Differential response of human cardiac stem cells and bone marrow mesenchymal stem cells to hypoxia-reoxygenation injury. *Mol. Cell. Biochem.* 425, 139–153. doi: 10.1007/s11010-016-2869-9

Rota, M., Kajstura, J., Hosoda, T., Bearzi, C., Vitale, S., Esposito, G., et al. (2007). Bone marrow cells adopt the cardiomyogenic fate *in vivo*. *Proc. Natl. Acad. Sci. U.S.A.* 104, 17783–17788. doi: 10.1073/pnas.0706406104

Rupp, S., Bauer, J., von Gerlach, S., Fichtlscherer, S., Zeiher, A. M., Dimmeler, S., et al. (2012). Pressure overload leads to an T increase of cardiac resident stem cells. *Basic Res. Cardiol.* 107:252. doi: 10.1007/s00395-012-0252-x

Sandstedt, J., Jonsson, M., Kajic, K., Sandstedt, M., Lindahl, A., Dellgren, G., et al. (2012). Left atrium of the human adult heart contains a population of side population cells. *Basic Res. Cardiol.* 107:255. doi: 10.1007/s00395-012-0255-7

Sandstedt, J., Jonsson, M., Lindahl, A., Jeppsson, A., and Asp, J. (2010). C-kit+ CD45- cells found in the adult human heart represent a population of endothelial progenitor cells. *Basic Res. Cardiol.* 105, 545–556. doi: 10.1007/s00395-010-0088-1

Smith, R. R., Barile, L., Cho, H. C., Leppo, M. K., Hare, J. M., Messina, E., et al. (2007). Regenerative potential of cardiosphere-derived cells expanded from percutaneous endomyocardial biopsy specimens. *Circulation* 115, 896–908. doi: 10.1161/CIRCULATIONAHA.106.655209

Townsend, N., Nichols, M., Scarborough, P., and Rayner, M. (2015). Cardiovascular disease in Europe 2015: epidemiological update. *Eur. Heart J.* 36, 2673–2674. doi: 10.1093/eurheartj/ehv428

Urbanek, K., Quaini, F., Tasca, G., Torella, D., Castaldo, C., Nadal-Ginard, B., et al. (2003). Intense myocyte formation from cardiac stem cells in human cardiac hypertrophy. *Proc. Natl. Acad. Sci. U.S.A.* 100, 10440–10445. doi: 10.1073/pnas.1832855100

Urbanek, K., Torella, D., Sheikh, F., Angelis, A., de, Nurzynska, D., Silvestri, F., et al. (2005). Myocardial regeneration by activation of multipotent cardiac stem cells in ischemic heart failure. *Proc. Natl. Acad. Sci. U.S.A.* 102, 8692–8697. doi: 10.1073/pnas.0500169102

Vicinanza, C., Aquila, I., Scalise, M., Cristiano, F., Marino, F., Cianflone, E., et al. (2017). Adult cardiac stem cells are multipotent and robustly myogenic: c-kit expression is necessary but not sufficient for their identification. *Cell Death Differ.* 24, 2101–2116. doi: 10.1038/cdd.2017.130

World Medical Association. (1975). *Declaration of Helsinki, 1st amendment.*

Zhang, Y. Y., Li, G., Che, H., Sun, H. Y., Li, X., Au, W. K., et al. (2014). Characterization of functional ion channels in human cardiac c-kit+ progenitor cells. *Basic Res. Cardiol.* 109:407. doi: 10.1007/s00395-014-0407-z

Zhou, Y., Pan, P., Yao, L., Su, M., He, P., Niu, N., et al. (2010). CD117-positive cells of the heart: progenitor cells or mast cells? *J. Histochem. Cytochem.* 58, 309–316. doi: 10.1369/jhc.2009.955146

Conflict of Interest Statement: The authors declare that the research was conducted in the absence of any commercial or financial relationships that could be construed as a potential conflict of interest.

Maria Athelogou was employed by company Definiens AG, Munich, Germany. All other authors declare no competing interests.

3. ZUSAMMENFASSUNG DER ARBEIT

Dissertation zur Erlangung des akademischen Grades Dr. med.

Qualitative und quantitative Analyse von lokalen Progenitorzellen in humanen Myokardbiopsien von Patienten mit Myokarditis und Kardiomyopathie

eingereicht von: Marie Gerisch, geb. Wegener

angefertigt am Biotechnologisch-Biomedizinischen Zentrum, Professur für Zelltechniken und angewandte Stammzellbiologie, Universität Leipzig

betreut von: Univ.-Prof. Dr. med. Augustinus Bader
Dr. rer. nat. Shibashish Giri (Ko-Betreuer)
Dr. med. Jan Smettan (Ko-Betreuer)

eingereicht: 07/2018

Ziel dieser Arbeit war es, lokale kardiale Progenitorzellen anhand von Oberflächenmarkern direkt in humanen Myokardbiopsien nachzuweisen und den Einfluss verschiedener kardialer Krankheitsbilder auf den lokalen Progenitorzellpool zu analysieren. Dabei sollte nicht nur eine traditionelle histologische Auswertung stattfinden, sondern auch eine Methode entwickelt werden, die eine quantitative, automatisierbare Analyse ermöglichen sollte. Dadurch konnten unterschiedlich große Gewebeproben im direkten Vergleich untersucht werden. Von besonderer Bedeutung für diese Arbeit waren die Progenitorzellmarker CD90 und CD117. Humane Myokardbiopsien von 23 Patienten mit folgenden Diagnosen wurden verwendet:

Dilatative Kardiomyopathie (DCM), ischämische Kardiomyopathie (ICM), Myokarditis und kardial gesunde Kontrollgruppen. Das Durchschnittsalter der Patienten mit DCM betrug 44 Jahre mit einer durchschnittlichen Krankheitsdauer seit der Erstdiagnose (ED) von 18 Jahren. Patienten mit ICM waren im Mittel 58 Jahre alt und die durchschnittliche Krankheitsdauer seit ED betrug 10 Jahre. Die Patienten mit Myokarditis waren durchschnittlich 24 Jahre alt und die Erkrankungsdauer seit ED lag zwischen eins und sechs Monaten. Das Durchschnittsalter der Kontrollgruppe betrug 35 Jahre. Zur Analyse lagen für diese Arbeit fertige, in Paraffin eingebettete und geschnittene Myokardbiopsien vom rechtsventrikulären und linksventrikulären Myokard und vom Septum interventrikulare vor. Zusätzlich wurden humane Gewebsbiopsien von Haut, Cerebellum und Niere als Positivkontrollen verwendet. Diese Proben wurden zunächst in Paraffin eingebettet und anschließend geschnitten und auf Objektträgern fixiert.

Nachfolgend wurde ein spezielles Protokoll zur immunhistochemischen Analyse von Progenitorzellmarkern der in Paraffin eingebetteten Gewebeproben entwickelt und etabliert. Pro Gewebeschnitt wurde eine Antikörperfärbung mit CD90 oder CD117 durchgeführt. Anschließend erfolgte die Digitalisierung der histologischen Präparate mittels eines virtuellen Mikroskops und einer speziell dafür entwickelten Software („*CellSens*“ der Firma „Olympus“). So entstanden qualitativ hochwertige digitale Bilder der gefärbten Paraffinschnitte. Das Besondere dieser Scan-Methode war, dass der gesamte Schnitt eingescannt wurde, und zwar so hochauflösend, dass jeder beliebige Ausschnitt des Bildes bis auf Zellebene vergrößert werden kann. Während des Scan-Vorganges wurden pro Präparat ca. 50 Fokuspunkte gesetzt, an welchen die Feinfokussierung manuell überprüft wurde, um fälschliches Fokussieren von Artefakten zu vermeiden. In den resultierenden digitalisierten Bildern konnten somit außerdem Unebenheiten des ursprünglichen histologischen Präparates ausgeglichen werden. Dies ist ein großer Vorteil zur konventionellen Mikroskopie, bei welcher bei jedem Einlegen eines Präparates die Fokussierung immer wieder nachjustiert werden muss, um Unschärfen ausgleichen zu können. Unter Nutzung der *CellSens*-Software konnte die Qualität der digitalen Bilder unter anderem durch Weißabgleich und Verbesserung des Phasenkontrastes weiter optimiert werden.

Die *qualitative* Analyse der gefärbten Präparate zeigte, dass bei allen Patienten $CD90^+$ und $CD117^+$ Signale auffindbar waren. Die CD90-Färbungen stellten sich als einzelne Signale zwischen den Kardiomyozyten dar. Im Gegensatz dazu konnte CD117 sowohl in Zellen zwischen den Kardiomyozyten, als auch in den Kardiomyozyten direkt nachgewiesen werden.

Mittels einer innovativen digitalen Bildanalyse gelang es eine gezielte *quantitative* Analyse unter Verwendung der gesamten Gewebeschnitte durchzuführen. Mithilfe der Software „*Developer XD"* (der Firma „Definiens®") war es möglich, im digitalisierten histologischen Bild zuerst den Vordergrund (das Biopsiematerial) vom Hintergrund (Bildregionen ohne Gewebematerial) zu separieren. Anhand der Farbintensität wurden die Signale für CD90 und CD117 automatisch erfasst. Die Signale wurden in 2 Gruppen unterteilt: in einzelne punktuelle Signale und in gruppierte bzw. miteinander verschmolzene Signale. Durch einen automatisierten Regelsatz der Software entstand zu jedem digitalisierten histologischen Bild ein neues bearbeitetes Bild, welches nur noch aus den Farben schwarz (Hintergrund), blau (nicht angefärbtes Gewebe), rot (einzelne Signale), grün (miteinander verschmolzene Signale) und gelb (randständiges Gewebe) bestand. Anschließend wurde durch die Software bei jedem Gewebeschnitt die Gesamtanzahl der Einzelsignale bestimmt. Bei der Analyse fiel auf, dass die höchste Expression von CD90 bei der Myokarditis gefunden wurde (mittlere Gesamtanzahl der Signale pro Gewebeschnitt: 9.741 Signale). Patienten mit einer ICM zeigten im Mittel 3.336 Signale pro Schnitt, Patienten mit DCM nur 2.144 Signale pro Schnitt. Die gesunde Kontrollgruppe enthielt im Mittel nur 1.036 Signale. Bei der Interpretation der Ergebnisse ergab sich jedoch die Schwierigkeit, dass die Größe der Gewebeschnitte stark variierte. Deshalb wurde durch die Software eine relative Anzahl an $CD90^+$ Signalen pro Gewebeschnitt berechnet.

Im Gegensatz zu CD90 beinhaltete die CD117-Färbung nicht nur einzelständige Signale, sondern auch viele gruppierte bzw. miteinander verschmolzene Signale. Aus diesem Grund wurde der Fokus der Analyse bei CD117 auf die relative Fläche an $CD117^+$ Signalen im Verhältnis zur Gesamtfläche gesetzt. Die Anzahl der Einzelsignale wurde vernachlässigt, da die überwiegend gruppierten Signale zu Verfälschungen der Anzahl geführt hätten. Verglichen mit der gesunden Kontrollgruppe zeigte sich ein signifikanter Anstieg der CD117-Expression sowohl bei der Myokarditis, als auch bei der ICM und DCM ($p < 0.05$). Zur besseren Vergleichbarkeit wurde auch bei CD90 die relative Fläche an positiven Signalen im Verhältnis zur Gesamtfläche errechnet. Die Ergebnisse zeigten wie auch schon die Anzahl der $CD90^+$ Signale einen Anstieg vor allem bei Myokarditispatienten. Die Erstellung einer relativen Größe ermöglichte es, alle Patienten hinsichtlich CD90 und CD117 miteinander zu vergleichen, ohne dass die unterschiedliche Größe der Gewebeschnitte die Analyse beeinflusste.

Neben der Auswertung der einzelnen Progenitorzellmarker wurde im Rahmen dieser Arbeit ein Procedere entwickelt, durch welches der Nachweis von mehreren Antigenen auf einer Zelle, die sogenannte „Ko-Expression“, möglich wurde. Die Identifizierung von Zellen mit einer Ko-Expression von CD90 und CD117 erfolgte mittels visuellem Vergleich von zwei Serienschnitten. Es wurde auf beiden Schnitten ein identischer, 4 mm^2 großer Bildausschnitt gewählt. Im visuellen Vergleich der beiden Gewebeschnitte wurden alle Zellen gezählt, die sowohl für CD90 als auch für CD117 eine positive Reaktion zeigten, die Anzahl wurde zur besseren Übersicht auf Anzahl n / mm^2 genormt. Die Auswertung ergab, dass bei allen Patienten Zellen gefunden wurden, welche sowohl für CD90 als auch für CD117 positiv waren. Die niedrigste Anzahl an Ko-Expressionen war bei der gesunden Kontrollgruppe zu finden (1 ± 0,43 $CD90^+CD117^+$ Zellen/mm^2), gefolgt von den Patienten mit DCM (1,67 ± 0.58 $CD90^+CD117^+$ Zellen/mm^2) und ICM (4 ± 1,89 $CD90^+CD117^+$ Zellen/mm^2). Bei den Patienten mit Myokarditis zeigten sich die meisten Zellen mit Ko-Expression von CD90 und CD117 (6,75 ± 3,25 $CD90^+CD117^+$ Zellen/mm^2). Mithilfe der Ko-Expression der beiden Progenitorzellmarker CD90 und CD117 gelang in dieser Arbeit der immunhistologische Nachweis von lokalen Progenitorzellen direkt im humanen Myokard. Durch die Expression beider Marker konnte ausgeschlossen werden, dass es sich bei den gefärbten Zellen um Mastzellen ($CD117^+/CD90^-$) oder um eingewanderte Stammzellen zum Beispiel aus dem Knochenmark handelt. Eine zusätzliche Färbung mit CD105 bestätigte, dass im Herzen lokale $CD90^+/CD117^+/CD105^+$ Progenitorzellen vorhanden sind. Des Weiteren zeigte die Analyse, dass bei Patienten mit Myokarditis ein Anstieg der lokalen Progenitorzellen zu verzeichnen ist. Dieses Ergebnis korreliert mit den allgemeinen klinischen Symptomen dieser Patientengruppe, denn Myokarditispatienten unterlaufen oftmals einen kompletten Heilungsprozess. Die Aktivierung lokaler Progenitorzellen bei der Myokarditis ist höchstwahrscheinlich maßgebend an dem guten funktionellen Outcome und der ausbleibenden Narbenbildung beteiligt. Im Gegensatz dazu zeigen chronische Herzerkrankungen wie die DCM oder ICM einen geringeren oder gar keinen Anstieg lokaler Progenitorzellen, was sich klinisch durch den ausbleibenden Heilungseffekt äußert und stattdessen mit einer Narbenbildung einherzugehen scheint.

In der hier vorliegenden Arbeit konnte nachgewiesen werden, dass im menschlichen Herzen sowohl bei Gesunden als auch bei kardial Erkrankten lokale Progenitorzellen zu finden sind. Der Nachweis der lokalen Progenitorzellen gelang hier mithilfe der Ko-Expression von den Progenitorzellmarkern CD90 und CD117. Da die Identifizierung der Marker durch

immunhistochemische Analyse direkt in den Myokardbiopsien stattfand, spiegeln die Ergebnisse den Nativzustand des Gewebes wider und enthalten Informationen über die unverfälschte Anzahl und Verteilung der Progenitorzellen. Die Ergebnisse dieser Arbeit unterstützen die These, dass die Aktivierung lokaler Progenitorzellen Teil eines Reparaturmechanismus ist, welcher nach einem akuten, entzündlichen Myokardschaden in Gang gesetzt wird. Man kann nun davon auszugehen, dass in jedem Herzen lokale Progenitorzellen ruhen, welche bei Aktivierung zu einer narbenfreien Regeneration des Myokards führen könnten. Hinweisend dafür ist der Anstieg lokaler $CD90^+/CD117^+$ Progenitorzellen vor allen Dingen bei Patienten mit Myokarditis.

Des Weiteren wurde im Rahmen dieser Arbeit ein Verfahren entwickelt, welches traditionelle histologische Methoden mit einer neuartigen Technologie der digitalen Bildanalyse verbindet. Mittels eines virtuellen Mikroskops konnten aus den histologischen Präparaten so genannte „Whole Slide Images“ erzeugt werden. Unter Verwendung der digitalisierten histologischen Bilder konnten nicht nur qualitative Analysen an einzelnen Bildausschnitten vorgenommen werden, sondern auch quantitative Analysen des gesamten Schnittes in einem effizienten, automatisierten Prozess durchgeführt werden. Somit wurde mit dieser Arbeit eine neuartige Methode entwickelt, in Paraffin eingebettete humane Myokardbiopsien hinsichtlich des Vorkommens lokaler Progenitorzellen qualitativ und quantitativ auszuwerten und miteinander vergleichen zu können.

Zukünftige Studien mit größerem Patientenumfang könnten neben dem Nachweis auch Mechanismen zur Aktivierung lokaler kardialer Progenitorzellen analysieren und somit einen signifikanten Beitrag zu der Entwicklung neuer Therapiestrategien kardiovaskulärer Erkrankungen liefern.

4. LITERATURVERZEICHNIS

1. http://www.who.int/mediacentre/factsheets/fs317/en/
2. http://www.who.int/gho/mortality_burden_disease/causes_death/top_10/en/
3. Smits AM, Vliet P, Hassink RJ et al. (2005) The role of stem cells in cardiac regeneration. J Cellular Mol Med 9(1): 25–36. doi: 10.1111/j.1582-4934.2005.tb00334.x
4. Lewis EF, Moye LA, Rouleau JL et al. (2003) Predictors of late development of heart failure in stable survivors of myocardial infarction: the CARE study. J Am Coll Cardiol 42(8): 1446–1453
5. Zak R (1973) Cell proliferation during cardiac growth. The American Journal of Cardiology 31(2): 211–219. doi: 10.1016/0002-9149(73)91034-5
6. Landmesser U, Drexler H (2005) Chronic heart failure: an overview of conventional treatment versus novel approaches. Nat Clin Pract Cardiovasc Med 2(12): 628–638. doi: 10.1038/ncpcardio0371
7. Lund LH, Khush KK, Cherikh WS et al. (2017) The Registry of the International Society for Heart and Lung Transplantation: Thirty-fourth Adult Heart Transplantation Report-2017; Focus Theme: Allograft ischemic time. J Heart Lung Transplant 36(10): 1037–1046. doi: 10.1016/j.healun.2017.07.019
8. https://www.nature.com/subjects/pluripotent-stem-cells. https://www.nature.com/subjects/pluripotent-stem-cells. Accessed 30 Apr 2018
9. Thomson JA, Itskovitz-Eldor J, Shapiro SS et al. (1998) Embryonic stem cell lines derived from human blastocysts. Science 282(5391): 1145–1147
10. He J-Q, Ma Y, Lee Y et al. (2003) Human embryonic stem cells develop into multiple types of cardiac myocytes: action potential characterization. Circ Res 93(1): 32–39. doi: 10.1161/01.RES.0000080317.92718.99
11. Takahashi K, Tanabe K, Ohnuki M et al. (2007) Induction of pluripotent stem cells from adult human fibroblasts by defined factors. Cell 131(5): 861–872. doi: 10.1016/j.cell.2007.11.019
12. Nelson TJ, Martinez-Fernandez A, Yamada S et al. (2009) Repair of acute myocardial infarction by human stemness factors induced pluripotent stem cells. Circulation 120(5): 408–416. doi: 10.1161/CIRCULATIONAHA.109.865154

13. Li X, Zhang F, Song G et al. (2013) Intramyocardial Injection of Pig Pluripotent Stem Cells Improves Left Ventricular Function and Perfusion: A Study in a Porcine Model of Acute Myocardial Infarction. PLoS ONE 8(6): e66688. doi: 10.1371/journal.pone.0066688
14. Zhang J, Wilson GF, Soerens AG et al. (2009) Functional cardiomyocytes derived from human induced pluripotent stem cells. Circ Res 104(4): e30-41. doi: 10.1161/CIRCRESAHA.108.192237
15. Zhang Y, Wang D, Chen M et al. (2011) Intramyocardial transplantation of undifferentiated rat induced pluripotent stem cells causes tumorigenesis in the heart. PLoS ONE 6(4): e19012. doi: 10.1371/journal.pone.0019012
16. Du Pré BC, Doevendans PA, van Laake LW (2013) Stem cells for cardiac repair: an introduction. J Geriatr Cardiol 10(2): 186–197. doi: 10.3969/j.issn.1671-5411.2013.02.003
17. Dawn B, Bolli R (2005) Adult bone marrow-derived cells: regenerative potential, plasticity, and tissue commitment. Basic Res Cardiol 100(6): 494–503. doi: 10.1007/s00395-005-0552-5
18. Wollert KC, Meyer GP, Lotz J et al. (2004) Intracoronary autologous bone-marrow cell transfer after myocardial infarction: the BOOST randomised controlled clinical trial. The Lancet 364(9429): 141–148. doi: 10.1016/S0140-6736(04)16626-9
19. Lunde K, Solheim S, Aakhus S et al. (2006) Intracoronary injection of mononuclear bone marrow cells in acute myocardial infarction. N Engl J Med 355(12): 1199–1209. doi: 10.1056/NEJMoa055706
20. Schächinger V, Erbs S, Elsässer A et al. (2006) Intracoronary bone marrow-derived progenitor cells in acute myocardial infarction. N Engl J Med 355(12): 1210–1221. doi: 10.1056/NEJMoa060186
21. Sürder D, Manka R, Lo Cicero V et al. (2013) Intracoronary injection of bone marrow-derived mononuclear cells early or late after acute myocardial infarction: effects on global left ventricular function. Circulation 127(19): 1968–1979. doi: 10.1161/CIRCULATIONAHA.112.001035
22. Choudry F, Hamshere S, Saunders N et al. (2016) A randomized double-blind control study of early intra-coronary autologous bone marrow cell infusion in acute myocardial infarction: the REGENERATE-AMI clinical trial†. Eur Heart J 37(3): 256–263. doi: 10.1093/eurheartj/ehv493

23. Traverse JH, Henry TD, Pepine CJ et al. (2012) Effect of the use and timing of bone marrow mononuclear cell delivery on left ventricular function after acute myocardial infarction: the TIME randomized trial. JAMA 308(22): 2380–2389. doi: 10.1001/jama.2012.28726
24. Nygren JM, Jovinge S, Breitbach M et al. (2004) Bone marrow-derived hematopoietic cells generate cardiomyocytes at a low frequency through cell fusion, but not transdifferentiation. Nat Med 10(5): 494–501. doi: 10.1038/nm1040
25. Koh BI, Kang Y (2012) The pro-metastatic role of bone marrow-derived cells: a focus on MSCs and regulatory T cells. EMBO Rep 13(5): 412–422. doi: 10.1038/embor.2012.41
26. Caplan AI (1991) Mesenchymal stem cells. J Orthop Res 9(5): 641–650. doi: 10.1002/jor.1100090504
27. Chen S-l, Fang W-w, Ye F et al. (2004) Effect on left ventricular function of intracoronary transplantation of autologous bone marrow mesenchymal stem cell in patients with acute myocardial infarction. The American Journal of Cardiology 94(1): 92–95. doi: 10.1016/j.amjcard.2004.03.034
28. Jeong H, Yim HW, Park H-J et al. (2018) Mesenchymal Stem Cell Therapy for Ischemic Heart Disease: Systematic Review and Meta-analysis. Int J Stem Cells. doi: 10.15283/ijsc17061
29. Gnecchi M, Danieli P, Cervio E (2012) Mesenchymal stem cell therapy for heart disease. Vascul Pharmacol 57(1): 48–55. doi: 10.1016/j.vph.2012.04.002
30. Buckingham M, Montarras D (2008) Skeletal muscle stem cells. Curr Opin Genet Dev 18(4): 330–336. doi: 10.1016/j.gde.2008.06.005
31. Menasché P (2008) Skeletal myoblasts and cardiac repair. J Mol Cell Cardiol 45(4): 545–553. doi: 10.1016/j.yjmcc.2007.11.009
32. Yu H, Lu K, Zhu J et al. (2017) Stem cell therapy for ischemic heart diseases. Br Med Bull 121(1): 135–154. doi: 10.1093/bmb/ldw059
33. Schenke-Layland K, Strem BM, Jordan MC et al. (2009) Adipose tissue-derived cells improve cardiac function following myocardial infarction. J Surg Res 153(2): 217–223. doi: 10.1016/j.jss.2008.03.019
34. Ji SQ, Cao J, Zhang QY et al. (2013) Adipose tissue-derived stem cells promote pancreatic cancer cell proliferation and invasion. Braz J Med Biol Res 46(9): 758–764. doi: 10.1590/1414-431X20132907

35. Anversa P, Nadal-Ginard B (2002) Myocyte renewal and ventricular remodelling. Nature 415(6868): 240–243. doi: 10.1038/415240a
36. Beltrami AP, Urbanek K, Kajstura J et al. (2001) Evidence that human cardiac myocytes divide after myocardial infarction. N Engl J Med 344(23): 1750–1757. doi: 10.1056/NEJM200106073442303
37. Urbanek K, Torella D, Sheikh F et al. (2005) Myocardial regeneration by activation of multipotent cardiac stem cells in ischemic heart failure. Proc Natl Acad Sci U S A 102(24): 8692–8697. doi: 10.1073/pnas.0500169102
38. Beltrami AP, Barlucchi L, Torella D et al. (2003) Adult cardiac stem cells are multipotent and support myocardial regeneration. Cell 114(6): 763–776
39. Gonzalez A, Rota M, Nurzynska D et al. (2008) Activation of cardiac progenitor cells reverses the failing heart senescent phenotype and prolongs lifespan. Circ Res 102(5): 597–606. doi: 10.1161/CIRCRESAHA.107.165464
40. Johnston PV, Sasano T, Mills K et al. (2009) Engraftment, Differentiation, and Functional Benefits of Autologous Cardiosphere-Derived Cells in Porcine Ischemic Cardiomyopathy. Circulation 120(12): 1075–1083. doi: 10.1161/CIRCULATIONAHA.108.816058
41. Makkar RR, Smith RR, Cheng K et al. (2012) Intracoronary cardiosphere-derived cells for heart regeneration after myocardial infarction (CADUCEUS): a prospective, randomised phase 1 trial. The Lancet 379(9819): 895–904. doi: 10.1016/S0140-6736(12)60195-0
42. Edling CE, Hallberg B (2007) c-Kit—A hematopoietic cell essential receptor tyrosine kinase. The International Journal of Biochemistry & Cell Biology 39(11): 1995–1998. doi: 10.1016/j.biocel.2006.12.005
43. Castaldo C, Di Meglio F, Nurzynska D et al. (2008) CD117-positive cells in adult human heart are localized in the subepicardium, and their activation is associated with laminin-1 and alpha6 integrin expression. Stem Cells 26(7): 1723–1731. doi: 10.1634/stemcells.2007-0732
44. Di Meglio F, Castaldo C, Nurzynska D et al. (2010) Localization and origin of cardiac CD117-positive cells: Identification of a population of epicardially-derived cells in adult human heart. Ital J Anat Embryol 115(1-2): 71–78
45. Sandstedt J, Jonsson M, Kajic K et al. (2012) Left atrium of the human adult heart contains a population of side population cells. Basic Res Cardiol 107(2): 255. doi: 10.1007/s00395-012-0255-7

46. Bearzi C, Rota M, Hosoda T et al. (2007) Human cardiac stem cells. Proc Natl Acad Sci U S A 104(35): 14068–14073. doi: 10.1073/pnas.0706760104
47. Urbanek K, Quaini F, Tasca G et al. (2003) Intense myocyte formation from cardiac stem cells in human cardiac hypertrophy. Proc Natl Acad Sci U S A 100(18): 10440–10445. doi: 10.1073/pnas.1832855100
48. Altarche-Xifró W, Curato C, Kaschina E et al. (2009) Cardiac c-kit+AT2+ cell population is increased in response to ischemic injury and supports cardiomyocyte performance. Stem Cells 27(10): 2488–2497. doi: 10.1002/stem.171
49. Kubo H, Jaleel N, Kumarapeli A et al. (2008) Increased cardiac myocyte progenitors in failing human hearts. Circulation 118(6): 649–657. doi: 10.1161/CIRCULATIONAHA.107.761031
50. Itzhaki-Alfia A, Leor J, Raanani E et al. (2009) Patient characteristics and cell source determine the number of isolated human cardiac progenitor cells. Circulation 120(25): 2559–2566. doi: 10.1161/CIRCULATIONAHA.109.849588
51. Rupp S, Bauer J, Gerlach S von et al. (2012) Pressure overload leads to an increase of cardiac resident stem cells. Basic Res Cardiol 107(2): 252. doi: 10.1007/s00395-012-0252-x
52. Nurzynska D, Di Meglio F, Romano V et al. (2013) Cardiac primitive cells become committed to a cardiac fate in adult human heart with chronic ischemic disease but fail to acquire mature phenotype: Genetic and phenotypic study. Basic Res Cardiol 108(1): 320. doi: 10.1007/s00395-012-0320-2
53. Bolli R, Chugh AR, D'Amario D et al. (2011) Cardiac stem cells in patients with ischaemic cardiomyopathy (SCIPIO): Initial results of a randomised phase 1 trial. Lancet 378(9806): 1847–1857. doi: 10.1016/S0140-6736(11)61590-0
54. Gambini E, Pompilio G, Biondi A et al. (2011) C-kit+ cardiac progenitors exhibit mesenchymal markers and preferential cardiovascular commitment. Cardiovasc Res 89(2): 362–373. doi: 10.1093/cvr/cvq292
55. Fang S, Wei J, Pentinmikko N et al. (2012) Generation of functional blood vessels from a single c-kit+ adult vascular endothelial stem cell. PLoS Biol 10(10): e1001407. doi: 10.1371/journal.pbio.1001407
56. Matuszczak S, Czapla J, Jarosz-Biej M et al. (2014) Characteristic of c-Kit+ progenitor cells in explanted human hearts. Clin Res Cardiol 103(9): 711–718. doi: 10.1007/s00392-014-0705-3

57. Li T-S, Cheng K, Malliaras K et al. (2012) Direct comparison of different stem cell types and subpopulations reveals superior paracrine potency and myocardial repair efficacy with cardiosphere-derived cells. J Am Coll Cardiol 59(10): 942–953. doi: 10.1016/j.jacc.2011.11.029
58. Smith RR, Barile L, Cho HC et al. (2007) Regenerative potential of cardiosphere-derived cells expanded from percutaneous endomyocardial biopsy specimens. Circulation 115(7): 896–908. doi: 10.1161/CIRCULATIONAHA.106.655209
59. Davis DR, Zhang Y, Smith RR et al. (2009) Validation of the cardiosphere method to culture cardiac progenitor cells from myocardial tissue. PLoS ONE 4(9): e7195. doi: 10.1371/journal.pone.0007195
60. Mishra R, Vijayan K, Colletti EJ et al. (2011) Characterization and functionality of cardiac progenitor cells in congenital heart patients. Circulation 123(4): 364–373. doi: 10.1161/CIRCULATIONAHA.110.971622
61. Chan HHL, Meher Homji Z, Gomes RSM et al. (2012) Human cardiosphere-derived cells from patients with chronic ischaemic heart disease can be routinely expanded from atrial but not epicardial ventricular biopsies. J Cardiovasc Transl Res 5(5): 678–687. doi: 10.1007/s12265-012-9389-0
62. Masson NM, Currie IS, Terrace JD et al. (2006) Hepatic progenitor cells in human fetal liver express the oval cell marker Thy-1. American Journal of Physiology-Gastrointestinal and Liver Physiology 291(1): G45-G54. doi: 10.1152/ajpgi.00465.2005
63. Gourdie RG, Dimmeler S, Kohl P (2016) Novel therapeutic strategies targeting fibroblasts and fibrosis in heart disease. Nat Rev Drug Discov 15(9): 620–638. doi: 10.1038/nrd.2016.89
64. Bader A, Lorenz K, Richter A et al. (2011) Interactive role of trauma cytokines and erythropoietin and their therapeutic potential for acute and chronic wounds. Rejuvenation Res 14(1): 57–66. doi: 10.1089/rej.2010.1050
65. Lorenz K, Sicker M, Schmelzer E et al. (2008) Multilineage differentiation potential of human dermal skin-derived fibroblasts. Exp Dermatol 17(11): 925–932. doi: 10.1111/j.1600-0625.2008.00724.x
66. Günter CI, Bader A, Dornseifer U et al. (2013) A multi-center study on the regenerative effects of erythropoietin in burn and scalding injuries: Study protocol for a randomized controlled trial. Trials 14: 124. doi: 10.1186/1468-6708-14-124

67. Cameli M, Righini FM, Sparla S et al. (2016) First Evidence of Cardiac Stem Cells From the Left Ventricular Apical Tip in Patients With Left Ventricular Assist Device Implantation. Transplant Proc 48(2): 395–398. doi: 10.1016/j.transproceed.2015.12.045
68. Gago-Lopez N, Awaji O, Zhang Y et al. (2014) THY-1 receptor expression differentiates cardiosphere-derived cells with divergent cardiogenic differentiation potential. Stem Cell Reports 2(5): 576–591. doi: 10.1016/j.stemcr.2014.03.003
69. Fung G, Luo H, Qiu Y et al. (2016) Myocarditis. Circ Res 118(3): 496–514. doi: 10.1161/CIRCRESAHA.115.306573
70. National Heart, Lund and Blood Institute Cardiomyopathy. https://www.nhlbi.nih.gov/health-topics/cardiomyopathy#Signs,-Symptoms,-and-Complications. Accessed 08 Apr 2018
71. Pantanowitz L, Farahani N, Parwani A (2015) Whole slide imaging in pathology: advantages, limitations, and emerging perspectives. PLMI: 23. doi: 10.2147/PLMI.S59826
72. Villa I, Mathieu M-C, Bosq J et al. (2018) Daily Biopsy Diagnosis in Surgical Pathology: Concordance Between Light Microscopy and Whole-Slide Imaging in Real-Life Conditions. Am J Clin Pathol 149(4): 344–351. doi: 10.1093/ajcp/aqx161

III ANHANG

Supplemental Material

https://www.frontiersin.org/articles/10.3389/fgene.2018.00072/full#supplementary-material

Qualitative and Quantitative Analysis of Cardiac Progenitor Cells in Cases of Myocarditis and Cardiomyopathy

Marie Gerisch, Jan Smettan, Sabine Ebert, Maria Athelogou, Beate Brand-Saberi, Nick Spindler, Wolf C. Mueller, Shibashish Giri, Augustinus Bader

Supplementary Figures 1-3 (Abbildungen A - E)

Positive, negative and IgG - controls for Immunohistochemistry (IHC)

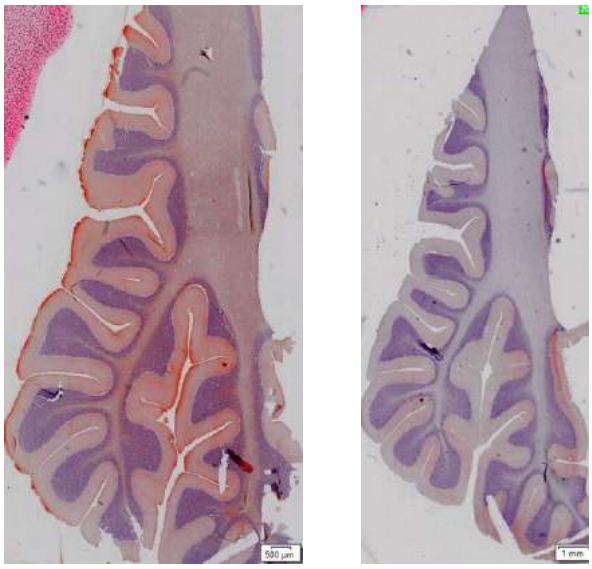

A **B**

Supplementary Figure 1. Histological images of the positive controls (human cerebellum, **A:** CD90 and **B:** CD117)

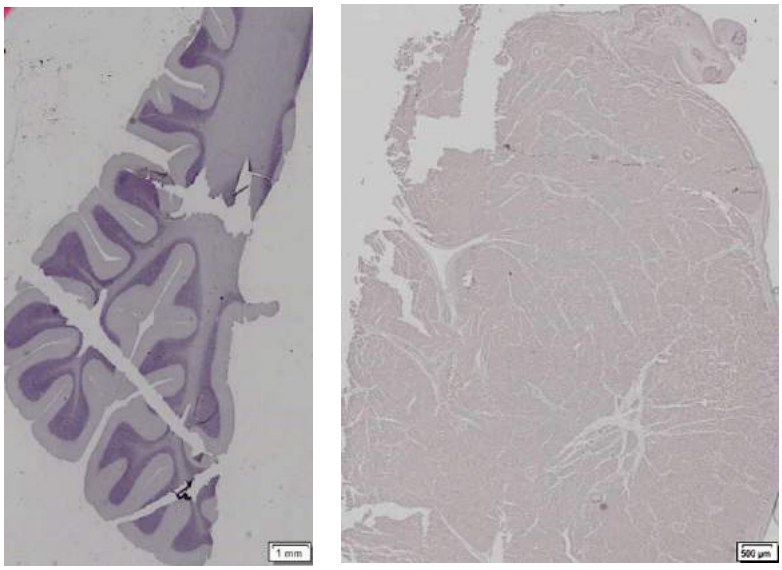

C **D**

Supplementary Figure 2. Histological images of the IgG - control (**C:** human cerebellum, **D:** human myocardium)

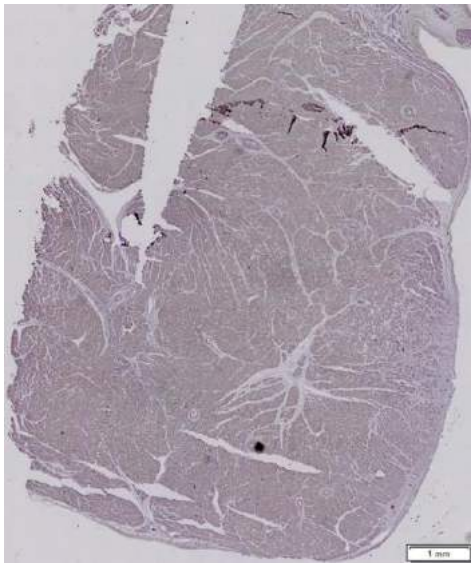

E

Supplementary Figure 3. Histological image of the negative control (**E:** human myocardium)

IV DARSTELLUNG DES EIGENEN WISSENSCHAFTLICHEN BEITRAGS

An die
Universität Leipzig
Dekanat der Medizinischen Fakultät
Referat für Akademische Angelegenheiten
Liebigstraße 27b
04103 Leipzig

Bestätigung des Eigenanteils der Doktorandin an einer Publikations-Dissertation gemäß § 6 (1) und § 7 (6) der Fakultätspromotionsordnung

Hiermit wird bestätigt, dass

Die Doktorandin **Marie Gerisch**, geb. Wegener

Zu den Publikationen

1. **"How to mend a broken heart: adult and induced pluripotent stem cell therapy for heart repair and regeneration"**, Wegener M, Bader A, Giri S. Drug Discov Today. 2015 Jun; 20:667-85. doi: 10.1016/j.drudis.2015.02.010

2. **"Qualitative and Quantitative Analysis of Cardiac Progenitor Cells in Cases of Myocarditis and Cardiomyopathy."** Gerisch M, Smettan J, Ebert S *et al.* Front Genet. 2018 Mar 6;9:72. doi: 10.3389/fgene.2018.0007

wie folgt beigetragen hat:

- Literaturrecherche und Analyse früherer Studien
- Organisieren von humanem Probematerial sowohl in Form fertiger Paraffinschnitte und fertig eingebetteter Biopsien als auch frischer Proben aus dem OP aus Kliniken der Universität Leipzig und deren histologische Aufarbeitung (z.T. Einbettung und Anfertigung von Paraffinschnitten)
- Maßgebender Beitrag bei der Neuentwicklung und Etablierung spezifischer Protokolle zur immunhistochemischen Analyse der speziellen in Paraffin eingebetteten humanen Gewebeproben
- Durchführung der immunhistochemischen Färbungen
- Digitalisierung der histologischen Präparate mittels spezieller Software
- Auswertung der histologischen Ergebnisse und der Ergebnisse der digitalen Bildanalyse
- Erstellung der Grafiken
- Manuskriptentwurf und Mitarbeit an der kritischen Revision

	Vor- und Nachname	Datum	Unterschrift
Doktorandin	Marie Gerisch	17.04.2018	M. Gerisch
Betreuer	Augustinus Bader	16.6.2018	
Betreuer	Jan Smettan	8.7.2018	
Ko-Betreuer	Shibashish Giri	04.06.2018	Shibashish Giri
Ko-Autor 1	Sabine Ebert	11.06.2018	Sabine Ebert
Ko-Autor 2	Maria Athelogou	11.05.2018	Athelogou
Ko-Autor 3	Beate Brand-Saberi	23.4.2018	B. Brand-Saberi

V ERKLÄRUNG ÜBER DIE EIGENSTÄNDIGE ABFASSUNG DER ARBEIT

Hiermit erkläre ich, dass ich die vorliegende Arbeit selbstständig und ohne unzulässige Hilfe oder Benutzung anderer als der angegebenen Hilfsmittel angefertigt habe. Ich versichere, dass Dritte von mir weder unmittelbar noch mittelbar eine Vergütung oder geldwerte Leistungen für Arbeiten erhalten haben, die im Zusammenhang mit dem Inhalt der vorgelegten Dissertation stehen, und dass die vorgelegte Arbeit weder im Inland noch im Ausland in gleicher oder ähnlicher Form einer anderen Prüfungsbehörde zum Zweck einer Promotion oder eines anderen Prüfungsverfahrens vorgelegt wurde. Alles aus anderen Quellen und von anderen Personen übernommene Material, das in der Arbeit verwendet wurde oder auf das direkt Bezug genommen wird, wurde als solches kenntlich gemacht. Insbesondere wurden alle Personen genannt, die direkt an der Entstehung der vorliegenden Arbeit beteiligt waren. Die aktuellen gesetzlichen Vorgaben in Bezug auf die Zulassung der klinischen Studien, die Bestimmungen des Tierschutzgesetzes, die Bestimmungen des Gentechnikgesetzes und die allgemeinen Datenschutzbestimmungen wurden eingehalten. Ich versichere, dass ich die Regelungen der Satzung der Universität Leipzig zur Sicherung guter wissenschaftlicher Praxis kenne und eingehalten habe.

.....	.....
Datum	Unterschrift

VI CURRICULUM VITAE

Persönliche Daten

Name:	Marie Gerisch, geb. Wegener
Nationalität:	Deutsch
Geburtsdatum und -ort:	21.09.1991 in Peine
Familienstand:	verheiratet, 1 Kind

Medizinische Ausbildung

03-08/2018	Praktisches Jahr in der Klinik für Kinder- und Jugendmedizin, Klinikum St. Georg Leipzig
01-03/2018	Praktisches Jahr am Institut für Humangenetik, Universitätsklinikum Leipzig
10-12/2017	Praktisches Jahr in der Klinik für Allgemein-, Visceral-, MIC- und Gefäßchirurgie, Sana Kliniken Leipziger Land
05-10/2017	Praktisches Jahr in der Klinik für Innere Medizin, Sana Kliniken Leipziger Land Elternzeit (05/2016 - 05/2017)
04/2013 – 04/2016	Klinischer Abschnitt des Studiums der Humanmedizin, Medizinische Fakultät der Universität Leipzig (Abschlussnote der zweiten ärztlichen Prüfung: 3,0)
10/2010 – 03/2013	Vorklinischer Abschnitt des Studiums der Humanmedizin, Medizinische Fakultät der Universität Leipzig (Abschlussnote der ersten ärztlichen Prüfung: 3,0)

Praktische Erfahrungen

07-08/2015	Famulatur in der Klinik für Kinder- und Jugendmedizin, Klinikum St. Georg Leipzig
03/2015	Famulatur im Paediatric Department, St Mary's Hospital Newport, Isle of Wight, Great Britain
02/2015	Famulatur in der Klinik und Poliklinik für Kinder- und Jugendmedizin/Kinderonkologie, Universitätsklinikum Leipzig

08-09/2014	Famulatur in der Klinik für Innere Medizin/Kardiologie im Herzzentrum Leipzig
02-03/2014	Famulatur in der Allgemeinmedizinischen Praxis Dr. med. Sören Heinrich, Leipzig
07-08/2011	Krankenpflegepraktikum in der Klinik für Gefäßchirurgie, Krankenhaus St. Elisabeth und St. Barbara, Halle (Saale)
02-03/2011	Krankenpflegepraktikum OKL Station B2/Orthopädie, Universitätsklinikum Leipzig
06-07/2010	Krankenpflegepraktikum in der Inneren Medizin, Muldentalkliniken GmbH, Krankenhaus Grimma

Dissertation

Seit 04/2013	Doktorandin am Biotechnologisch-Biomedizinischen Zentrum, Professur für Zelltechniken und Angewandte Stammzellbiologie, Universität Leipzig

Publikationen

2015	How to mend a broken heart: adult and induced pluripotent stem cell therapy for heart repair and regeneration. Wegener M, Bader A, Giri S (2015) Drug Discov Today. 20:667-85. doi: 10.1016/j.drudis.2015.02.010
2018	Qualitative and Quantitative Analysis of Cardiac Progenitor Cells in Cases of Myocarditis and Cardiomyopathy. Gerisch M, Smettan J, Ebert S *et al.* (2018) Front Genet. 6;9:72. doi:10.3389/fgene.2018.00072

Schulische Ausbildung

2001-2010	Gymnasium St. Augustin, Grimma (Abiturnote: 1,4)
1997-2001	Grundschule am Wallgraben, Grimma

Sonstige Tätigkeiten

09/2013-12/2015	Studentische Hilfskraft in der Praxis Dipl.-Med. Babette Schmidt, Fachärztin für Neurologie und Psychiatrie, Leipzig
03/2012-03/2013	Studentische Hilfskraft am Berufsgenossenschaftlichen Klinikum Bergmannstrost in Halle (Saale), neurologische Frührehabilitation und Stroke Unit

Weiterbildungen und Zertifikate

04/2015-07/2015	„Praxisbezogener systematischer EKG-Kurs“, Teil II - Aufbaukurs
10/2014-02/2015	„Praxisbezogener systematischer EKG-Kurs“
10/2014-07/2015	English Language Course „Speaking in Medicine“
04-07/2011	Wahlfach „Medizinische Informatik für Mediziner“ (Note: gut)
10/2010-07/2011	Wahlfach „Englisch für Mediziner“ (Note: gut)

Sprach- und EDV-Kenntnisse

Sprachkenntnisse	Englisch (fließend) Französisch gut (A2) Latein (Latinum)
EDV-Kenntnisse	Microsoft-Office: Word, Excel, PowerPoint, Outlook SAP
Führerschein	Klassen B, M, L, T/S

VII DANKSAGUNG

An erster Stelle danke ich meinem Betreuer Prof. Augustinus Bader und meinen Ko-Betreuern Dr. Shibashish Giri und Dr. Jan Smettan sehr für die angenehme Zusammenarbeit, wertvolle Unterstützung, Förderung und Geduld in den vergangenen Jahren.
Ein ganz besonderer Dank gilt Sabine Ebert, die mir insbesondere bei der Durchführung der Experimente eine große Stütze war und mich während der gesamten Zeit stets bestmöglich angeleitet und beraten hat.
Ich danke Dr. Maria Athelogou, die mit ihrer professionellen Unterstützung bei der Auswertung der Ergebnisse diese Arbeit in die richtigen Bahnen lenkte. Ich danke auch allen weiteren Koautoren der Publikationen für ihr Engagement, ihre Ausdauer und ihre konstruktive Kritik an den Manuskripten, wodurch beide Publikationen erfolgreich veröffentlicht werden konnten.

Ich bedanke mich herzlich bei meinen Eltern Manuela Wegener und Gerd Wegener, die mich immer unterstützten, förderten, mir den nötigen Rückhalt gaben, und damit die Voraussetzungen für mein Studium und diese Promotionsarbeit gelegt haben.
Einen besonderen Dank richte ich an meinen Ehemann Stefan Gerisch, der mich mit seinem Engagement, seinen Anregungen, Ermutigungen und Optimismus bis zur Fertigstellung dieser Arbeit bestens motiviert hat. Ein abschließender Dank geht an meine Tochter Emma Charlotte Gerisch, die während der Fertigstellung dieser Arbeit oftmals auf mich verzichten musste und mir das dennoch nicht nachträgt.